AHTD TRC TRANSPORTATION RESEARCH COMMITTEE

TRC8902

Effect of Truck Tire Contact Pressures

R. P. Elliott, R. P. Selvam, L. K. Mun

Final Report

1991

Effect of Truck Tire Contact Pressures

Dept. of Civil Engineering
College of Engineering
University of Arkansas
Fayetteville, Arkansas

FINAL REPORT
TRC 8902

FINAL REPORT

TRC-8902

EFFECT OF TRUCK TIRE CONTACT PRESSURE

PRINCIPAL INVESTIGATOR - Robert P. Elliott

CO-PRINCIPAL INVESTIGATOR - R. Panneer Selvam

GRADUATE ASSISTANT - Low Keng Mun

Conducted by

Arkansas Highway and Transportation Research Center
Department of Civil Engineering
Engineering Experiment Station
University of Arkansas

in cooperation with

Arkansas State
Highway and Transportation Department

and

U.S. Department of Transportation
Federal Highway Administration

Report No. UAF-AHTRC-91-001

University of Arkansas
Fayetteville, Arkansas

February, 1991

Technical Report Documentation Page

1. Report No.	2. Government Accession No.	3. Recipient's Catalog No.
FHWA/AR-91/006		

4. Title and Subtitle	5. Report Date
TRC-8902, Effect of Truck Tire Contact Pressure	February, 1991
	6. Performing Organization Code
	8. Performing Organization Report No.
7. Author(s)	
Elliott, R. P., Selvam, R. P., and Mun, L. K.	UAF-AHTRC-91-001
9. Performing Organization Name and Address	10. Work Unit No. (TRAIS)
Arkansas Highway and Transportation Research Center Department of Civil Engineering University of Arkansas Fayetteville, AR 72701	11. Contract or Grant No. TRC-8902
	13. Type of Report and Period Covered
12. Sponsoring Agency Name and Address	Final Report
Arkansas State Highway and Transportation Department Materials and Research Division P. O. Box 226 Little Rock, AR 72206	14. Sponsoring Agency Code FHWA/AR-91/006

15. Supplementary Notes

Study conducted in cooperation with the U.S. Department of Transportation, Federal Highway Administration

16. Abstract

A survey of truck tire pressures was conducted at numerous sites around Arkansas. The average inflation pressure was found to be 105 psi with pressures in excess of 120 psi not being uncommon. In comparison, the AASHTO Guide for Design of Pavement Structures is based on empirical data in which truck tire pressures did not exceed about 80 psi. This study examined the effect of the higher pressure on pavement performance and included laboratory measurement of tire contact pressures at various inflation pressures and loads. The major effect was found to be increased rutting potential within the upper 2 to 3 inches of asphalt surfacing. This effect cannot be taken into account in thickness design but must be considered in material selection. Other effects are increased fatigue cracking and greater rut development in the base, subbase, and subgrade. Recommendations for thickness design modifications to account for these effects are presented.

17. Key Words	18. Distribution Statement
Tire Pressure, Contact Pressure, Rutting, Fatigue, Thickness Design	NO RESTRICTIONS

19. Security Classif. (of this report)	20. Security Classif. (of this page)	21. No. of Pages	22. Price

Form DOT F 1700.7 (8-72) Reproduction of completed page authorized

ACKNOWLEDGEMENTS/DISCLAIMER

This report is based on the findings of Project TRC-8902, Effect of Truck Tire Contact Pressure.

TRC-8902 is sponsored by the Arkansas State Highway and Transportation Department and the U.S. Department of Transportation, Federal Highway Administration.

SI CONVERSION FACTORS

1 inch = 25.4 mm

1 foot = 0.305 m

1 pcf = 16 kg/m^2

1 psi = 6.9 kN/m^2

1 ksi = 6.9 MN/m^2

1 lb = 4.45 N

TABLE OF CONTENTS

List of Tables

List of Figures

ACKNOWLEDGEMENTS/DISCLAIMER

This report is based on the findings of Project TRC-8902, Effect of Truck Tire Contact Pressure.

TRC-8902 is sponsored by the Arkansas State Highway and Transportation Department and the U.S. Department of Transportation, Federal Highway Administration.

SI CONVERSION FACTORS

1 inch = 25.4 mm

1 foot = 0.305 m

1 pcf = 16 kg/m^2

1 psi = 6.9 kN/m^2

1 ksi = 6.9 MN/m^2

1 lb = 4.45 N

CHAPTER 1

INTRODUCTION

1.1 Introduction

The effect of high tire pressure on pavement performance has been the topic of many research studies in recent years. These studies [8,10,11,15,16, 17,26] have generally concluded that increased tire pressures accelerate pavement deterioration, especially for thin flexible pavements. The studies suggest that increased tire pressures cause more rapid development of alligator cracking and surface rutting in asphalt concrete pavements.

The Arkansas State Highway and Transportation Department designs pavements using the AASHTO Guide for the Design of Pavement Structures [1]. Within the framework of the Guide procedures, there is no convenient method for considering the effects of higher tire pressures. The Guide procedures were derived empirically from data obtained from the AASHO Road Test (1958-1960). Being empirical in nature, the AASHTO Guide design procedures reflects only those conditions prevalent at the AASHO Road Test. The average tire pressures used during the AASHO Road Test ranged from 75 psi to 80 psi, and the tires were of bias ply construction. However, recent surveys [11,17,26] indicate that tire pressures have increased to an average of 105 psi, and radial tires have replaced bias ply tires as the commonly used tire

type.

Since high tire pressures contribute to premature pavement deterioration which results in increased maintenance and rehabilitation cost, changes are needed in the design process to account for the effect of high tire pressure on pavements.

1.2 Scope and Purpose

The purpose of this study was to investigate the effects of high tire pressure on pavements commonly built in Arkansas and to provide recommendations on how to account for the effects within the framework of the AASHTO Guide. The contact pressure effect of two types of tires, radial and bias ply, was studied. The radial tire represented the typical tire used today and the bias ply tire represented the tires used during the AASHO Road Test (1958) period.

1.3 Tire Pressure Study Work Plan

The following are brief descriptions of the activities under this study.

A) Literature Review

The available literature was reviewed throughout the course of the project to provide constant feedback on the findings of others involved in similar research.

B) Truck Tire Pressure Survey.

A truck tire pressure survey was carried out by the Arkansas State Highway and Transportation Department (AHTD). The data collected were analyzed under this study to obtain the trend of tire types and inflation pressures used by truckers in Arkansas.

C) Contact Pressure Measurements.

Mechanistic pavement analyses typically assume that the tire-pavement contact pressure is equal to the tire inflation pressure. Literature reviews prior to the study revealed some information relative to measured contact pressures. To supplement this information contact pressure measurements were made as a part of this study.

A testing frame was designed and set up to investigate the pattern and magnitude of tire contact pressures. Two types of tire, radial and bias ply, were used for this investigation. The radial tire was inflated to four different inflation pressures: 80 psi, 100 psi, 120 psi, and 140 psi. The bias ply tire was inflated to three different inflation pressures: 60 psi, 80 psi, and 100 psi.

D) Pavement Structural Analysis.

Pavement structural analyses were performed to investigate the effects of higher tire pressures on the load induced stresses and strains. Two types of analyses were made - elastic layer analyses using

ELSYM5 and finite element analyses using ILLIPAVE. ILLIPAVE was modified as a part of the study so that it could handle the non-uniform contact pressures measured in the study.

E) Recommendation Development

Based on the findings of this and other research, recommendations were developed for modifications to the AHTD standard pavement design practice. The recommendations are intended to compensate for the effect of today's higher tire pressures within the framework of the AASHTO Guide.

CHAPTER 2

LITERATURE REVIEW

2.1 Pavement Design Procedures

There are two general approaches to pavement design: 1) empirical and 2) mechanistic. In the empirical approach, the design procedure is derived from experience and observation of the performance of existing pavements. The reliability of an empirically based design procedure is dependent on the materials, thicknesses, loadings, and environment being similar to that for which the experience and performance data were obtained. Design procedures based on the mechanistic approach, on the other hand, are derived from the analyses of load-induced stresses, strains, and deformations on the behavior of the pavement materials. A fully developed mechanistic procedure can be expected to provide a better design in situations where experience (e.g. high tire pressure) is not applicable; however, the wide range of pavement materials and the complexity in their behavior have thus far limited the development of mechanisitc design procedures.

2.1.1 AASHTO Flexible Pavement Thickness Design Procedure

The AASHTO design procedure [1] which is used by AHTD was derived empirically from data obtained from the AASHO Road Test. The AASHTO flexible pavement thickness design

procedure relates pavement thickness to the required structural number (SN) for the pavement. The SN is defined as the sum of the products of thickness and layer coefficient for each of the pavement layers.

$$SN = a_1D_1 + a_2D_2 + \ldots\ldots\ldots \qquad \text{[Eq. 2-1a]}$$

This equation was later modified to take into account the effect of drainage. The equation is:

$$SN = a_1D_1 + a_2D_2m_2 + a_3D_3m_3 \qquad \text{[Eq. 2-1b]}$$

where,

a_i = layer coefficient of layer i

D_i = thickness of layer i, inches

m_i = drainage modifying factor for layer i

The required SN for a particular pavement is determined from the estimated future traffic, effective roadbed soil resilient modulus, the design serviceability loss and the desired level of design reliability. The equation to determine the required SN [1] is:

$$\begin{aligned} Log_{10}W_{18} = {} & z_R*s_o + 9.36*log_{10}(SN+1) - 0.20 + 2.32* log_{10}M_R \\ & - 8.07 + (log_{10}\,(dPSI/(4.2-1.5))/(0.40 + \\ & 1094/\,(SN + 1)^{5.19})) \end{aligned} \qquad \text{[Eq. 2-2]}$$

where,

W_{18} = 18 kip equivalent single axle load applications (ESALs) expected for the design period.

Z_R = Factor dependent upon the desired level of design reliability.

s_o = Overall standard deviation of pavement performance prediction.

dPSI = Design serviceability loss, $p_o - p_t$.

M_R = subgrade resilient modulus, psi.

The AASHO Road Test was conducted in the late 1950's and early 1960's in northern Illinois. At that time only bias ply tires were being used and the inflation pressure for heavily loaded trucks was typically 75 to 80 psi. Bias ply tires and pressures in this range were used on the trucks trafficking the Road Test pavements. Recent surveys have shown that wheel loads and tire pressures have increased, and radial tires are more commonly used than bias ply tires. In this respect, the empirical data from the AASHO Road Test are not consistent with current conditions and note that there is no provision in the AASHTO design equation for consideration of tire types or tire pressures. Some modification of the AASHTO design process is needed so that the effects of high tire pressures are properly considered.

2.1.2 Mechanistic-Empirical Design Procedure

Mechanistic-Empirical design procedures combine both the empirical and theoretical approaches in pavement design

through the development of transfer functions. Transfer functions relate the number of 18 kip ESAL applications a pavement can carry before service failure to load-induced, mechanical pavement responses (stresses, strains, and deformations) [19]. The stresses, strains, and deformations are determined from structural analyses, and the number of load applications to service failure are established from field performance data (empirical). Thus, mechanistic-empirical design procedures provide the means for the consideration of the variability in loading conditions (tire pressure, load, suspension etc).

Two transfer functions are typically used for mechanistic analyses of flexible pavements. These are based on the two structural response parameters generally considered as most critical to pavement performance. The two response parameters are: 1) maximum tensile strain at the bottom of the AC layer, and 2) maximum vertical strain at the top of the subgrade. The transfer functions based on these parameters are generally referred to as fatigue transfer functions and rutting transfer functions. The locations of the two critical response parameters are chosen because they are generally considered to control the fatigue and rutting failure modes of the pavement. Fatigue transfer functions are developed to control the development of alligator cracking in the asphalt concrete (AC), and usually take the form:

$$\log N_f = K + n \log (1/e_{ac}) \qquad \text{[Eq. 2-3]}$$

where,

N_f = number of load applications to failure.

e_{ac} = maximum tensile strain at the bottom of AC.

K & n = constants determined by testing and/or empirical data.

Rutting transfer functions, on the other hand, are developed to control permanent subgrade deformation. The general form of rutting transfer functions is:

$$\log N_r = k + a \log (1/e_z) \qquad \text{[Eq. 2-4]}$$

where,

N_r = number of load applications to failure.

e_z = the load-induced vertical strain at the top of the subgrade.

k & a = constants determined from analysis.

Transfer functions based on these response parameters are used in some well-known mechanistic-empirical design procedures - 1) FHWA's VESYS procedure [20], 2) The Asphalt Institute's (TAI) procedure [21], and 3) the Shell design procedure [22].

The accuracy of a transfer function is dependent on the particular field performance data and the structural response parameters that formed the basis for the development of the function.

Because the transfer functions are at least partially

based on empirical data, the mechanistic-empirical design procedures can be subjected to the same shortcomings with regard to tire pressure effects as are empirical procedures. For example, research [15,17] has found that the effects of high tire pressures are greatest within the AC layer with the primary effect being increased potential for rutting. The base layer can also be affected by high tire pressures. However, since the base is not normally evaluated in mechanistic-empirical analyses, the commonly used transfer functions (described above) may not be adequate for analyzing the effects of higher pressures on the base. A detailed study of the effects of higher tire pressures should include the analyses of the traditional traffic-induced responses as well as responses at various other locations within the AC and base layers.

2.2 Changes in Tire Technology

The tire manufacturing industry has prospered from improved production technology. As a result of the improved technology, the tire manufacturers have managed to produce high quality radial tires that are capable of withstanding higher inflation pressures and supporting heavier loads. However, the increased tire pressure poses a major concern for pavement engineers as it (increased pressure) is widely suspected to be one of the major causes of some premature pavement failures.

2.2.1 High Pressure Tire and Low Pressure Tire

The increased tire pressure is influenced by factors such as the change from bias ply to radial tires, the increase in allowable axle loads, and the prevalent perception that high tire pressures result in lower fuel consumption.

High pressure tires support heavier wheel loads, reduce rolling resistance, and reduce hydroplaning potential. However, despite the perception that high tire pressure reduces fuel consumption, several studies [2,3] have demonstrated that the effect of tire pressure on fuel economy is not very significant. Test data generated at Calspan [2] in Buffalo, New York, indicated that a 10 psi increase in inflation pressure would result in approximately 4% reduction in bias ply tire rolling resistance but only a 2-1/2% reduction for radial tires. This 2-1/2% reduction in rolling resistance results in less than 1% reduction in fuel consumption.

Stuart et al [3] studied the economics of using high (90 psi to 110 psi) and low (less than 70 psi) pressure tires on vehicles used in transporting forest products over unpaved low-volume roads. Fuel consumption data from several field test sites showed little difference between trucks of high and low tire pressure. However, the researchers did find that the use of low tire pressure caused less damage to pavement, trucks and cargo, while providing better driving comfort.

2.2.2 Radial Tire and Bias Ply Tire.

The bias ply tire, commonly used during the AASHO Road Test (1958) era, is constructed of multiple cross-angled fabric layers (body plies) and multiple-angled fabric breakers in the crown region (Figure 2-1). The radial ply tire, commonly used today, is constructed of a single radially oriented steel ply and multiple-angled steel belts in the crown region (Figure 2-2).

Radial tires are the products of improved tire manufacturing technology. The radial tires are capable of withstanding higher inflation pressures and supporting heavier axle loads. The deregulation of the trucking industry, the increase in legal axle load, and the demand for surface transportation have resulted in the growth of radial tires usage. Figure 2-3 shows the growth of radial tire usage in this country. Figure 2-4 compares the performance of standard aspect ratio radial tires versus bias ply tires in line haul trucking. A '+' denotes an improvement of performance; a '-' denotes a loss of performance; and '=' denotes similar performance.

The usage of low profile radial tire has also grown relative to standard aspect ratio radials, accounting for 18% of replacement sales and 35% of original equipment radial medium truck tire sales [4]. Low profile tires have a lower diameter but wider section width (Figure 2-5). Figure

DIAGONAL PLY (BIAS)

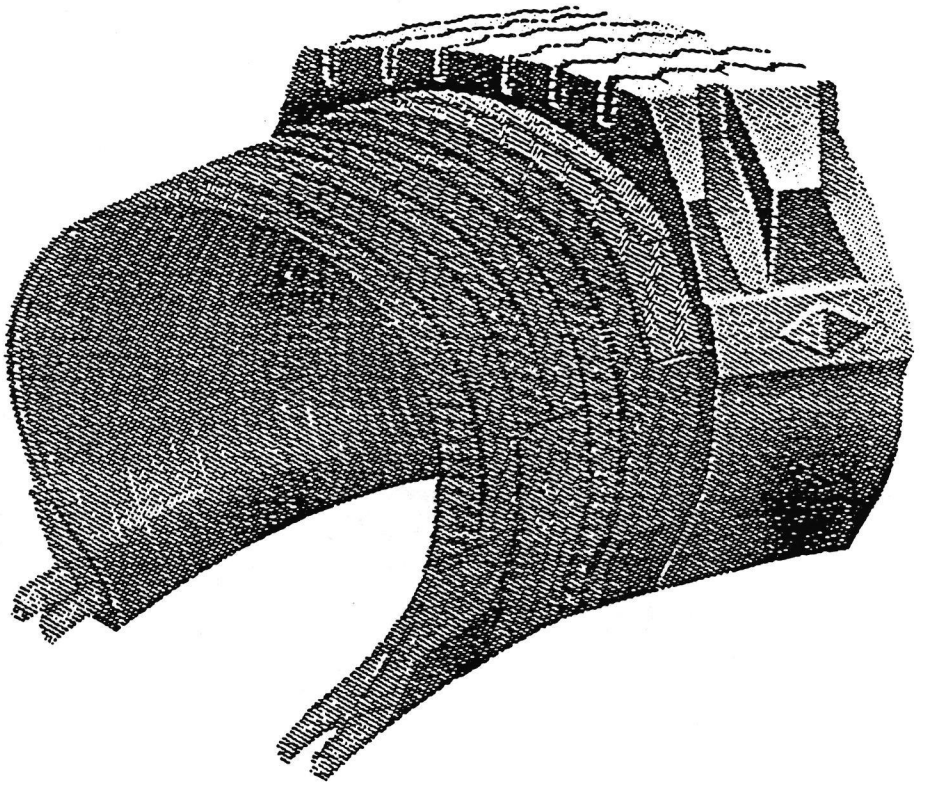

Figure 2-1. Bias Ply Tire (Yap [6]).

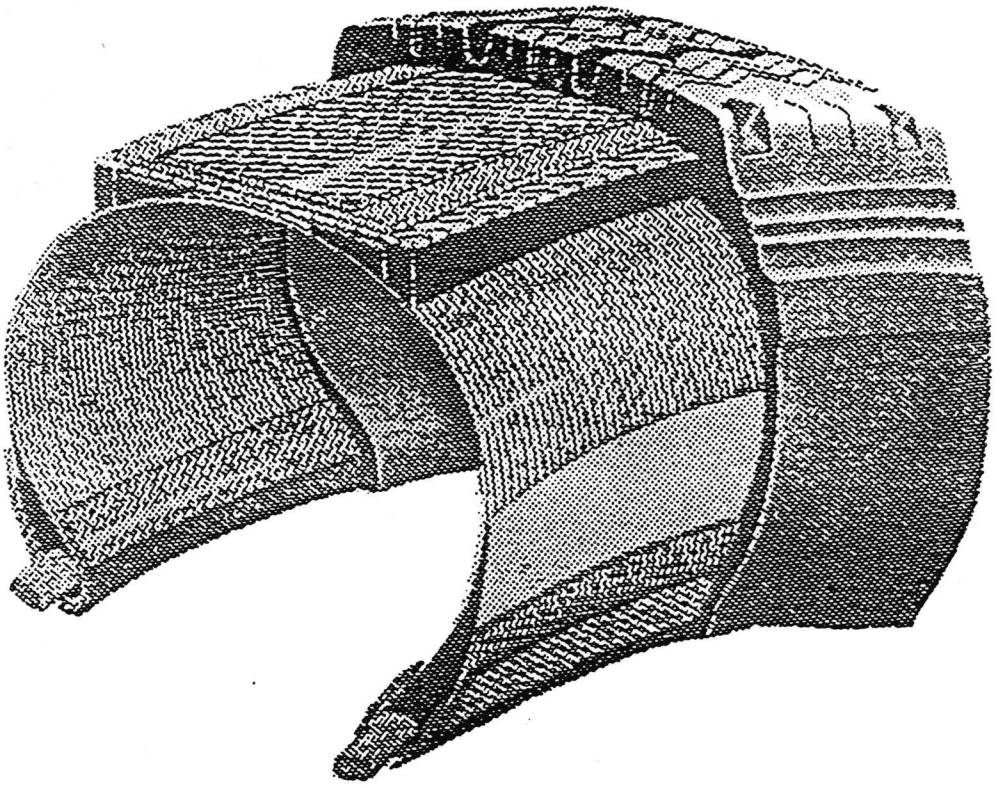

Figure 2-2. Radial Tire (Yap [6]).

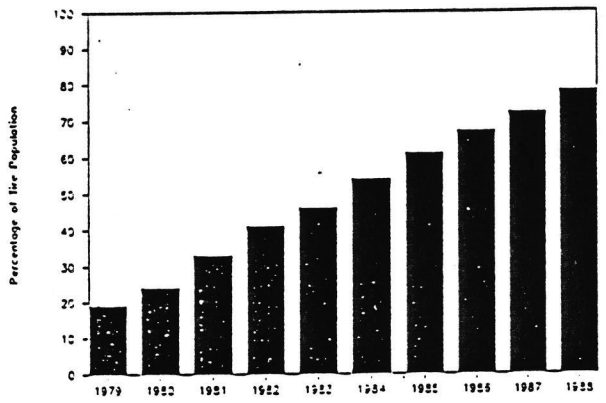

Figure 2-3. Radial Tire Population in Tractors and Trailers (Courtesy of Michelin Tire Corporation)

RADIAL VS BIAS

● CASING DURABILITY	+
● TREAD WEAR	+
● FUEL ECONOMY	+
● HANDLING/STABILITY	+
● DOWNTIME	+
● POTENTIAL PAYLOAD VOLUME	=
● INVENTORY COMPLEXITY	=
● EASE OF MAINTENANCE	=
● PAYLOAD WEIGHT	–
● TIRE/WHEEL COST	–

Figure 2-4. Radial vs. Bias Ply Tire Performance (Ford [4]).

2-6 compares (in a similar manner as that used in Figure 2-4) the performance of low profile tires against standard aspect ratio tires.

Another type of tire gaining popularity in the trucking industry is the wide base single (Figure 2-7). The wide base tire (or super single tire) is used alone on a wheel in place of the two (dual) tires normally used. The wide base tire is wider but has a lower profile than the standard tire. Figure 2-8 compares the performance of wide base singles against duals.

Besides being capable of withstanding high inflation pressures and supporting heavier axle load, radial tires also provide better vehicular tracking. While this may improve driving comfort, it may also lead to an increase in the rate of pavement rutting and could explain the dual tire rutting observed on some pavements in recent years (Figure 2-9). As the ruts develop, they become channels or guideways for the truckers, thus concentrating all loadings to a single, narrow path.

2.3 Inflation Pressure and Contact Pressure.

Mechanistic pavement analyses generally assume that the tire-pavement contact pressure equals the tire inflation pressure. Inflation pressure refers to the internal tire pressure whereas contact pressure refers to the vertical interface pressure between the tire treads and the pavement

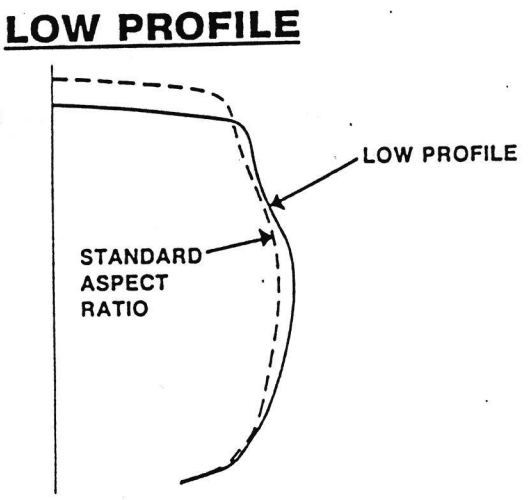

Figure 2-5. Low Profile Tire (Ford [4]).

LOW PROFILE VS STANDARD ASPECT RATIO

RADIAL CONSTRUCTION

● PAYLOAD WEIGHT	+
● POTENTIAL PAYLOAD VOLUME	+
● FUEL ECONOMY	=/+
● HANDLING/STABILITY	=/+
● TREADWEAR	=/+
● CASING DURABILITY	=
● INVENTORY COMPLEXITY	=
● DOWNTIME	=
● EASE OF MAINTENANCE	=
● TIRE/WHEEL COST	=

Figure 2-6. Low Profile vs. Standard Aspect Ratio Tire Performance (Ford [4]).

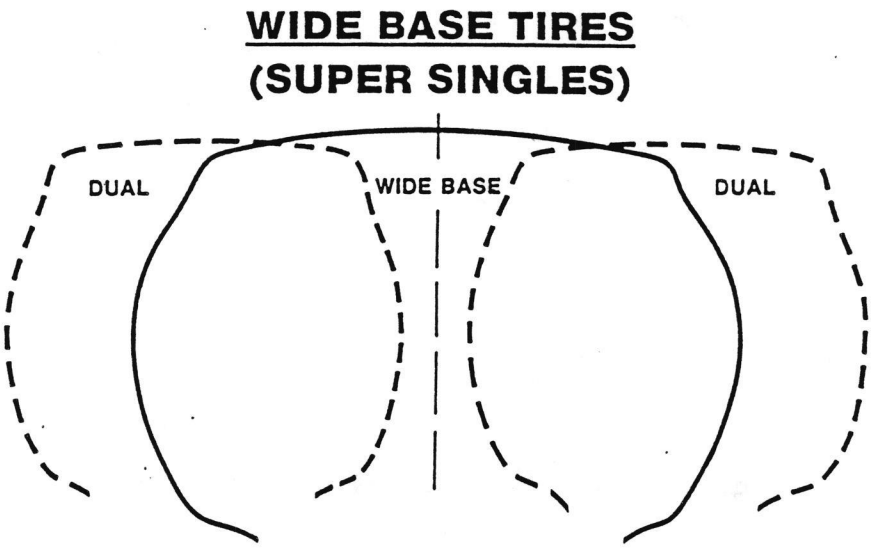

Figure 2-7. Wide Base Tires (Ford [4]).

WIDE BASE SINGLES VS DUALS

POTENTIAL	
● PAYLOAD WEIGHT	+
● PAYLOAD VOLUME	+
● EASE OF MAINTENANCE	+
● TIRE/WHEEL COST	+
● FUEL ECONOMY	=/+
● TREADWEAR	/+
● HANDLING/STABILITY	−/+
● CASING DURABILITY	−/=
● DOWNTIME	−
● INVENTORY COMPLEXITY	−

Figure 2-8. Wide Base Singles vs. Duals (Ford [4]).

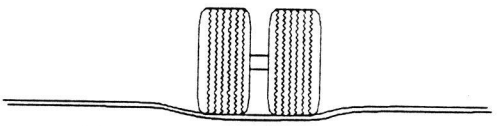

Normal Rut Pattern

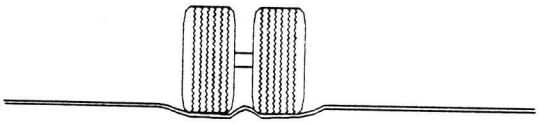

Dual Wheel Rut Pattern

Figure 2-9. Typical Rut Shape vs. the Dual Tire Ruts Observed on Some Pavements.

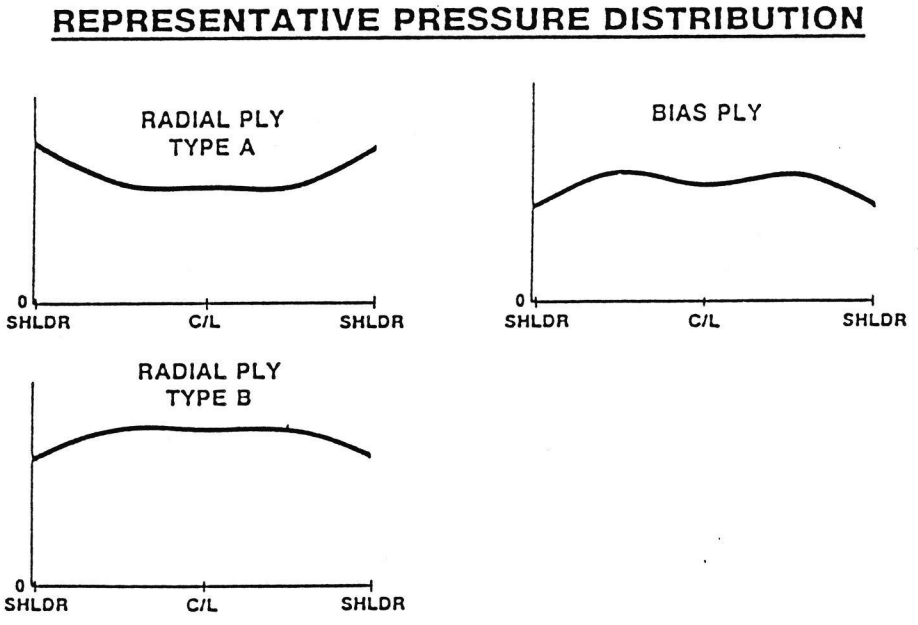

Figure 2-10. Representative Pressure Distribution (Ford [4]).

surface. Research [6,7] has shown that the tire contact pressure does not equal the inflation pressure, and the contact pressure is not uniform over the entire contact area (Figure 2-10).

Lister and Nunn [5] reported that while the contact area of a low wall stiffness smooth tire approximately equals the wheel-load divided by the inflation pressure, the contact area of a heavily treaded and of high wall stiffness tire is only about 60% of the area calculated by dividing the wheel-load by the inflation pressure. In other words, the average contact pressure for a tire can be as high as 167% of the inflation pressure. At certain points, the contact pressure is almost double the inflation pressure (Figure 2-11).

Pedro Yap [6] measured the contact pressure of a very slow moving tire (0.10 mph) over an instrumented flat bed (Figure 2-12). Besides measuring the vertical contact force, the instrumentation measured other forces along the lateral and longitudinal directions ("inplane" forces). The "inplane forces" occur as a result of the bending of the tire as it is deformed from its normally toroidal shape at the tire/road interface. He reported that the vertical forces are relatively large compared to the "inplane" forces. Thus, it may be assumed that the contribution of the "inplane" forces to pavement rutting and fatigue cracking is not as significant as the contribution of the vertical forces.

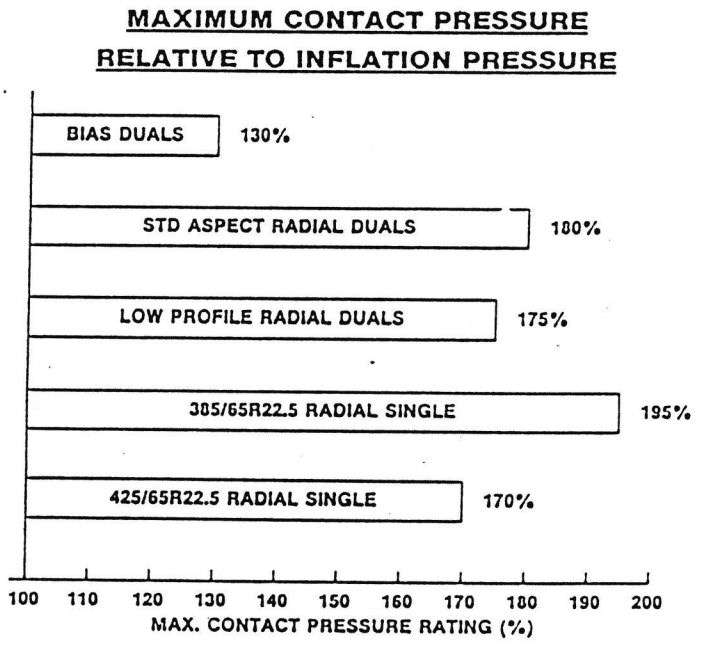

Figure 2-11. Maximum Contact Pressure Relative to Inflation Pressure (Ford [4]).

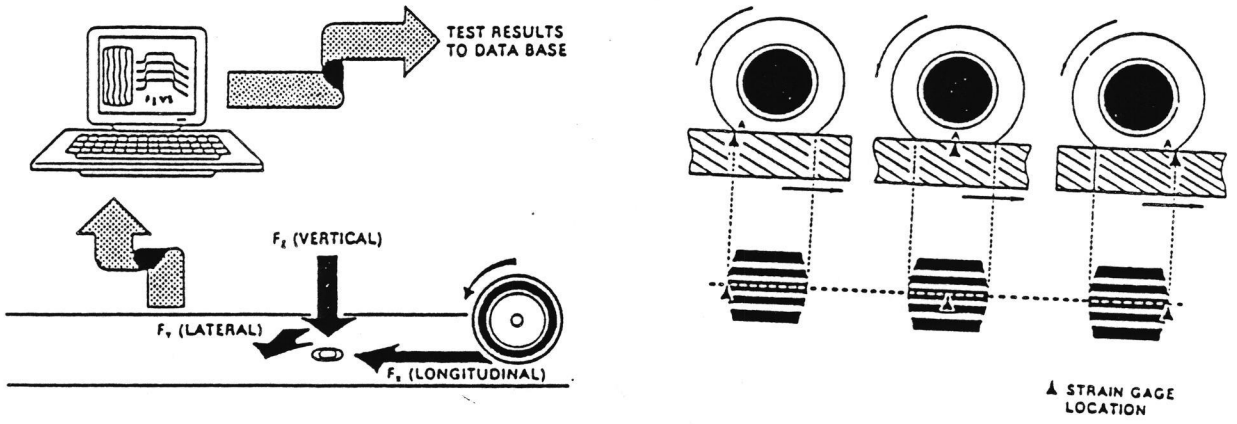

Figure 2-12. Moving Tire Contact Pressure Measuring Device Used by Yap [6].

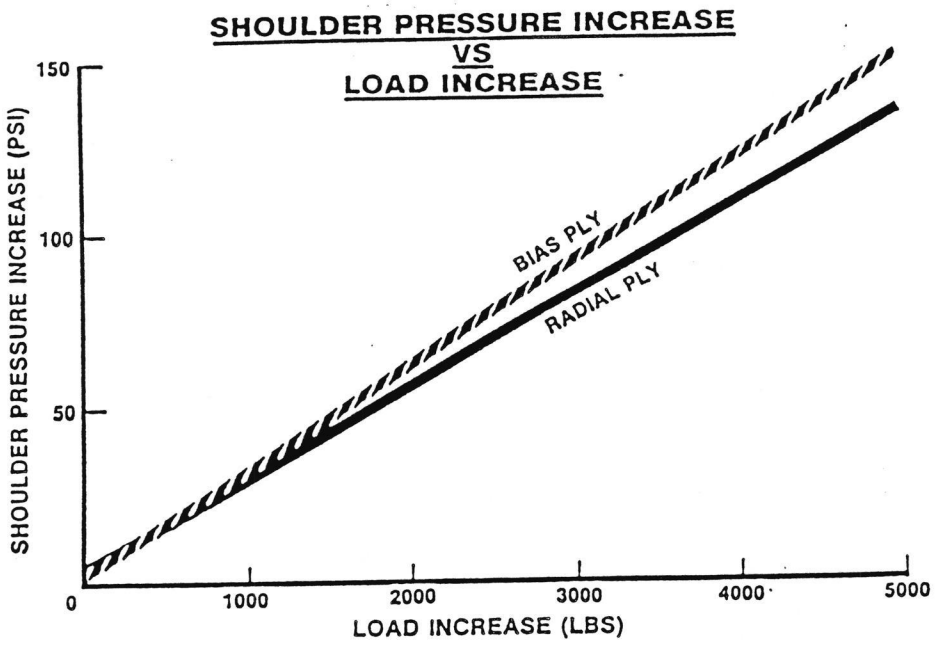

Figure 2-13. Shoulder Pressure Increase vs. Load Increase (Ford [4]).

The contact pressures of both tire types change with different load and inflation pressures. T.L. Ford [4] reported that bias ply tires are more sensitive to load increment at fixed inflation pressure than are radial tires. For example, a 100 pound load increase produces a 3 psi shoulder pressure increase in bias tires compared to 2 psi increase in radial tires (Figure 2-13). There is little change in the contact pressure along the centerline with increasing load. On the other hand, the centerline pressure increases with increasing inflation pressure. The effect is more significant in radial tires. A 1 psi increase in inflation pressure results in a 1.3 psi increase in centerline pressure for radial tires compared to 1 psi increase in bias tires (Figure 2-14). The disproportionate increase in centerline pressure with respect to increase in inflation pressure for radial tires results in high stress concentration at the middle of the tire track.

Tielking [7] developed a finite element program to model the behavior of radial tires. This program was used to study the pattern of contact pressure distribution for use in pavement analyses. The program accepts tire properties input, and uses an assembly of homogeneous orthotropic, axisymmetric shell elements positioned along the carcass mid-ply surface (Figure 2-15) to calculate the contact pressure distribution.

The contact pressure distribution calculated from the

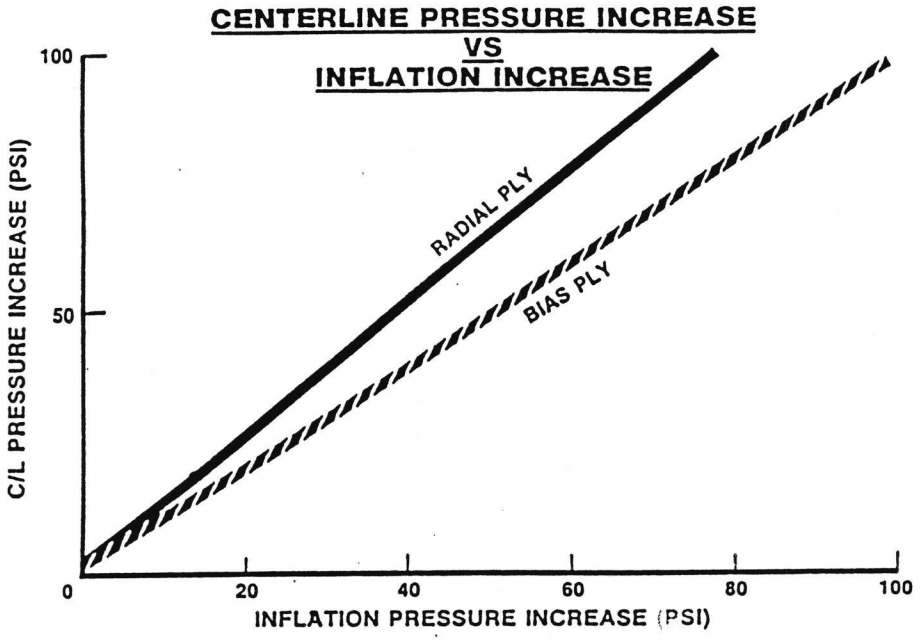

Figure 2-14. Centerline Pressure Increase vs. Inflation Increase (Ford [4]).

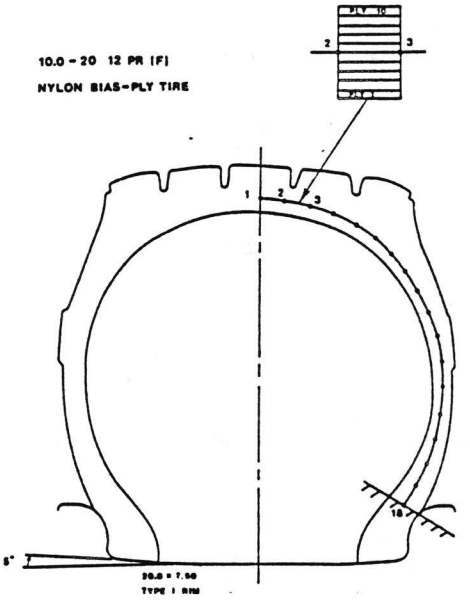

Figure 2-15. Assembly of Finite Element Modelling of Truck Tire (Tielking [7]).

Tielking model was similar to the findings reported by Pedro Yap [6]. The maximum contact pressure calculated from the Tielking tire model is almost double the inflation pressure. T.L. Ford [4] reported similar results with a maximum of contact pressure/inflation pressure ratio of 1.95.

2.4 Pavement Responses to Higher Tire Pressure.

Several studies [8,10,11,15,16,17,25] have indicated that high tire pressures affect pavement performance. The effects are reported to be especially significant on thin pavement structures. Craus et al [8] investigated the effects of contact pressure (inflation pressure) on the fatigue behavior of various flexible pavement configurations. The pavement and contact (tire) pressure variations studied are shown in Figure 2-16. The fatigue response of the AC was modeled using the relationship developed by Finn [9] for fatigue cracking occurring over 10 percent of the pavement surface area:

$$\log N_f = 15.947 - 3.291 \log e_t - 0.854 \log E \quad \text{[Eq. 2-5]}$$

where,

N_f = number of load applications to produce up to 10 percent cracking.

e_t = maximum tensile micro strain on the underside of asphalt bound layer, in. per in.

E = complex modulus of asphalt concrete, ksi.

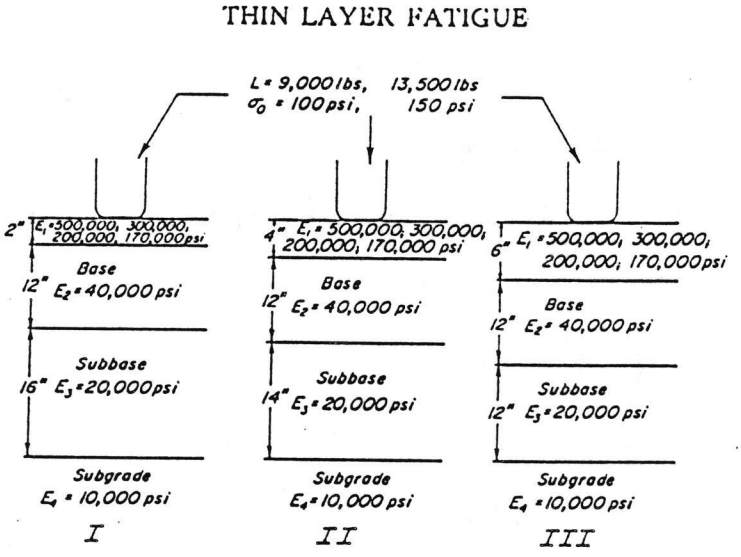

Figure 2-16. Pavement Detail in Craus et al Study (Craus [8]).

The maximum tensile strains were predicted using the elastic layer theory.

In investigating the effects of load and contact pressure on fatigue life of the AC pavement, Craus et al found that a 50 percent increase in contact pressure reduced the fatigue life of a 2", 6", and 10" AC layer by 85%, 40 %, and 20% respectively. The higher reductions in fatigue life of the thinner AC layers clearly show that thin AC pavements (thickness less than or equal to 4 ") are more severely affected by higher contact pressure than are thick pavements. For thick AC layer, load increase was found to be more significant than contact pressure increase in reducing the fatigue life of a pavement.

In addition, Craus et al reported that a reduction in the resilient modulus of the base, subbase, and subgrade had a very strong influence on the fatigue life of the pavement, especially in thin pavements. Craus et al concluded that thin AC pavements should be designed with an asphalt mix having low stiffness modulus; and thick AC pavements should be designed with a high stiffness asphalt mix. Although they did not find much influence due to base and subbase thickness, they recommended that both courses should have high resilient moduli.

Saraf et al [10] studied the effect of tire pressure and load on pavement performance using a pavement analysis program (TEXGAP-3D) that could model a non-uniform tire-

pavement contact pressure. They used a pressure sensitive film and a pressure/color intensity optical converter to measure the non-uniform tire contact pressure. The measured values were used as input to the pavement analysis program. They also used a standard elastic layer program (ELSYM5) that assumes a uniform contact pressure typically equal to the tire inflation pressure.

The variables considered in their analysis were AC thickness (1.5", 2", 3", and 4"), wheel load (4,500 lb and 5,400 lb), and inflation pressure (75 psi, 90 psi, and 110 psi). They reported that by maintaining the wheel load at 4,500 lb and increasing the inflation pressure from 75 psi to 110 psi, the ELSYM5 (uniform pressure) analysis showed a 69.3% increase in the critical tensile strain for the 1.5" AC layer and a 41.8% increase for the 4" thick AC layer. By comparison, the TEXGAP-3D analysis (non-uniform pressure) showed increases of 32.6% and 8.8% for the 1.5" and 4" thick AC layer respectively. The increased inflation pressure showed only minimal effect on the compressive strain at the top of the subgrade. Both analyses showed that the compressive strain increased by only 2.2% for the 1.5" layer and 1.6% for the 4" layer.

Roberts et al [11] investigated the effect of increased tire pressures on low-volume flexible pavements (1" to 4" thick AC layer on a 8" thick granular base) using non-uniform contact pressures. The contact pressures were not

measured. They were predicted using a finite element computer model developed by Tielking [7]. The predicted pressures were used as input to a modified ILLIPAVE program (a finite element pavement analysis program). They concluded that high tire pressures result in a pavement life reduction. Based on their investigation, they discouraged the construction of 1" to 3" thick AC surfaces. Their analyses showed that high tire pressures produce the greatest increase in tensile strains at the bottom of AC surfaces in this thickness range. They recommended that pavements should be designed as "thin and flexible" or "thick and stiff."

Thompson [12], on the other hand, studied the effect of high tire pressure on thick flexible pavements. He used three uniform pressures (80 psi, 100 psi, and 120 psi) and a circular wheel-load of 9 kip as input to the ILLIPAVE model. He reported that AC strains increased nonlinearly with the contact pressure increases. Pavements with thicker AC layers and stiffer moduli were found to be less affected by the contact pressure increases. For example, a 12" full-depth AC with moduli of 200 ksi and 500 ksi experiences a tensile strain increase of less than 6% for a 50% increment in contact pressure.

Thompson also noted that high contact pressures do not significantly affect subgrade deviator stresses in thick AC pavements. For a 6" full-depth pavement having a moduli of 200 ksi, a 50% increase in contact pressure produced a 17%

increase in deviator stress. With an AC modulus of 500 ksi, the deviator stress increase was only 6%.

Thompson also reported that surface deflections and subgrade compressive strains are not sensitive to contact pressures. The most affected pavement sections, 6" full-depth AC with moduli of 200 ksi and 500 ksi, produced approximately 11% compressive strain increase for a 50% increase in contact pressure.

In comparing both F.L. Roberts and M.R. Thompson's reports, one notices how the thickness of the AC layer affects the pavement response to high contact pressures. While Roberts found high contact pressures severely detrimental to thin AC pavements, Thompson suggests that high contact pressure is not a significant concern in the design of thick AC pavement.

Patterson [13] examined the effect of contact pressure on fatigue distress in untreated and cement-bound layers. He concluded that on thin asphalt pavements with untreated bases high contact pressure influences performance more than increased wheel loads.

Eisenmann and Hilmer [14] carried out both laboratory tests and theoretical pavement analyses to investigate the effect of both wheel load and inflation pressure on the rutting behavior of asphalt pavements. A wheel tracking test system was set up for laboratory dynamic rolling tests. Both single and dual radial bias tires were tested under a con-

trolled summer environment.

The wheel-loads for the single and dual tires ranged from 7.1 kip to 10.2 kip and 7.1 kip to 10.3 kip respectively. The inflation pressures for the single tire ranged from 116 psi to 180 psi, and the dual tires ranged from 116 psi to 160 psi. The net contact area was measured from the inked tire footprint, and the average contact pressure was obtained by dividing the wheel-load by the net contact area. The average contact pressure was used as input for theoretical analyses using the BISAR elastic layer program.

From the results of both laboratory and theoretical analyses, Eisenmann and Hilmer observed that increase in axle load caused rutting at the bottom of the pavement, while increase in contact pressure caused rutting near the AC layer. They concluded that the main mechanism of rutting is shear deformation, not material densification. They indicated that rutting is a flow phenomenon and not compaction of the different layers.

Haas and Papagianakis [15] used the elastic layer program ELSYM5 to investigate the effect of tire pressure and wheel-loads on an 8" Full-Depth AC pavement. Pavement rutting was estimated by using the sum of the compressive strains of each layer in the pavement. They reported that increased wheel loads causes significant increases in tensile strains at the bottom of the AC layer and compressive strains at the top of subgrade but no changes to the com-

pressive strains near the surface of the AC layer. However, by increasing the inflation pressure, the compressive strains near the surface increase significantly. The Haas and Papagianakis analysis suggests that to study the rutting effect caused by high tire pressure, the traditional critical location (i.e. the top of the subgrade) is no longer the only location to be considered. A complete evaluation of rutting caused by high tire pressures must include detailed analysis near the top of the AC layer.

Sebaaly and Tabatabaee [16] presented perhaps the most comprehensive study of the tire pressure effect on pavement performance. Three different types of tires were used in their study - an 11R22.5 dual radial, an 11-22.5 bias ply, and a 385/65R22.5 wide base radial single tire. Each was subjected to three inflation pressures (bias ply - 75, 100, 125 psi ; radial - 80, 105, 130 psi) and three wheel-loads (10, 17, and 22 kips). The tire inflation pressures were selected to reflect the past average pressures, the present average pressures, and the present maximum pressures. The inflation pressures and wheel-loads ranged from 75 to 130 psi and 10 to 22 kips respectively. Asphalt thicknesses ranged between 2" and 8" over an 8" granular base.

A moving, flat bed machine equipped with strain gages was used to measure the non-uniform contact pressures of slow moving tires. Sebaaly and Tabatabaee observed that none of the contact pressures measured exceeded 1.75 times the

tire inflation pressure. For pavement analysis purposes, a modified BISAR elastic program capable of accepting non-uniform contact pressure was used.

Similar to other tire pressure studies, Sebaaly and Tabatabaee employed the fatigue and rutting response parameters defined in the Finn's study. The responses evaluated were the tensile strains at the bottom of the asphalt layer for fatigue analyses, deflections at the surface of the asphalt layer, and the compressive stresses at the top of the subgrade for the rutting analyses.

The significance of high tire pressure on thin asphalt pavement performance was clearly established in their research. For a 2" thick AC layer, they reported that an axle load of 10,000 lb with an inflation pressure of 130 psi is more damaging than an axle load of 17,000 lb axle load with an inflation pressure of 80 psi. Similarly, a 17,000 lb axle load and 130 psi pressure was found to be more damaging than a 22,000 lb load and 80 psi pressure. They also reported that increasing the inflation pressure of the wide base single tire from 130 psi to 145 psi causes the AC tensile strains due to a 20000 lb load to increase 40 percent. Their findings concur with those of other investigators in that high tire pressure has a more pronounced effect on thin AC pavements than on thick AC pavements.

Hudson and Seeds [17] conducted a comprehensive study directed towards developing a modified flexible pavement

design process that accounts for the effects of higher tire pressures. They evaluated truck traffic data in Arizona, and used elastic layer analyses to study the effect of increased inflation pressures. The pavement responses to two different axle loads, 18 kips and 28 kips, and to inflation pressures ranging from 70 psi to 160 psi at 10 psi increments were analyzed.

Figure 2-17 shows the responses of several important pavement distress parameters to varying inflation pressures at a constant 18 kip load. The Figure indicates that horizontal tensile strain and shear strain at the bottom of the AC layer increase with inflation pressure but that the vertical pressure at the top of the subgrade remains fairly constant. They concluded: "The implication is that tire pressure increases may affect the surface layer in terms of reduced fatigue life, increased surface rutting, or increased roughness but that there is very little effect in terms of pavement damage attributable to vertical strain on the roadbed soil."

Hudson and Seeds studied the effects of inflation pressures of 90 psi and 120 psi. These were identified as being the lower and upper limits of tire pressures that formed 90% of the tire pressure distributions measured in the Arizona survey. They reported that this 35% increase in inflation pressures produces 38% reduction in fatigue life of the pavement. The fatigue effect was estimated using

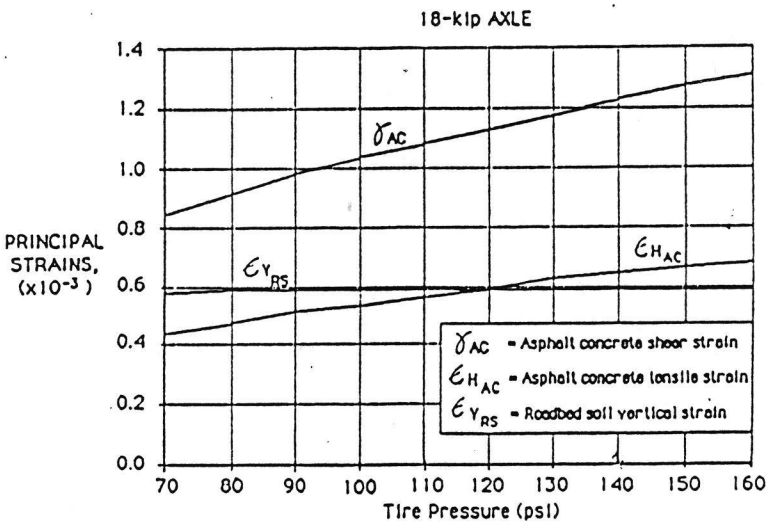

Figure 2-17. Plot of principal strain in the pavement structure vs. tire pressure from ARE Inc. study (Hudson and Seeds [17]).

Finn's equation (see Eq. 2-5).

Finn's equation was derived from the analysis of AASHO Road Test data in which bias ply tires were used with an inflation pressure of approximately 75 psi. To present more insight into the effect of high tire pressure, a comparison to the 75 psi pressure should be made. Even though the use of uniform pressures and ELSYM5 may not accurately reflect the actual pressure distribution shape and material behavior, Hudson and Seeds research provides support that tire pressure changes should be considered in the design process.

Bonaquist et al [18] studied the effect of wheel load, tire pressure, and tire type on an AC pavement at the Federal Highway Administration (FHWA) Pavement Testing Facility (PTF) using the Accelerated Loading Facility (ALF). ALF is a test machine capable of applying a large number of moving wheel loads to a pavement in a short time. The load applied can range from 9,400 lb to 22,500 lb. The pavement tested had a 2" AC wearing course, a 5" AC binder course, and a 12" granular base course. Thermocouples, moisture cells, strain gages, and a surface deflection measuring devices were placed at various depths within the pavement section to record the responses of the pavement under load. The loading conditions included two types of tires (radial and bias), three different axle-loads (9,400 lb, 14,100 lb, and 19,000 lb), and three different inflation pressures (76 psi, 108 psi, and 140 psi).

The data collected in the Bonaquist et al study included tire contact area, surface deflection, surface strain, strain at the bottom of the asphalt layer, and pavement temperature. Bonaquist et al reported that the measured contact areas were larger than the computed contact area by 12 to 58 sqi. However, the measured contact areas were the gross areas. A better representation of average contact pressures should include measurements of the net contact areas.

Bonaquist et al also performed a sensitivity analysis on the data using ELSYM5. Table 2.1 illustrates the results of the ELSYM5 analysis for critical pavement responses at the center of one of the dual wheels. The analysis shows that the effect of higher tire pressure is mostly confined to the AC surface layer. From Table 2.1 it is observed that pressure does not affect the vertical stress at the top of the subgrade. The results from the ELSYM5 analysis indicate that, in contrast with all other critical responses, the vertical compressive stresses within the asphalt layer are influenced more by contact pressure than by load (Figure 2-18). Since vertical compressive stresses is considered to be a rut prediction parameter, it can be concluded that high pressure contributes to rutting distress of AC pavement.

Bonaquist et al compared the values of tensile strains at the bottom of the AC layer computed with ELSYM5 and the field measured values. They reported that wheel-load plays a

TABLE 2.1 EFFECT OF TIRE PRESSURE ON CRITICAL PAVEMENT RESPONSES AS DETERMINED BY BONNAQUIST [18].

	Tire Pressure, psi		
Pavement Response	76	108	140
Surface Deflection	.0381"	.0396"	.0411"
AC Radial Microstrain	482	544	588
Vertical Stress on Base	24 psi	27 psi	28 psi
Vertical Subgrade Stress	8 psi	8 psi	8 spi

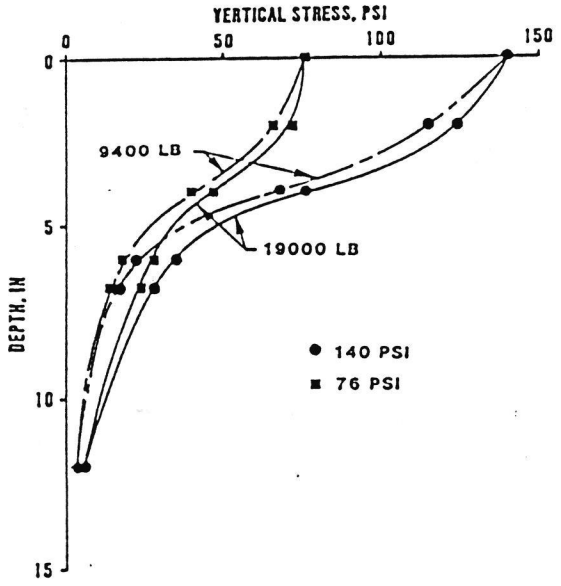

Figure 2-18. Effect of load and contact pressure on vertical stress based on ELSYM5 (Bonaquist [18]).

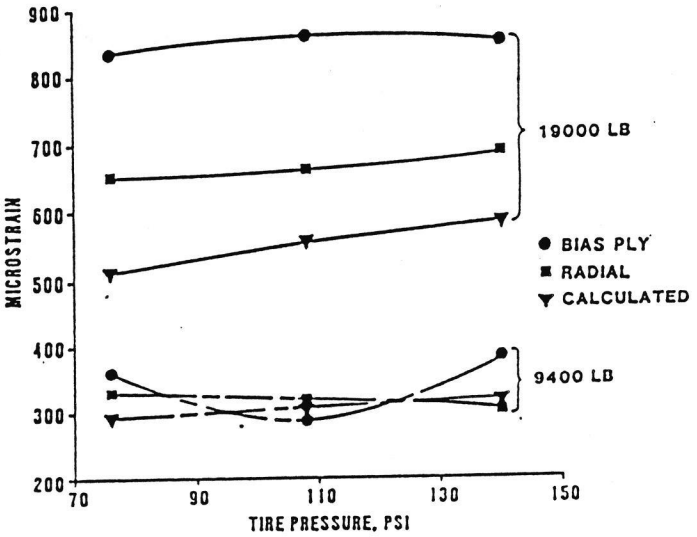

Figure 2-19. Effect of Load, Tire Pressure, and Tire Type on Longitudinal Strain at the Bottom of the Asphalt Layer (Bonaquist [18]).

more significant role in fatigue cracking than does higher tire pressure (Figure 2-19). This conclusion is compatible with the conclusions of other researchers in that the pavement being studied is a thick asphalt pavement having a 7" surface.

Although Bonaquist et al's report is based on an evaluation of field measurements, it's findings must be treated with caution because of the lack of environmental controls in their testing. For example, one section of the pavement was tested from January to June 1987 when the pavement temperature was low. Another section of the pavement was tested in October when the pavement temperature was higher.

2.5 Proposed Design Procedure Modifications

Hudson et al suggested modifications to ESAL factors in order to solve the rutting and fatigue cracking distress associated with high tire pressures. Hudson et al used ELSYM5 and the data from the AASHO Road Test among several other criteria in deriving a mechanistic damage model relating number of pavement loadings to pavement failures. The mechanistic damage model was then used to formulate a new set of 18-kip ESAL factors comprising the effects of load, load configuration, and tire pressure. The equivalence factor was calculated as the ratio of the allowable 18-kip single axle load at 75 psi tire pressure, to the allowable load applications at different load, load configuration, and

tire pressure:

$$e_{x/c/p} = (N_f)_{18/1/75} / (N_f)_{x/c/p}$$

where,

$e_{x/c/p}$= Equivalence factor for x-kip applications, c axle configuration, and p tire pressure.

$(N_f)_{18/1/75}$= Allowable 18-kip applications, single axle load, and 75 psi tire pressure.

$(N_f)_{x/c/p}$ = Allowable x-kip load applications, c axle configuration, and p tire pressure.

Hudson et al used two sets of damage models to derive the equivalence factors. The first set of models were developed for pavement of 3" and 6" surface thicknesses, using the critical tensile strain (fatigue transfer function) at the bottom of the AC layer as the response parameter. The second set of models for thin surface treatments were developed with the critical vertical strain (rut transfer function) at the subgrade as the response parameter. Table 2.2 shows the comparison of AASHTO and ARE Inc. ESAL factors. ARE Inc. equivalence factors refer to factors generated by Hudson et al's mechanistic damage models.

The Hudson et al's approach to solving the problem of high tire pressure by modifying (in most cases, increasing) the ESAL does not appear to be the appropriate solution. An increase in the ESAL means an increase in 18 kip ESAL applications. Looking back at the AASHTO design equation [Eq. 2-

TABLE 2.2 COMPARISON OF LOAD EQUIVALENCY FACTORS DETERMINED BY HUDSON WITH THE AASHTO ESAL FACTORS [17].

Axle Load	AASHTO (75 psi)	Hudson et al Equivalency Factors (75 psi)	(110 psi)	(145 psi)
4 kips	0.003	0.0026	0.0060	0.0096
10 kips	0.102	0.1446	0.5555	1.2790
18 kips	1.000	1.0000	5.2950	15.5170
30 kips	6.800	6.9700	25.3000	90.1000
50 kips	60.000	60.5000	236.9000	427.7000

P_t = 2.5 and SN = 4.0

2], an increase in the left term of the equation will result in an increase in the SN, other factors being constant. That implies either an increase in the total pavement thickness or an increase in the thickness of certain layer while maintaining the same total pavement thickness. However, the effect of high tire pressure is more localized to the surface layer, especially for thick AC pavement. In fact, Hudson et al wrote:

> **"The implication is that tire pressure increases may affect the surface layer in terms of reduced fatigue life, increased surface rutting, or increased roughness but that there is very little effect in terms of pavement damage attributable to vertical strain on the roadbed soil."**

Thus, increased pavement thickness may increase fatigue life of the pavement but will not solve the more likely problem caused by high tire pressure - rutting in the surface layers.

2.6 Asphalt Mix Modifications and Higher Tire Pressures.

Rutting occurs in many different ways: i) shear deformation which is a flow phenomenon, ii) densification of pavement layers, and iii) loss of surface material due to use. Of these, shear deformation appears to be the major form of rutting in the AC layer due to the nature of its composition.

Since shear deformation is the major form of rutting in

the AC layer, it is important to understand the factors that influence the shear resistance properties of the AC layer. Shear stress is described as a function of material characteristics (mixture properties), environment (temperature), load (gross load and tire contact pressure), and pavement structural geometry (layer characteristics and thickness). On the other hand, the shear strength of AC is a function of several properties of the mixture including aggregate and binder characteristics, and voids content (on-site) of the mixture. Pavlovich and Shuler [23] noted that some AC mixtures exhibit strengths much in excess of applied stress whereas other mixtures show significantly lesser strength than imposed shear stress. They hypothesized that mixture properties or structural geometries can be appropriately designed to accommodate present and predicted high pressure tire loads.

E.R. Brown [24] reported several factors that relate high tire pressure and heavy axle load to premature AC rutting. One of the factors identified is an excess of asphalt cement which is mainly due to inadequate laboratory compaction during mix design. The Marshall method of sample preparation (50, or 75 blows) may result in sample density that is significantly lower than the ultimate field density given the loading condition (high tire pressure and heavier axle load) that the pavement faces today. Higher compactive effort, and not higher asphalt content nor higher filler

content, should be exercised to produce AC field density that conforms to specifications. Brown also proposes the possibility of using larger size aggregate (> 3/4 ") and closer monitoring the amount of minus No. 200 materials in the mix to provide better mixture stability.

The type, shape, size, and texture of the aggregates used affect the shear resistance of the AC. Crushed aggregate has better bonding with asphalt, resulting in better mix stability through increase resistance to flow. Presently, there is indication that natural sand in the mix reduces the performance of AC pavement. Present AHTD specifications limit the use of natural sand to 15% in mix design. Wong [27] reported that mixtures with Donafil, a very angular, manufactured sand, have better rutting resistance than mixtures with natural sand in both static and dynamic loading tests.

Kim et al [25], instead of modifying the ESAL, concentrated on reviewing the asphalt mix design criteria to solve severe wheel track rutting associated with high tire pressures. They contend that both the empirically based Marshall and Hveem mix design methods are obsolete and inadequate due to the increase in traffic loads, tire pressures, and number of trucks. They investigated the Hveem mix design process used by the Oregon State Highway Division by evaluating the rutting potential of AC specimens. Aggregates for these AC specimens were obtained from four different sources. Speci-

mens with six different aggregate gradations, including the Fuller's maximum density gradation, were tested in a simple creep test. Among several conclusions they made are: i) Hveem stability has little relationship with creep stiffness - mixes with high Hveem stability value do not always resist creep deformation better than mixes with low Hveem stability, ii) Creep stiffness decreases with an increasing percentage of aggregate passing No. 200 sieve, and controlling the amount of material passing No. 200 clearly improves the deformation resistance of the mix, and iii) using one percent lime slurry results in some improvement in creep stiffness.

CHAPTER 3

TRUCK TIRE SURVEY

In the summer of 1988, AHTD conducted a survey of truck tire pressures in Arkansas. Tire pressures were measured on 488 trucks at 19 locations (Table 3.1) in the state. The locations ranged from interstate highways to relatively low volume local state highways. The purpose of the survey was to determine: 1) whether the tire pressures and types on Arkansas trucks were similar to those reported in other states and 2) whether the pressures differed by highway type or area within the state.

The data collected included the tire size, inflation pressure, temperature, vehicle class, state license plate, type of commodity and trip, and air and pavement temperatures. A statistical analysis of the data was performed to obtain information regarding the distribution of tire types and tire pressures in the state of Arkansas. Table 3.2 shows the results of the analysis. Figure 3-1 and Figure 3-2 show the tire pressure distributions of bias ply and radial tires found from the truck tire survey. Figure 3-3 and Figure 3-4 show the cumulative pressure distributions of bias ply and radial tires from the truck tire survey.

Seventy-two percent of the tires surveyed were of radial construction, and 28% were of bias ply construction.

TABLE 3.1 TRUCK TIRE SURVEY LOCATIONS.

Location	Highway	Region	Survey Date
1. Mayflower	I-40W	Central	6/14/88
2. Lonoke	I-40E&W	Central	6/15/88
3. Benton	I-30E&W	Central	6/16/88
4. Thornton	US 167	South	6/20/88
5. Fordyce (South)	SH 274	South	6/21/88
6. Leola	SH 46	South	6/21/88
7. Mena	SH 8	West	6/23/88
8. Harrison Weight Station (US)		North West	6/27/88
9. Alpena	SH 68/21	North West	6/28/88
10. Fayetteville	US 71N&S	North West	6/28/88
11. Springdale	SH 68/45	North West	6/29/88
12. Brashears	SH 16	North West	6/29/88
13. Mt. Pine	SH 227	West	7/1/88
14. Lake Village	US 65	South East	7/5/88
15. Huttig	SH 129	South	7/6/88
16. Lewisville	SH 29S	South West	7/7/88
17. Batesville Wt. Stn.	US 167	North	7/11/88
18. -----	SH 14 & SH 373	North East	8/13/88
19. Jonesboro (North)	US 29	North East	-----

TABLE 3.2 SUMMARY OF AHTD TIRE PRESSURE SURVEY.

Tire Type	# Tires	% Total	Pressure, psi Max*	Mean	Min	Std. Dev.
1. All Axles Combined.						
Bias	545	28	160*	93.0	28	21.1
Radial	1423	72	160*	105.2	30	14.9
2. Front Axles Only.						
Bias	128	--	148	88.6	40	20.7
Radial	354	--	160*	107.5	60	14.5
3. Drive Axles Only.						
Bias	252	--	160*	92.9	30	22.0
Radial	622	--	160*	103.9	32	14.4
4. All Axles Except Front and Drive.						
Bias	165	27	160*	96.6	28	19.4
Radial	447	73	160*	105.1	30	15.9

* Pressures in excess of 160 psi could not be measured.

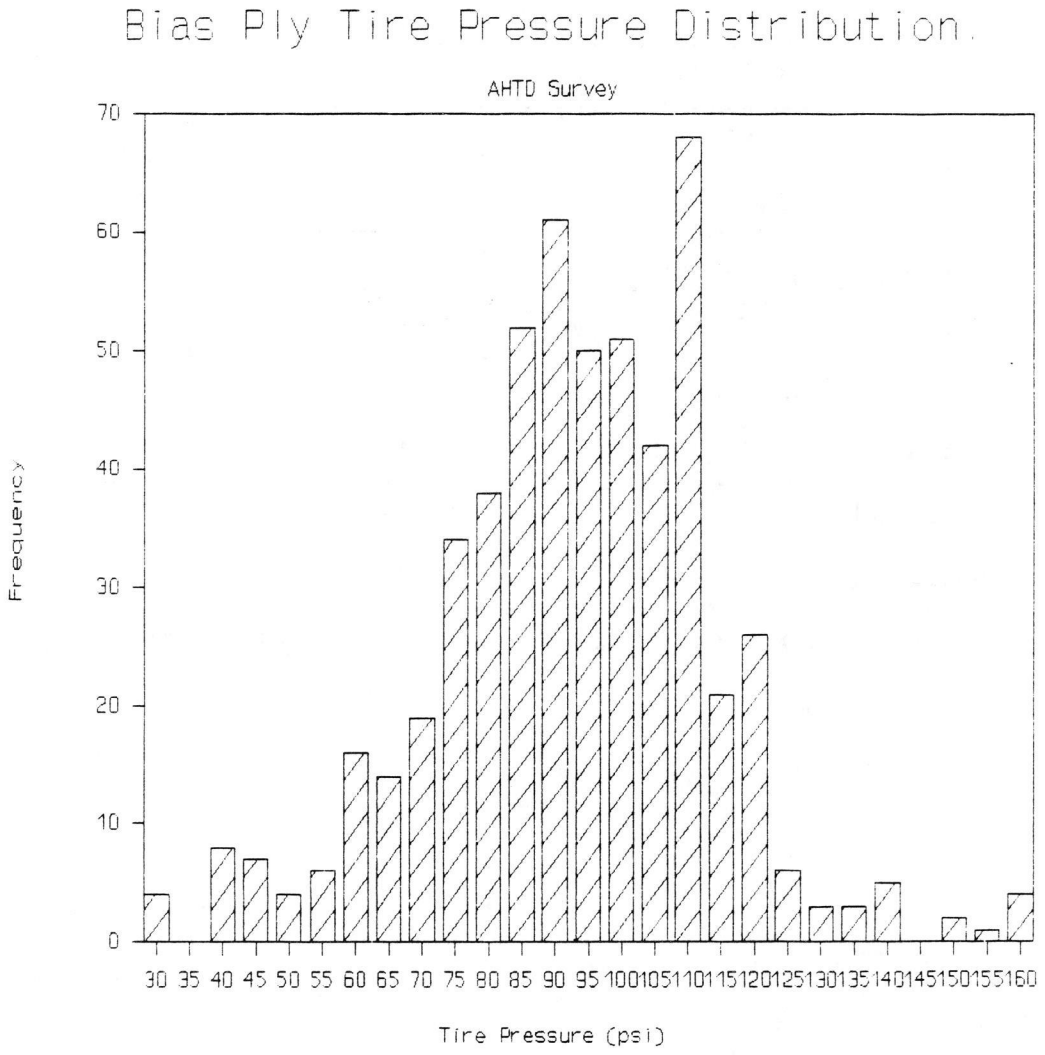

Figure 3-1. Distribution of Bias Ply Tire Pressures.

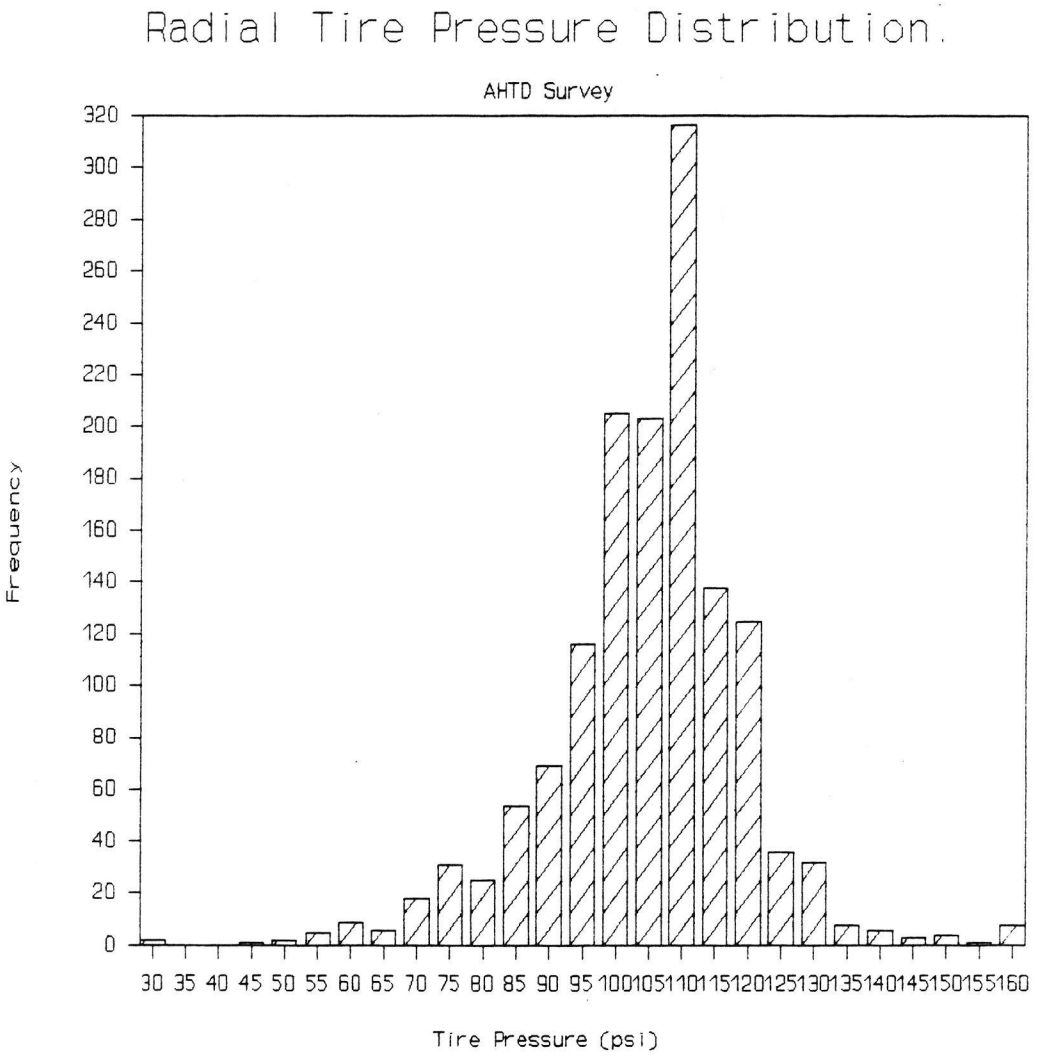

Figure 3-2. Distribution of Radial Tire Pressures.

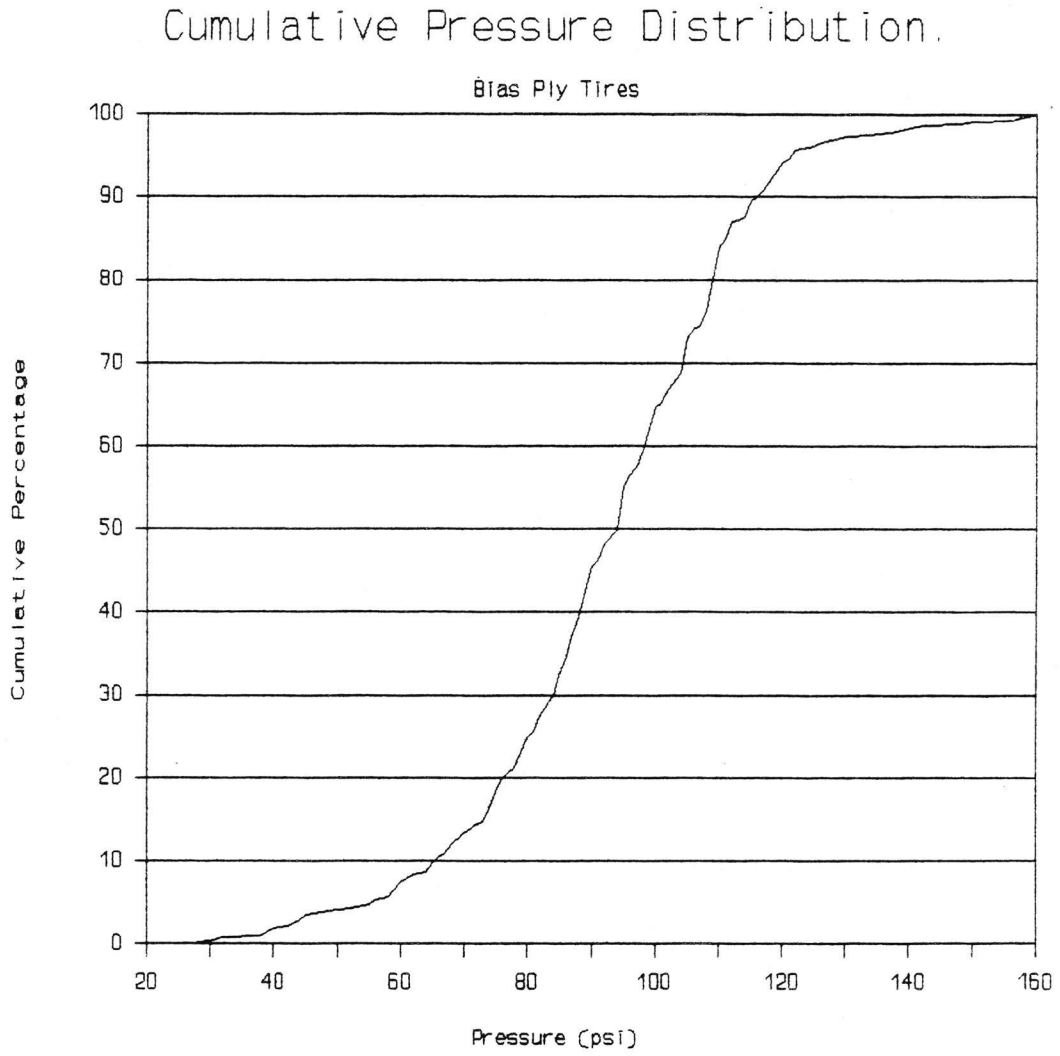

Figure 3-3. Cumulative Distribution of Bias Ply Tire Pressures.

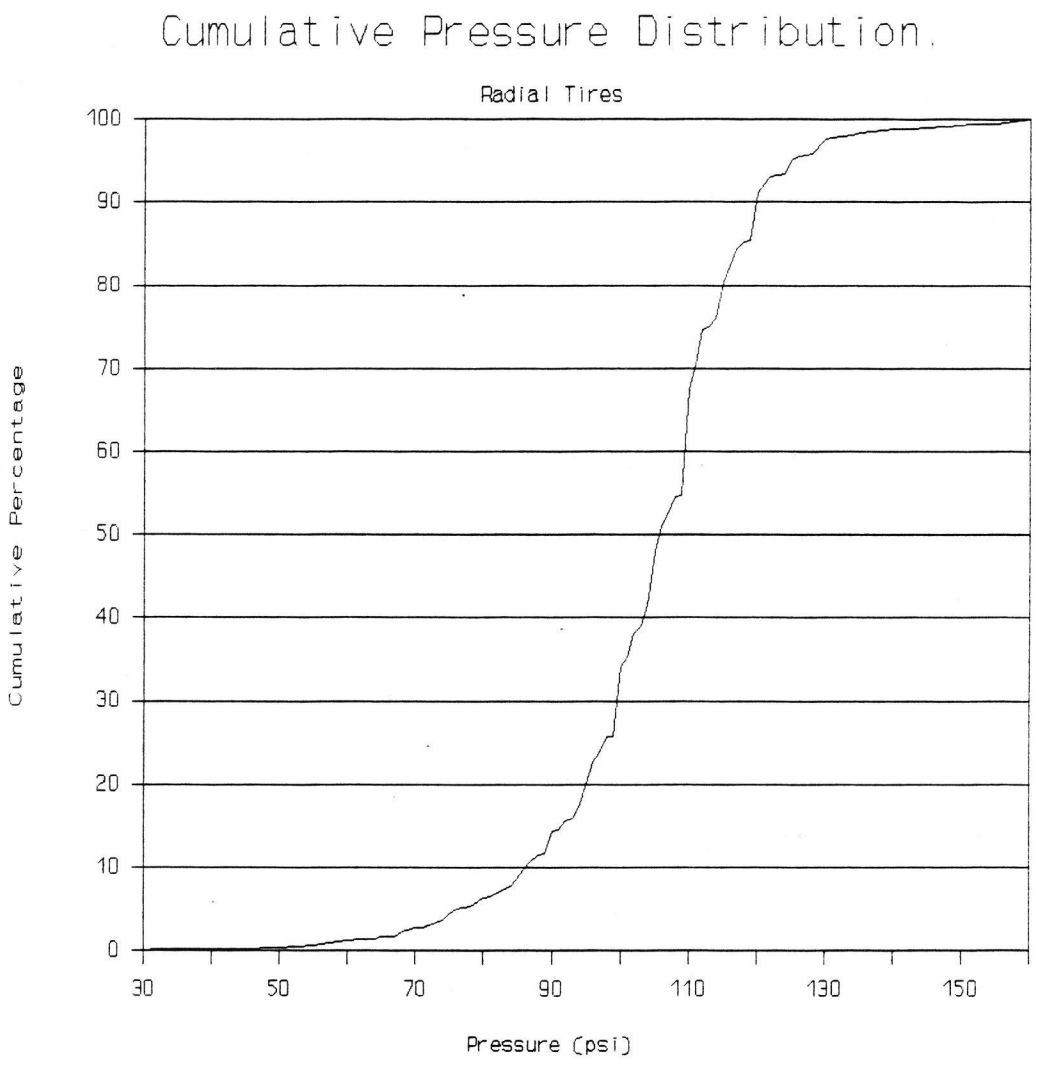

Figure 3-4. Cumulative Distribution of Raidal Tire Pressures.

The average measured inflation pressure for bias ply and radial tires were 93.0 psi and 105.2 psi respectively. About one percent (radial and bias ply combined) of the measured inflation pressures were in excess of 160 psi. Six percent of the bias ply tires measured and nine percent of the radial tires measured were in excess of 120 psi inflation pressure.

The results from the statistical analyses also showed some variations in tire pressure distributions and tire types either according to highway or regional classifications (Table 3.3). Radial tires were more widely used on all types of highways and were more highly inflated than bias ply tires. However, in some regions bias ply tires are still widely used on state highways. The average radial tire pressures computed according to both highway and regional classifications were in the range of 86 to 110 psi, whereas the computed average bias ply tire pressures were in the range of 72 to 102 psi. Table 3.3 shows that the average tire pressures (radial and bias ply tires) measured in the northeast region were significantly lower than those measured in other regions (e.g. for radial tires 93 psi vs. 99 psi in the next lowest region).

A similar survey of trucks in Arizona revealed that 83% were using radial tires and that the average radial tire pressures was 105.9 psi for the front axles [17]. Another survey conducted by the Oregon Department of Trans-

TABLE 3.3 TIRE PRESSURE DISTRIBUTIONS BY REGION AND HIGHWAY CLASSIFICATIONS.

		Radial		Bias Ply	
		%	Pressure	%	Pressure
Central	Interstate	84	109.0	16	101.7
	U.S. Highway	--	-----	--	-----
	State Highway	--	-----	--	-----
	All	84	109.0	16	101.7
South	Interstate	--	-----	--	-----
	U.S. Highway	84	106.5	16	100.3
	State Highway	54	102.9	45	97.1
	All	63	104.3	37	97.5
West	Interstate	--	-----	--	-----
	U.S. Highway	--	-----	--	-----
	State Highway	55	99.0	45	91.9
	All	55	99.0	45	91.9
No. West	Interstate	--	-----	--	-----
	U.S. Highway	79	106.8	21	93.3
	State Highway	71	103.1	29	91.3
	All	75	105.0	25	92.1
So. East	Interstate	--	-----	--	-----
	U.S. Highway	65	103.5	35	82.8
	State Highway	--	-----	--	-----
	All	65	103.5	35	82.8
So. West	Interstate	--	-----	--	-----
	U.S. Highway	--	-----	--	-----
	State Highway	72	102.2	28	84.8
	All	72	102.2	28	84.8
North	Interstate	--	-----	--	-----
	U.S. Highway	78	109.6	22	98.7
	State Highway	--	-----	--	-----
	All	78	109.6	22	98.7
No. East	Interstate	--	-----	--	-----
	U.S. Highway	86	85.9	14	72.0
	State Highway	58	96.1	42	79.9
	All	64	93.2	36	79.2

portation (ODOT) indicated that 87% of the tires measured were of radial construction and that the average measured tire pressures (hot) of radial and bias tires were 102 psi and 82 psi respectively [26].

Results from other surveys conducted in Texas, New Mexico, and Florida also showed that current tire pressures average between 105 psi to 110 psi with a range of 40 to 150 psi. Those surveys also indicated the diminishing use of bias ply tires.

These surveys confirmed that radial tires have replaced bias ply tires as the common truck tire type and tire inflation pressures have increased significantly from 80 psi to an average of about 105 psi over a period of about 30 years.

Based on the results of the AHTD truck tire survey, it was concluded that tire pressures and tire types used on Arkansas highways are similar to those reported in other states. The AHTD truck tire survey showed some variations in tire pressure distributions and tire types either according to highway classification or regional classification. Truck tire pressures were lower in the northeast region, and bias ply tires were widely used on state highways.

CHAPTER 4

LABORATORY MEASUREMENT OF CONTACT PRESSURE

A common assumption in most pavement analyses is that the tire to pavement contact pressure is uniform and equal to the tire's inflation pressure. In fact, the actual distribution of contact pressure is neither uniform nor equal to the inflation pressure. The shape and magnitude of the distribution depend on variables such as tire pressure, axle load, tire type, and tire condition. At the start of this study only a limited amount of measured contact pressure data was found in the literature. To augment these data, laboratory tests were conducted to measure the net contact area and contact pressure of a radial tire and bias ply tire. In certain cases, the tire contact pressure was found to be almost double the inflation pressure.

4.1 Test Frame.

The laboratory tests were conducted using a 100 kip MTS unit. To conduct the tests, a test frame (Figure 4-1) was constructed to hold the tire and to measure the contact pressures. The test frame had two main parts: i) top frame (to which the tire was mounted), and ii) bottom frame (which served as the tire contact surface and held the pressure measurement device). The top frame (Figure 4-2)

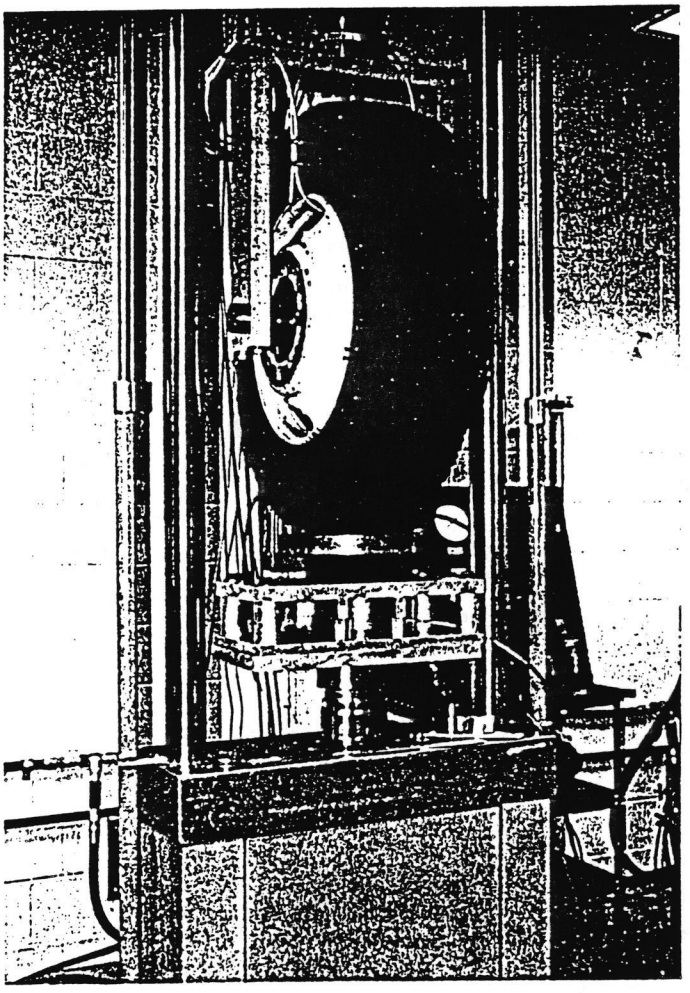

Figure 4-1. Contact Pressure Measurement Test Frame.

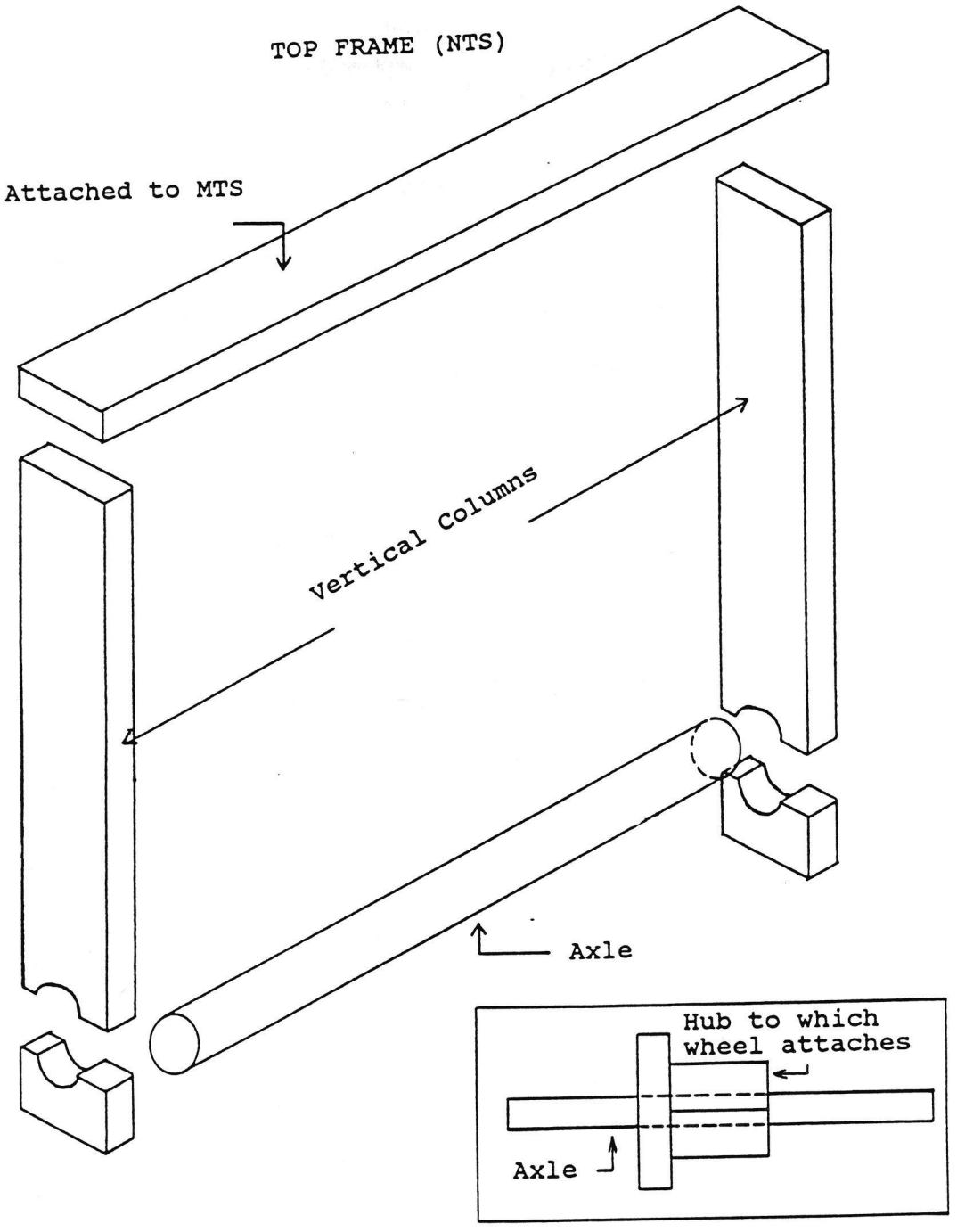

Figure 4-2. Top Frame for Contact Pressure Measurements.

consisted of a 3" diameter steel axle fixed to the tire with a square 6" x 6" steel box bolted to the tire rim. The two ends of the axle were attached to two vertical 2" x 6" aluminum bars, whose upper edges were held by a horizontal 2" x 6" aluminum bar. The top frame was attached to a 100 kip load cell which, in turn, was attached to the crosshead on the MTS load frame. The 100 kip load cell was used to control the load applied to the tire.

The bottom frame (Figure 4-3) consisted of two 24" x 12" x 1.5" aluminum plates separated by four 2.5" diameter, four inches high aluminum pillars. During testing, the tire was placed on the top plate and a load cell was placed on the bottom plate. Attached to the load cell was a 3/8" rod that extended through a hole in the top plate. The top of the 3/8" rod was adjusted flush with the surface of the top plate. The load exerted on the 3/8" rod was used as a measure of the contact pressure.

The holes in the top plate were spaced to permit contact pressure measurements at numerous locations in the contact area. One row of holes was located in the middle of the plate. The other two rows are located two and four inches from the middle row. A ball bearing was placed at the center in between the bottom plate and another plate attached to the MTS. This allowed the bottom frame to slide one inch backward and forward and one-half inch sideways so that the holes could be shifted to various locations under

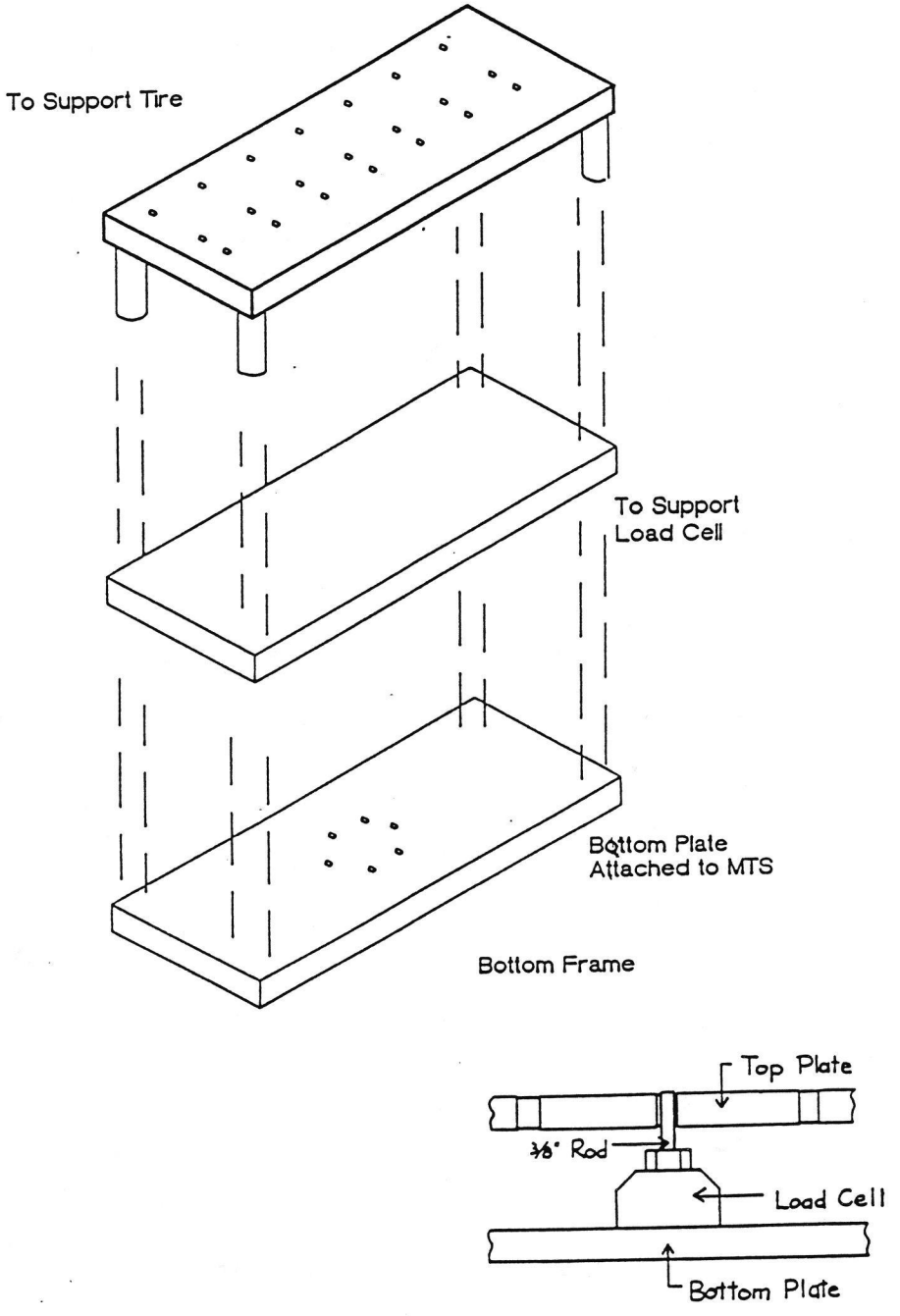

Figure 4-3. Bottom Frame for Contact Pressure Measurements.

the tire.

4.2 Contact Pressure Measurement

Tire contact pressure measurement was performed using the test frame described in Section 4.1. The purpose of contact pressure measurement was to obtain information regarding tire contact pressure distribution. The information obtained was used as input for ILLIPAVE pavement structural analysis.

4.2.1 Procedure in Setting Up the Tire

The following procedure was used in mounting and preparing the tire for contact pressure measurements.

1) Place the tire at the center of the axle.
2) Apply ink to the tread at the bottom of the tire (in the vicinity where contact is anticipated).
3) Place a 11" x 12" white posterboard on top of the bottom plate.
4) Move the bottom plate up, and load the tire to 6 kip.
5) Release the load by moving the bottom plate down.
6) After the ink on the posterboard has dried, superimpose a full scale transparency of the hole locations on top of the posterboard.
7) Count the number of holes that are in full contact with the tread.
8) Check whether the number of full contact holes can be

increased by rotating the tire.

9) If the tire is rotated, repeat steps 2 to 8.

10) After the exact position of the tire is determined, tighten all the nuts.

4.2.2 Procedure in Pressure Measurements

The following procedure was used in making the pressure measurements.

1) Apply ink to the bottom of the tire tread.
2) Take tire prints under wheel loads of 1 kip, 2 kips, 3 kips, 4 kips, 5 kips, and 6 kips.
3) Record the hole locations where full pin/tread contact is possible at each wheel load (use the full scale transparency).
4) Place the one kip load cell under a hole at which contact pressure is to be measured.
5) Insert the contact pin into the hole, and let it rest on top of the adjustable nut attached to the one kip load cell.
6) Stiffen the area surrounding the hole by inserting two sets of parallel bars and two pillars around the one kip load cell.
7) Adjust the top of the pin flush with the top plate. Use a smooth metal straight edge to check that it is flush.
8) Zero the reading for the one kip load cell, and then

start applying load on the top plate by moving up the bottom plate.

9) Increase the tire load in one kip increments until the maximum load (5 or 6 kips) is reached. Record the contact load on the one kip load cell (3/8" pin) at each full contact point (refer to step 3). The contact pressure is obtained by dividing the contact load by the area of the contact pin.

10) Repeat steps 7 to 9 three or four times.

11) Change hole location and repeat steps 4 to 10.

4.3 Accuracy of Test Frame

The accuracy of the contact pressure measurements was evaluated in three ways: i) by comparing the measured pressure with a "known" contact pressure, ii) by checking the repeatability of the results, and iii) by comparing the applied load to the load calculated using the pressure measurements and net contact area.

The "known" contact pressure was generated using a 10" x 6" x 3" rubber block having properties similar to the tire rubber. The block was placed on the top plate with a 1" thick steel plate on top of it. The tire was then lowered to the steel plate and a load applied. Because of the uniformity of the rubber and the stiffness of the steel plate above the rubber block, it was assumed that the contact pressure would be uniform. Thus, the "known" pres-

sure was obtained by dividing the total load applied by the area (10" x 6") of the rubber block.

The measured contact pressures, obtained according to the procedure (steps 4 to 11) described in 4.2.2, compared favorably with the "known" pressure (Figure 4-4). Table 4.1 shows that the maximum difference between the "known" pressure and the measured pressure was 20%, and that the measured pressures were larger than the "known" pressures. The differences occurred either due to the deflection of the top plate (bottom frame) or the intrusion of rubber into the contact hole.

The repeatability of the results was checked by performing two sets of tests using the radial tire at the same inflation pressure. Analysis of the test results indicated that the test frame produced repeatable results (Figure 4-5 and Figure 4-6) for most of the pin locations measured. The maximum differences between two readings were 52% and 27%, and the average differences were 13% and 11% for tire pressures of 80 psi and 120 psi respectively (Table 4.2).

The third method used to check the accuracy of the test frame involved the calculation of the products of measured pressures by the area (net) that each point represented, and then summing the products. The summation was compared to the total load applied. The comparison showed an error ranging from one to five percent.

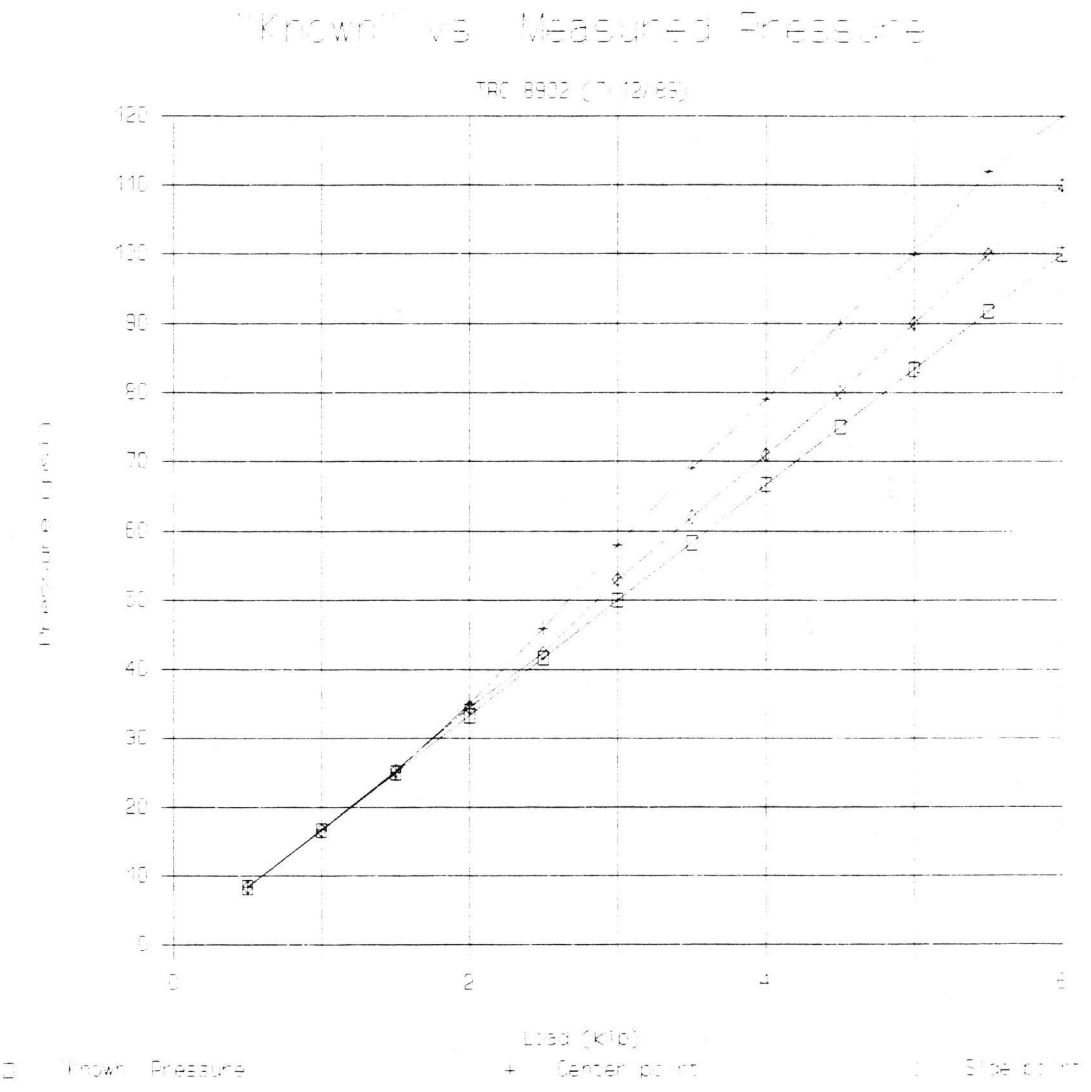

Figure 4-4. "Known" versus Measured Pressures.

TABLE 4.1 COMPARISON OF "KNOWN" AND MEASURED PRESSURES.

Load kips	"Known" Pressure psi	Measured Pressures Center psi	% Error	Edge psi	% Error
0.50	8.33	8.41	0.92	8.40	0.80
1.00	16.67	16.70	0.20	16.70	0.20
1.50	25.00	25.10	0.40	25.30	1.20
2.00	33.33	35.00	5.00	34.50	3.50
2.50	41.67	46.00	10.40	42.40	1.76
3.00	50.00	58.00	16.00	53.00	6.00
3.50	58.33	69.00	18.29	62.00	6.29
4.00	66.67	79.00	18.50	71.00	6.50
4.50	75.00	90.00	20.00	80.00	6.67
5.00	83.33	100.00	20.00	90.00	8.00
5.50	91.67	112.00	22.18	100.00	9.09
6.00	100.00	120.00	20.00	110.00	10.00

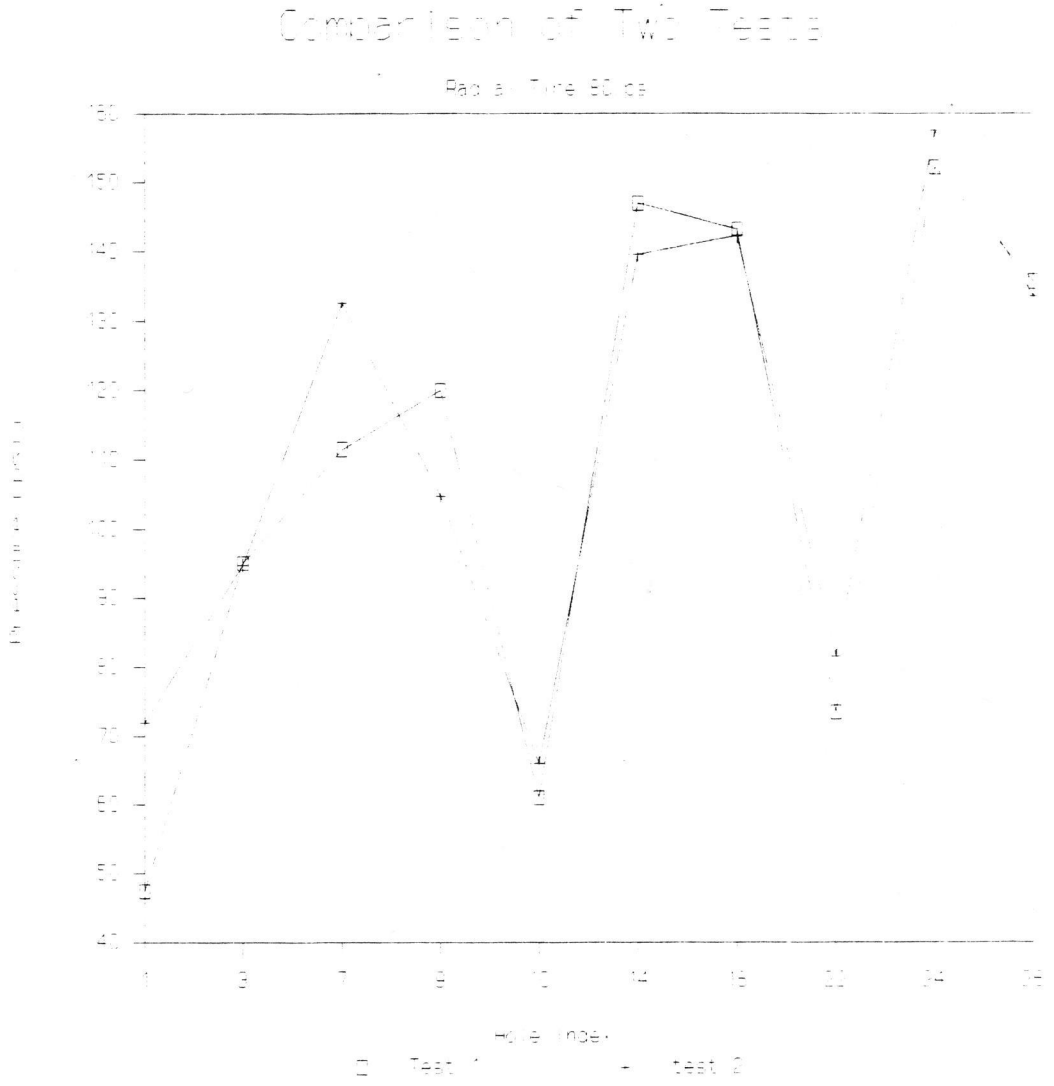

Figure 4-5. Comparison of Two Pressure Measurements at 80 psi.

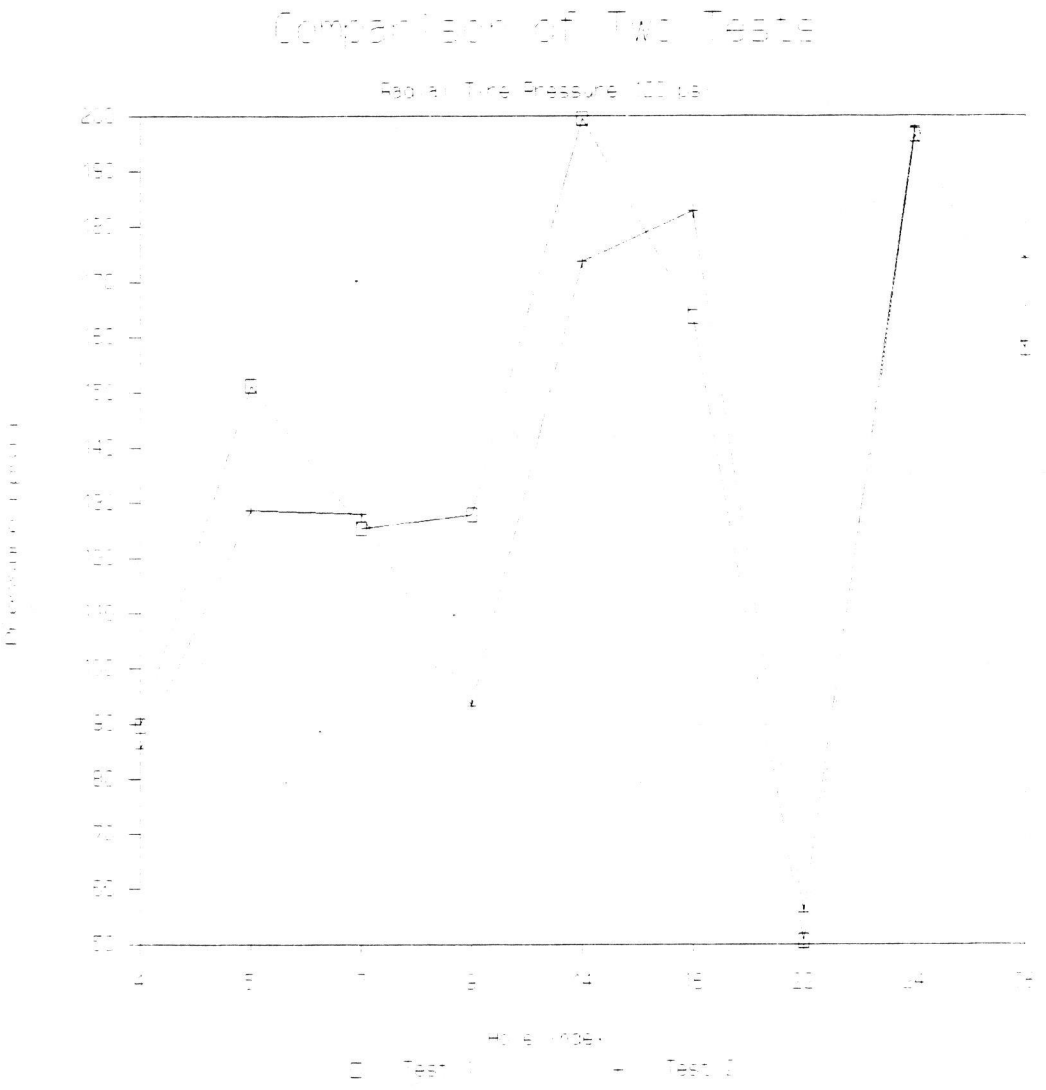

Figure 4-6. Comparison of Two Pressure Meawsurements at 120 psi.

TABLE 4.2 REPEATABILITY OF CONTACT PRESSURE MEASUREMENTS.

Pin Location	Radial Tire Inflated to 80 psi Pressure Measurements Test 1	Test 2	% Difference
1	47.41	72.00	52
3	95.05	94.80	0
7	111.50	132.60	19
9	120.05	104.80	13
14	146.98	139.60	5
16	143.24	142.30	1
26	135.70	133.60	2

Pin Location	Radial Tire Inflated to 120 psi Pressure Measurements Test 1	Test 2	% Difference
4	89.73	85.60	5
5	151.29	128.70	15
7	125.40	128.00	2
9	127.94	93.20	27
14	199.37	173.70	13
16	163.61	182.70	12
22	50.61	55.70	10
24	196.48	197.90	1
26	157.83	174.10	10

Although a maximum difference of 52% (80 psi radial tire) was reported in the repeatability test, the overall result obtained from the three methods described above indicated that the test frame was adequate for contact pressure measurements. The large discrepancy reported in the repeatability test could be attributed to experimental error (at hole 7).

4.4 Net Contact Area and Contact Pressure

Net contact area refers to the area of actual contact between the tire tread and the pavement; whereas gross contact area refers to the total area enclosed within the boundary of the tire print. The ratio of net contact area to gross contact area varies according to tread pattern, tire condition, load and pressure magnitude. Net contact area provides more relevant information regarding load transfer from tire to pavement than gross area does. The net contact areas of the tires at different inflation pressures and loads were obtained by tracing the tire prints (Figure 4-7) using the software "AutoCad." The contact areas and average contact pressures for the radial tire tested at different inflation pressures are given in Table 4.3.

Results from contact pressure measurement indicated that tire contact pressures were not uniform. The tire contact pressure distribution curves for both radial and bias ply

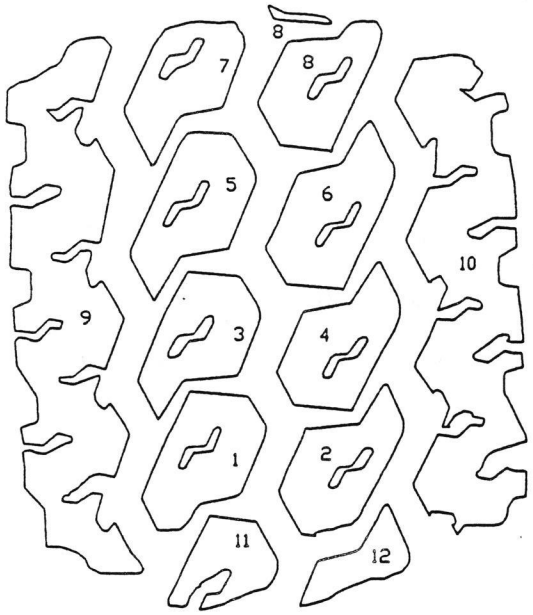

TRC-8902: TIRE PRESSURE STUDY

TIRE PRESSURE = 80 psi.

LOAD = 5 Kip.

DATE = 7/25/89

POINT	NET AREA (sq.)
1	2.7573
2	2.5678
3	2.5541
4	2.5806
5	2.8755
6	3.0301
7	2.3988
8	2.6208
9	10.3829
10	9.5213
11	1.5974
12	1.1700
TOTAL	44.0567

AREA OF CIRCLE = 89.8489 sq.

Figure 4-7. Radial Tire Print at 80 psi and 5 kip Load.

TABLE 4.3 NET CONTACT AREAS AND AVERAGE CONTACT PRESSURES.

Inflation Pressure psi	Applied Load kips	Net Contact Area sq in	Average Contact Pressure psi
Radial Tire			
80	1	11.26	88.0
	2	18.47	108.3
	3	30.17	99.4
	4	39.65	100.9
	5	44.06	113.5
	6	50.30	119.3
100	1	11.75	85.1
	2	17.90	111.7
	3	26.87	111.6
	4	34.21	116.9
	5	42.40	117.9
	6	45.10	133.0
120	1	9.90	101.0
	2	12.69	157.6
	3	21.79	137.7
	4	29.13	137.3
	5	36.65	136.4
	6	43.04	139.4
140	1	10.47	95.5
	2	14.70	136.0
	3	21.69	138.3
	4	28.45	140.6
	5	34.29	145.8
	6	42.30	141.8
Bias Ply Tire			
60	1	23.53	42.5
	2	37.49	53.4
	3	48.15	62.3
	4	57.38	69.7
	4.8	64.64	74.3
80	1	21.32	46.9
	2	34.28	58.3
	3	44.07	68.1
	4	50.70	78.9
	5	61.24	81.7
100	1	18.57	53.8
	2	31.25	64.0
	3	40.54	74.0
	4	48.48	82.5
	5	55.15	90.7

tires are shown in Chapter 5. Figure 5-2 shows that the contact pressure for bias ply tire is less uniform and the peak contact pressure occurs in between the shoulder and the center of the tire. On the other hand, Figure 5-4 shows that the contact pressure for the radial tire is more uniform and the pressure is higher at the center than at the shoulder of the tire. Both Figure 5-2 and Figure 5-4 show that the shapes of the contact pressure distribution curves obtained from this laboratory measurement are similar to those reported by Ford [4].

CHAPTER 5

ANALYSES OF TIRE PRESSURE EFFECTS

Mechanistic analyses were performed to evaluate the effect of higher tire pressures on conventional flexible pavements commonly built in Arkansas. The overall objective was to compare the relative effects of today's higher tire pressures and radial tires to the 80 psi, bias ply tire used at the time of the AASHO Road Test. The tires and pressures modelled in the analyses were bias ply tires at 80 and 100 psi and radial tires at 120 and 140 psi. A wheel load of 4500 pounds, representing the load on a single tire of a dual tired, 18 kip single axle, was used in the analyses.

Each of the analysis programs available have limitations in their ability to model the tire-pavement system. ELSYM5 has the capability to model dual tires but can only handle uniform contact pressures. ILLIPAVE can only model a single tire loading but, with modification, can model a non-uniform contact pressure. ILLIPAVE also has the ability to model the stress dependent nature of granular bases and subgrade soils. To compensate for these limitations, three types of analyses were performed: 1) ELSYM5 elastic layer analyses, 2) ILLIPAVE non-uniform contact pressure analyses, and 3) ILLIPAVE uniform contact pressure analyses.

5.1 Study Parameters

The conventional flexible pavements examined consist of an asphalt concrete surface over a granular base. The pavement variations included in the analyses were:

Surface Thicknesses: 2, 4, and 6 inches

Surface Elastic Moduli: 50 and 500 ksi

Base Thickness: 12 inches

Base Moduli:	ELSYM5 - 40 ksi
	ILLIPAVE - 7500 $O^{.45}$
Subgrade:	ELSYM5 - 8 ksi
	ILLIPAVE - see Figure 5-1

The pavement analyses examined the effect of tire pressure relative to fatigue cracking and surface rutting. Tensile strains in the asphalt surface layer were used as the measure of fatigue effects; and vertical strains in the surface, base, and top of subgrade were used as indicators of rutting effects.

5.2 ELSYM5 Analyses

The ILLIPAVE program provides the most realistic method of pavement analysis. It realistically models the stress dependent nature of base and subgrade materials; and, with the modifications made for this study, ILLIPAVE can model non-uniform contact pressures. However, ILLIPAVE can

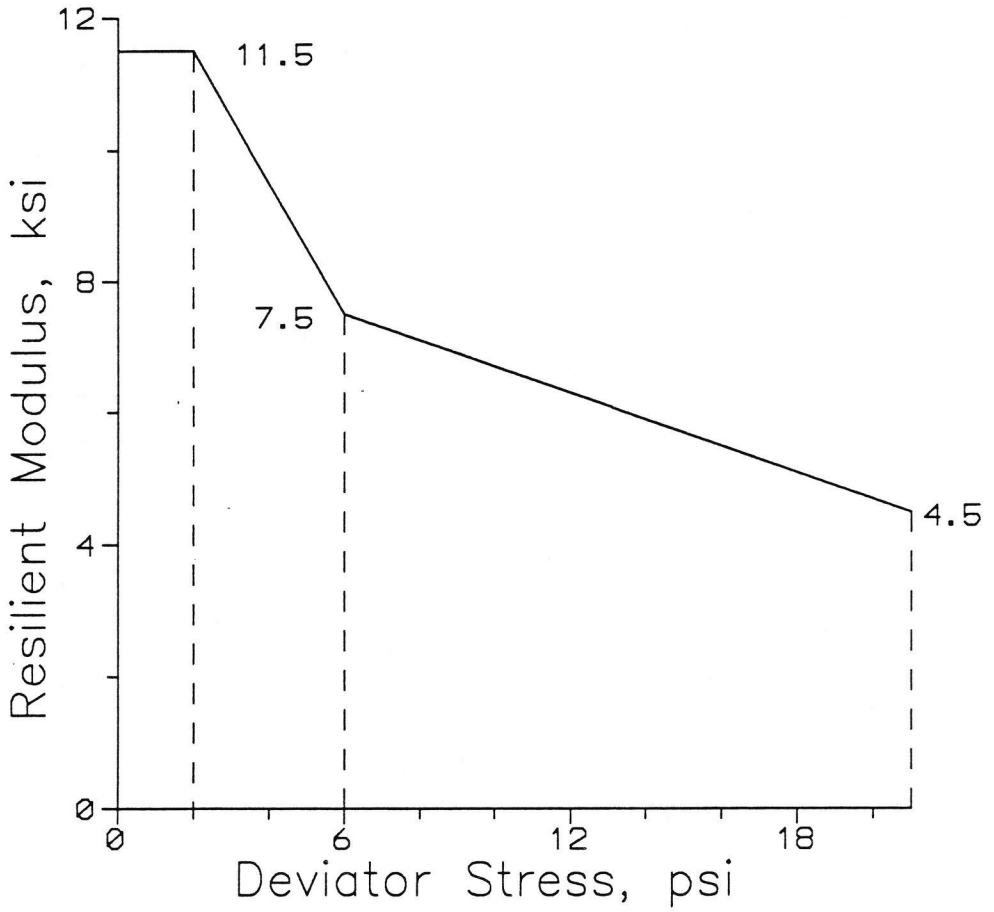

Figure 5-1. Subgrade Soil Resilient Modulus Model Used in ILLIPAVE Analyses.

handle only a single loading location and therefore cannot model the typical dual tire loading. Generally, this limitation is ignored and the total wheel loading (both wheels) is treated as being applied to a single area.

ELSYM5 analyses were performed to examine the influence of pressure increase with depth in the pavement and to determine whether the relative effect using a single tire loading (a restriction with ILLIPAVE) would be adequate. Quite obviously, the effect of a pressure increase must decrease with depth. This being the case, the effect with depth is more significant for thinner pavements. Consequently, this effect was studied by examining the vertical strain in the base and subgrade of the 2" AC surface pavement.

Table 5.1 shows the predicted vertical strains at various depths in the base and subgrade for both a single 4.5 kip tire and dual 4.5 kip tires at 80 and 120 psi contact pressure. The relative effect of the pressure increase is shown by the percent change in the predicted strain. Comparison of the single and dual tire percentages show that the relative effects are nearly identical (e.g. 13.8% vs 13.2%). The results also show that pressure increase has very little effect at the subgrade level (< 2% increase in strain).

Similar analyses performed on thicker pavements (4" and 6" AC surfaces) show identical results at the base and subgrade with regard to the relative effects of both single and dual tire pressure increase (Table 5.2 and Table 5.3).

Table 5.1 ELSYM5 Analyses of Vertical Strains in Base amd Subbase of a 14" Conventional Flexible Pavement.

Pavement - 2" AC with 12" Granular Base

		Single Tire, 1 @ 4.5 kips			Dual Tires, 2 @ 4.5 kips		
	Depth	Vertical Microstrain		%	Vertical Microstrain		%
Layer	inches	80 psi	120 psi	Change	80 psi	120 psi	Change
Base	5"	689	784	13.8	698	790	13.2
	8"	426	456	7.0	475	504	6.1
	11"	298	307	3.0	383	391	2.1
	14"	314	320	1.9	429	434	1.2
Subgrade	14"	478	487	1.9	659	667	1.2

Table 5.2 ELSYM5 Analyses of Vertical Strains in Base amd Subbase of a 16" Conventional Flexible Pavement.

Pavement - 4" AC with 12" Granular Base

		Single Tire, 1 @ 4.5 kips			Dual Tires, 2 @ 4.5 kips		
	Depth	Vertical Microstrain		%	Vertical Microstrain		%
Layer	inches	80 psi	120 psi	Change	80 psi	120 psi	Change
Base	7"	334	359	7.5	386	410	6.2
	10"	228	236	3.5	297	304	2.4
	13"	182	184	1.1	266	268	0.8
	16"	199	200	0.5	303	304	0.3
Subgrade	16"	304	306	0.7	466	468	0.4

Table 5.3 ELSYM5 Analyses of Vertical Strains in Base amd Subbase of a 18" Conventional Flexible Pavement.

Pavement - 6" AC with 12" Granular Base

		Single Tire, 1 @ 4.5 kips			Dual Tires, 2 @ 4.5 kips		
	Depth	Vertical Microstrain		%	Vertical Microstrain		%
Layer	inches	80 psi	120 psi	Change	80 psi	120 psi	Change
Base	9"	196	206	5.1	252	261	3.6
	12"	142	145	2.1	205	208	1.5
	15"	121	121	0.0	192	192	0.0
Subgrade	15"	203	203	0.0	334	335	0.3

The influence of a single tire versus a dual tire analysis on the AC layer was investigated by examining the predicted radial strains at the bottom of the AC of each of the thicknesses studied (2, 4, and 6 inches). The relative effects (percent change in Table 5.4) were found to be quite similar with the single tire model prediction being somewhat lower. The difference in relative effect predictions were insignificant for the 4" and 6" surfaces (20% vs 24% and 12% vs 13%); but there could be some concern for the 2" surface prediction (39% vs 49%).

Based on these analyses it was concluded that the ILLIPAVE single tire model provides an adequate representation of the relative effect of pressure increases except that the effect on thin AC surfaces may be somewhat underpredicted. It was also concluded that pressure increases would have little significant influence on the behavior of subgrade and only limited influence on the behavior of bases.

5.3 ILLIPAVE Analyses Using Non-uniform Contact Pressure

Non-uniform contact pressure, which reflects actual tire-pavement contact pressure, was selected as input for a modified ILLIPAVE program. Since the tire-pavement contact pressure is non-uniform, ILLIPAVE analyses using non-uniform contact pressure will provide a more accurate investigation of the effect of higher tire pressures on flexible pavements.

Table 5.4 Single Tire vs Dual Tire Pressure Effects on Maximum Tensile Strains at the Bottom of AC Surface.

	Single Tire, 1 @ 4.5 kips			Dual Tires, 2 @ 4.5 kips		
AC Thickness	Radial Microstrain		% Change	Radial Microstrain		% Change
	80 psi	120 psi		80 psi	120 psi	
2"	266	370	39.1	213	317	48.8
4"	181	217	19.9	146	181	24.0
6"	118	132	11.9	104	118	13.5

5.3.1 Non-uniform Contact Pressure Input For ILLIPAVE

The measured contact pressures described in Chapter 4 were used to select input data for the ILLIPAVE analyses. The contact pressure distribution curves for a 4500 pound wheel load (Figures 5-2, 5-3, 5-4, and 5-5) were obtained by taking the average of the contact pressures measured at 4,000 pounds and 5,000 pounds. The measured pressure distributions had to be adjusted for the analyses. The adjustments were necessary to compensate for the lack of contact in the areas between the treads and to make the total load equal to 4,500 pounds.

The first step in making the adjustments was to select the radius of the loaded area for each tire type and each pressure analyzed. The selection was complicated by differences in the shape of the contact areas and in the amount of non-contact area.

For the bias ply tire, the measured contact areas were nearly square with half the lengths of the sides being smaller than the circular radius normally assumed based on the inflation pressure. Also, because the tire was well worn, there was little area of non-contact between treads; the average ratio of net contact area (actual contact) to gross contact area was 0.90. Half the measured width (3.75") of the contact area was selected to represent the 80 psi and 100 psi bias ply tire.

The contact areas for the radial tires were elliptical

Tire Type: Bias Ply Tire

Tire Pressure: 80 psi

Radius: 3.75"

* Average 4 and 5 kip Measured Pressures

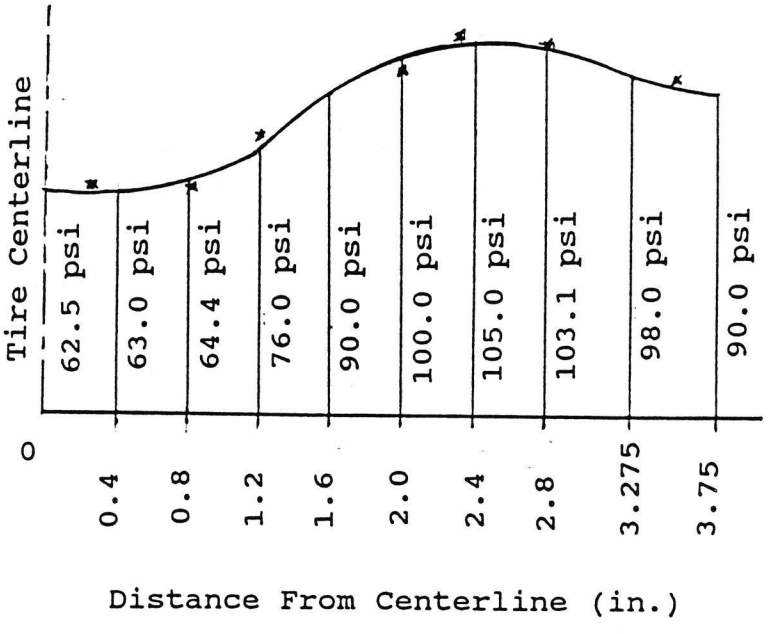

Figure 5-2. Contact Pressure Distribution for Bias Ply Tire at 4,500 pounds and 80 psi.

Tire Type: Bias Ply Tire

Tire Pressure: 100 psi

Radius: 3.75"

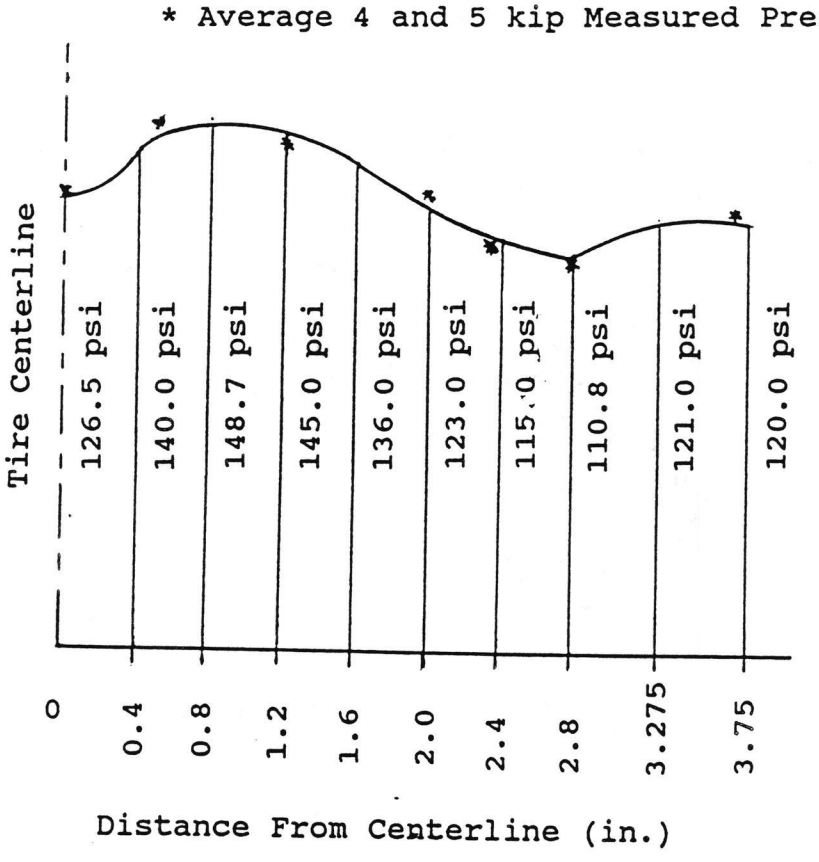

Figure 5-3. Contact Pressure Distribution for Bias Ply Tire at 4,500 pounds and 100 psi.

Tire Type: Radial Tire

Tire Pressure: 120 psi

Radius: 3.45"

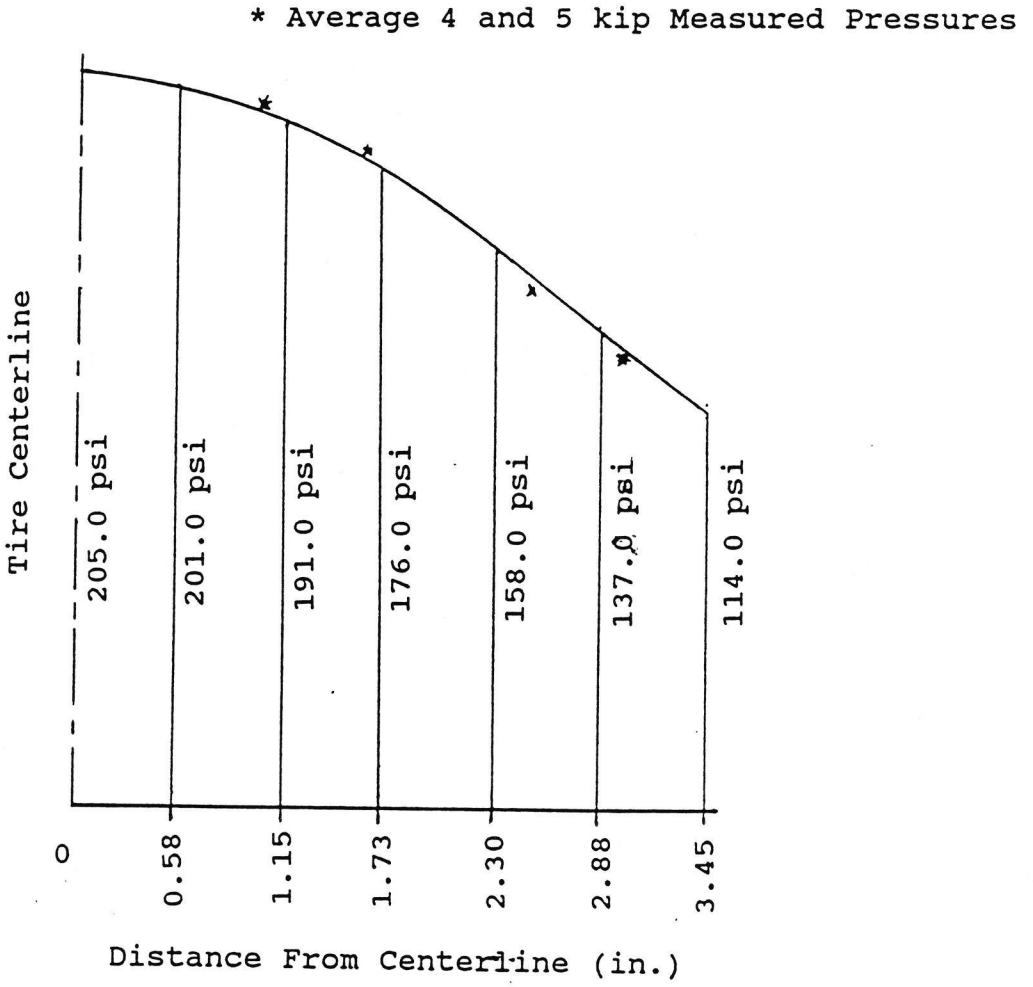

Figure 5-4. Contact Pressure Distribution for Radial Tire at 4,500 pounds and 120 psi.

Tire Type: Radial Tire

Tire Pressure: 140 psi

Radius: 3.20"

* Average 4 and 5 kip Measured Pressures

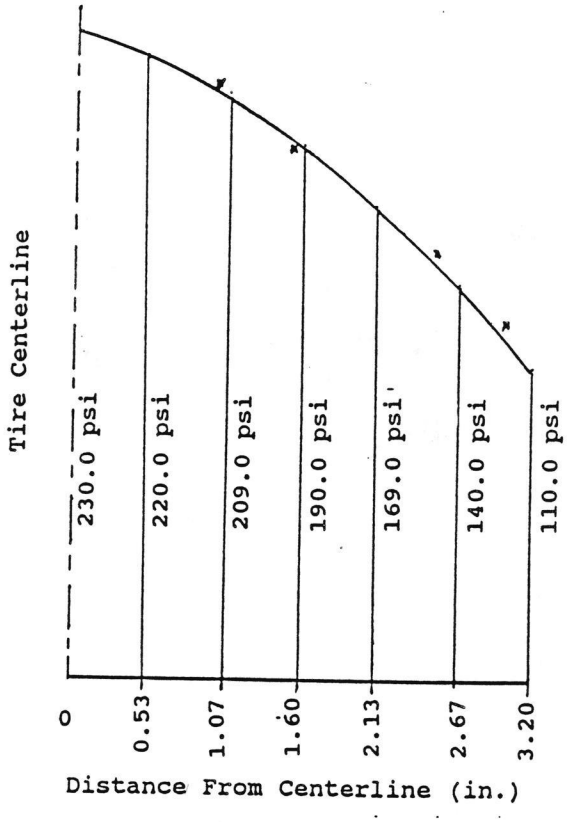

Figure 5-5. Contact Pressure Distribution for Radial Tire at 4,500 pounds and 140 psi.

with both axes exceeding the diameter normally assumed based on inflation pressure. There was also a considerable amount of non-contact area between treads. The average ratio of net contact area to gross contact area was 0.60. After some debate, the radius based on inflation pressure was selected to represent the radial tires. This radius is somewhat conservative but reasonable; it is smaller than half the length of the minor axis of the gross contact area (e.g. 3.45" vs 4.0" at 120 psi) and slightly larger than a radius based on the net contact area (e.g. 3.24" at 120 psi). The average ratio of the net contact area to the area based on inflation pressure was 0.93.

The procedure used to adjust the measured pressures is listed in Figure 5-6. The pressure adjustment calculations are shown in Table 5.5. An example of the input data set for ILLIPAVE analyses is shown in Figure 5-7.

5.3.2 Analyses of Critical Pavement Strains

Figures 5-8 and 5-9 show the effect of high tire pressure on tensile strain at the bottom of the AC surface. Figure 5-8 shows the change in tensile strain for an AC surface of varying thickness and with a modulus of 500 ksi. Figure 5-9 shows the same information for an AC surface with a modulus of 50 ksi.

The effect of increased tire pressure is especially significant on the 2" thick AC surface. Figures 5-8 and 5-9

1) Plot the averages (at different pin locations where measurements were taken) of the 4 kip and 5 kip contact pressure measurements. The averages are assumed to be the contact pressure for a 4.5 kip single wheel loading.

2) Fit a curve through the averaged contact pressure points described in step 1). This curve is assumed as the "Contact Pressure Distribution Curve For a 4.5 Kip Single Wheel Loading."

3) Divide the pavement under study to a number of elements within the criteria set in the ILLIPAVE analysis.

4) Set the nodal points on the 4.5 kip contact pressure distribution curve and obtain the contact pressure at each nodal point.

5) Adjust the pressures at the nodal points so that the summation of pressure x area equals 4500 pounds (Table 5.1).

6) Use the adjusted contact pressures as input for the ILLIPAVE analyses.

Figure 5-6. Contact Pressure Adjustment Procedure.

Table 5.5a Adjustment of Pressure Values to Get 4.5 kip Total Load (80 psi Bias Ply Tire).

Tire Type = Bias Ply			Pressure = 80 psi				Radius = 3.75"	
Nodal Point (1)	Coordinate (2)	Average Coordinate (3)	Pressure (psi) (4)	Average Pressure (5)	Load * lb (6)	Adjusted Pressure 4.5/TL1 x (4)	Average Pressure (7)	Load * lb (8)
1	0.00		62.5			67.45		
		0.20		62.8	31.55		67.7	34.04
2	0.40		63.0			67.98		
		0.60		63.7	96.03		68.7	103.63
3	0.80		64.4			69.44		
		1.00		70.2	176.39		75.7	190.35
4	1.20		76.0			82.01		
		1.40		83.0	292.08		89.6	315.19
5	1.60		90.0			97.12		
		1.80		95.0	429.83		102.5	463.84
6	2.00		100.0			107.91		
		2.20		102.5	566.82		110.6	611.67
7	2.40		105.0			113.31		
		2.60		104.1	680.07		112.3	733.88
8	2.80		103.1			111.28		
		3.04		100.6	911.74		108.5	983.88
9	3.28		98.0			105.75		
		3.51		94.0	985.54		101.4	1063.52
10	3.75		90.0			97.12		
				TL1	4170.04		TOTAL	4500.00

* Width x 2 x 3.142 x (3) x Average Pressure

Table 5.5b Adjustment of Pressure Values to Get 4.5 kip Total Load (100 psi Bias Ply Tire).

Tire Type = Bias Ply			Pressure = 100 psi				Radius = 3.75"	
Nodal Point (1)	Coordinate (2)	Average Coordinate (3)	Pressure (psi) (4)	Average Pressure (5)	Load * lb (6)	Adjusted Pressure 4.5/TL1 x (4)	Average Pressure (7)	Load * lb (8)
1	0.00		126.5			104.57		
		0.20		133.3	66.99		110.1	55.37
2	0.40		140.0			115.73		
		0.60		144.3	217.67		119.3	179.93
3	0.80		148.7			122.88		
		1.00		146.8	369.06		121.4	305.08
4	1.20		145.0			119.86		
		1.40		140.5	494.43		116.1	408.71
5	1.60		136.0			112.42		
		1.80		129.5	585.92		107.0	484.34
6	2.00		123.0			101.68		
		2.20		119.0	658.06		98.4	543.97
7	2.40		115.0			95.06		
		2.60		112.9	737.68		93.3	609.79
8	2.80		110.8			91.55		
		3.04		115.9	1050.60		95.8	868.46
9	3.28		121.0			100.02		
		3.51		120.5	1263.38		99.6	1044.35
10	3.75		120.0			99.20		
				TL1	5443.77		TOTAL	4500.00

* Width x 2 x 3.142 x (3) x Average Pressure

Table 5.5c Adjustment of Pressure Values to Get 4.5 kip Total Load (120 psi Radial Tire).

Tire Type = Radial			Pressure = 120 psi				Radius = 3.45"	
Nodal Point (1)	Coordinate (2)	Average Coordinate (3)	Pressure (psi) (4)	Average Pressure (5)	Load * lb (6)	Adjusted Pressure 4.5/TL1 x (4)	Average Pressure (7)	Load * lb (8)
1	0.00		205			158.99		
		0.29		203.0	210.88		157.4	163.55
2	0.58		201			155.89		
		0.86		196.0	610.83		152.0	473.73
3	1.15		191			148.13		
		1.44		183.5	953.12		142.3	739.19
4	1.73		176			136.50		
		2.01		167.0	1214.38		129.5	941.81
5	2.30		158			122.54		
		2.59		147.5	1379.04		114.4	1069.51
6	2.88		137			106.25		
		3.16		125.5	1434.10		97.3	1112.21
7	3.45		114			88.41		
				TL1	5802.35		TOTAL	4500.00

* Width x 2 x 3.142 x (3) x Average Pressure

Table 5.5d Adjustment of Pressure Values to Get 4.5 kip Total Load (140 psi Radial Tire).

Tire Type = Radial			Pressure = 140 psi					Radius = 3.45"
Nodal Point (1)	Coordinate (2)	Average Coordinate (3)	Pressure (psi) (4)	Average Pressure (5)	Load * lb (6)	Adjusted Pressure 4.5/TL1 x (4)	Average Pressure (7)	Load * lb (8)
1	0.00		230			196.68		
		0.27		225.0	201.09		192.4	171.96
2	0.53		220			188.13		
		0.80		214.5	575.11		183.4	491.81
3	1.07		209			178.73		
		1.33		199.5	891.49		170.6	762.36
4	1.60		190			162.48		
		1.87		179.5	1122.96		153.5	960.30
5	2.13		169			144.52		
		2.40		154.5	1242.72		132.1	1062.71
6	2.67		140			119.72		
		2.93		125.0	1228.87		106.9	1050.87
7	3.20		110			94.07		
				TL1	5262.25		TOTAL	4500.00

* Width x 2 x 3.142 x (3) x Average Pressure

```
TITLE "CONVENTIONAL 6 in. THK. 500,000 psi."
INCR 1 HPAV 18.0 HSUB 197.5
RAD 3.45 PSI 120.0
PRESS DISTALL 7 1 120
NCOL 15 R 7 3.45 R 9 6.465 R 10 8.62 R 12 14.0075 R 13 19.395
R 16 51.72
NROW 24 Z 1 215.5 Z 13 209.5 Z 17 197.5 Z 19 193.19 Z 21
184.57 Z 22 175.95 Z 23 150.0 Z 24 100.0 Z 25 0.0
ZMAT 1 1 ZMAT 13 2 ZMAT 17 3 ZMAT 19 3 ZMAT 21 3 ZMAT 22 3
ZMAT 23 3 ZMAT 24 3 ZMAT 25 3
PROP 1 3.0 DEN 1 145.0 KO 1 0.67 H 1 6.0 E 1 5.0E04 U1 0.4
PROP2 5. DEN2 135.0 KO 2 0.6 H2 12.0 U2 0.38 KONE 2 7500 X2
0.45 MAXSR 2 4.8 MINSIG 2 0.01 EFAIL 2 4000
PROP3 2. DEN3 120. KO3 0.82 H3 197.5 U3 0.45 KONE3 6.0 TAUSUB3
15.0 EFAIL3 3000. KTWO3 7500. KTHREE3 1000. KFOUR3 -200. DSLL3
2.0 DSUL3 21.0
PRINTALL
CALCULATE
     7    6    0.0        0.0         88.41          106.25
     6    5    0.0        0.0        106.25          122.54
     5    4    0.0        0.0        122.54          136.50
     4    3    0.0        0.0        136.50          148.13
     3    2    0.0        0.0        148.13          155.89
     2    1    0.0        0.0        155.89          158.99
YES 3 V
                 0.0       10.5
                40.0        0.0



"USER GENERATED MESH. FN = UMT6120.DAT"
```

Figure 5-7. Input Data Set for ILLIPAVE Analyses.

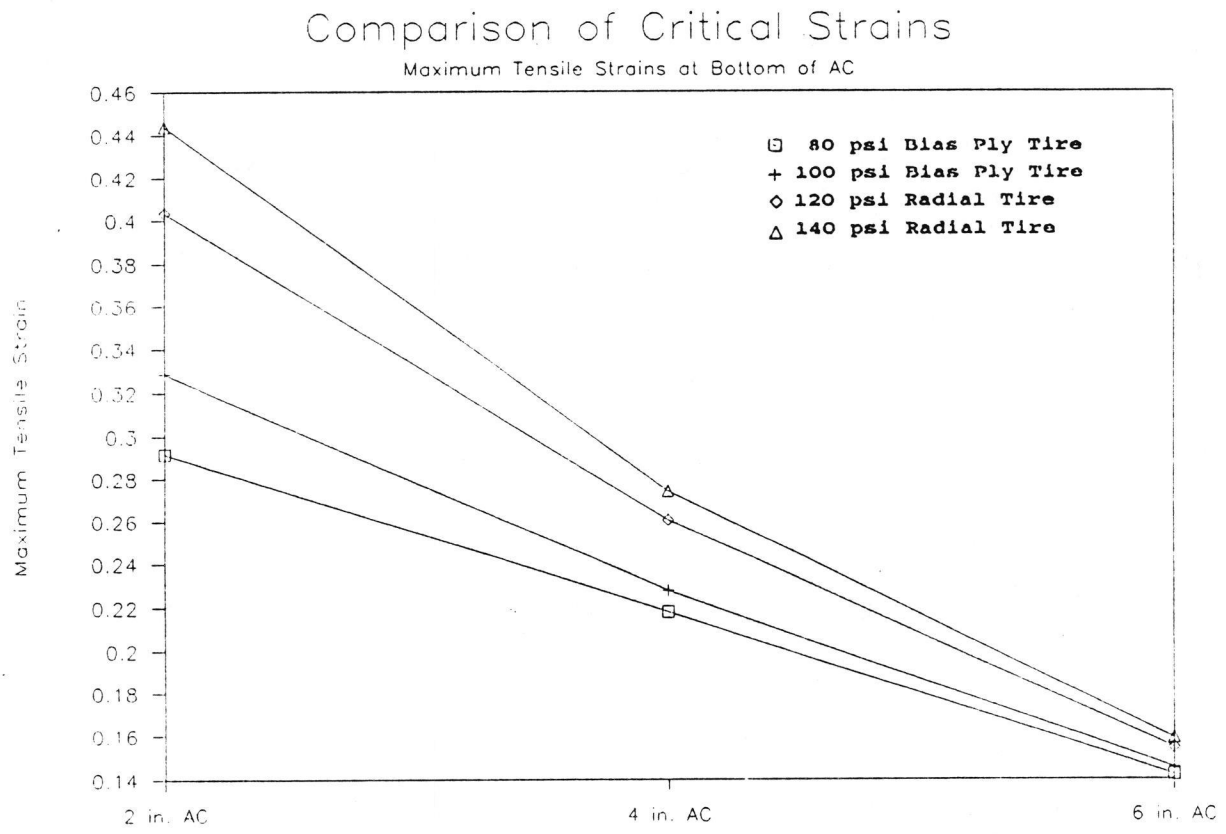

Figure 5-8. Maximum Tensile Strain at Bottom of Asphalt Concrete with E_{ac} = 500 ksi

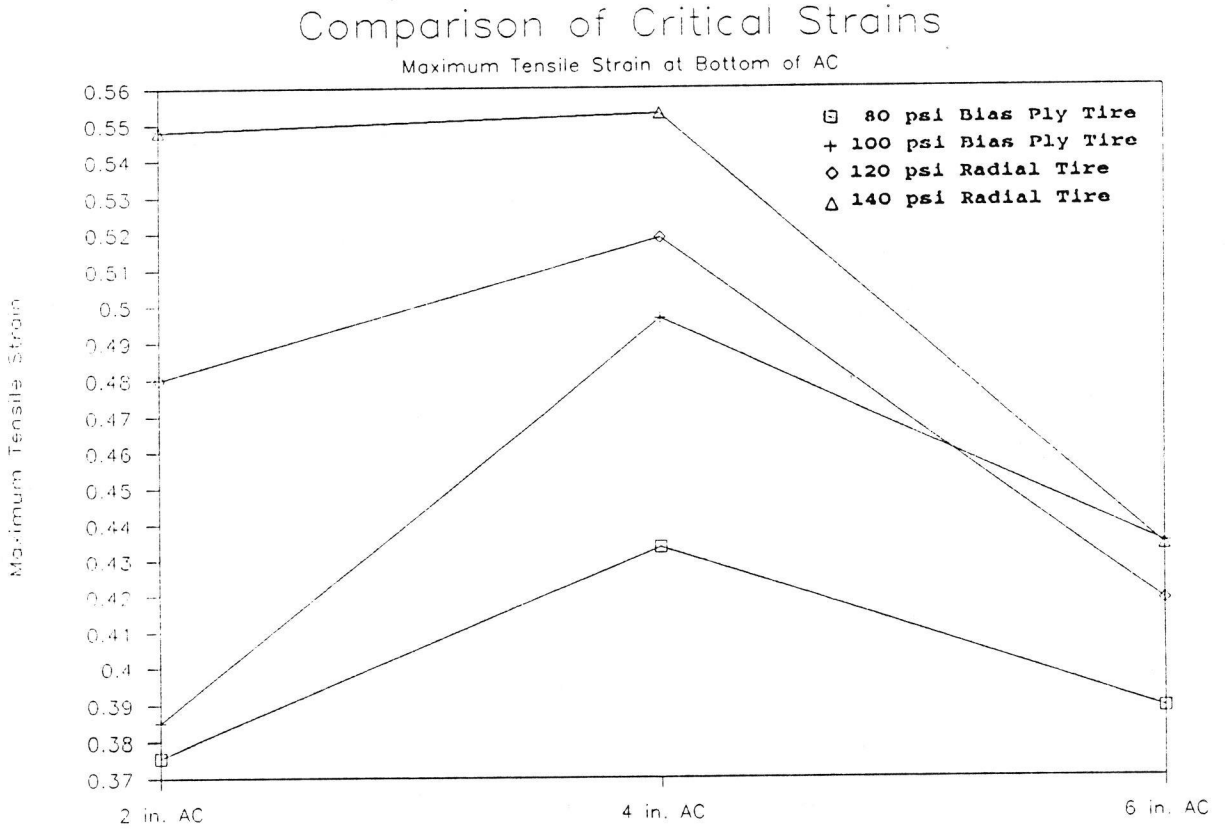

Figure 5-9. Maximum Tensile Strain at Bottom of Asphalt Concrete with E_{ac} = 50 ksi

show that higher tire contact pressures increase the tensile strain at the bottom of the 2" thick AC surface quite significantly. For an AC modulus of 500 ksi, the tensile strain increased 13% with the 100 psi bias ply, 38% with the 120 psi radial tire, and 52% with the 140 psi radial tire. Based on the findings from the ELSYM5 analyses described in Section 5.2, these increases in tensile strain (13% to 52%) can be expected to be somewhat larger when the effect of dual tires is taken into consideration.

The relative increases decreased significantly with greater thickness. With the 4" surface, the tensile strain increases were 4% with the 100 psi bias ply tire, 20% with the 120 psi radial tire, and 26% with the radial tire. These dropped to 2%, 9%, and 12% respectively with the 6" surface. The results of the above analyses are tabulated in Appendix A, Table A.1 and Table A.2.

Figures 5-10 and 5-11 show the effect of increased tire pressures on the vertical strain at the top of the subgrade for AC moduli of 500 ksi and 50 ksi respectively. Both Figure 5-10 and Figure 5-11 show that an increase in bias ply tire pressure does not affect the vertical strains at the top of the subgrade significantly; however, higher pressure radial tires seem to increase the vertical strains considerably. This effect could be explained by observing the shape of the contact pressure distribution curves for radial tires (the contact pressures at the center of the

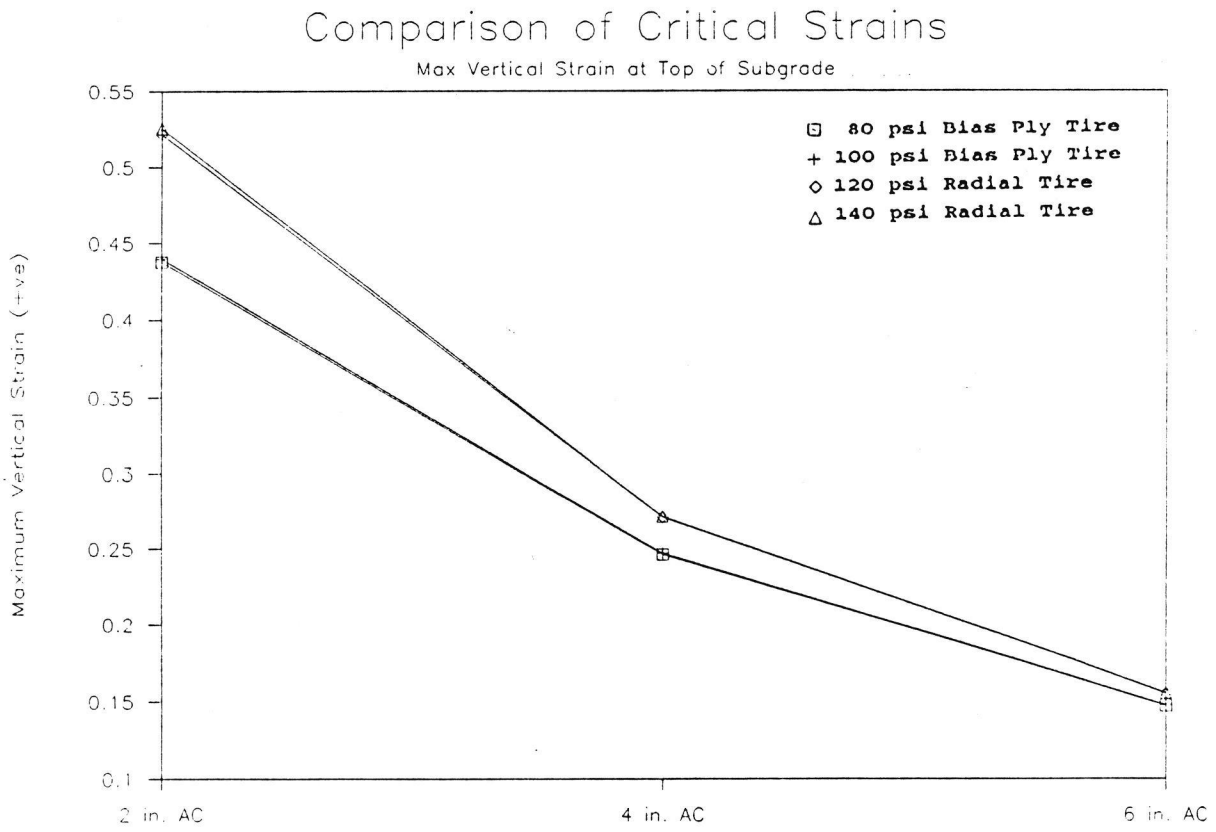

Figure 5-10. Vertical Strain at Top of Subgrade with E_{ac} = 500 ksi

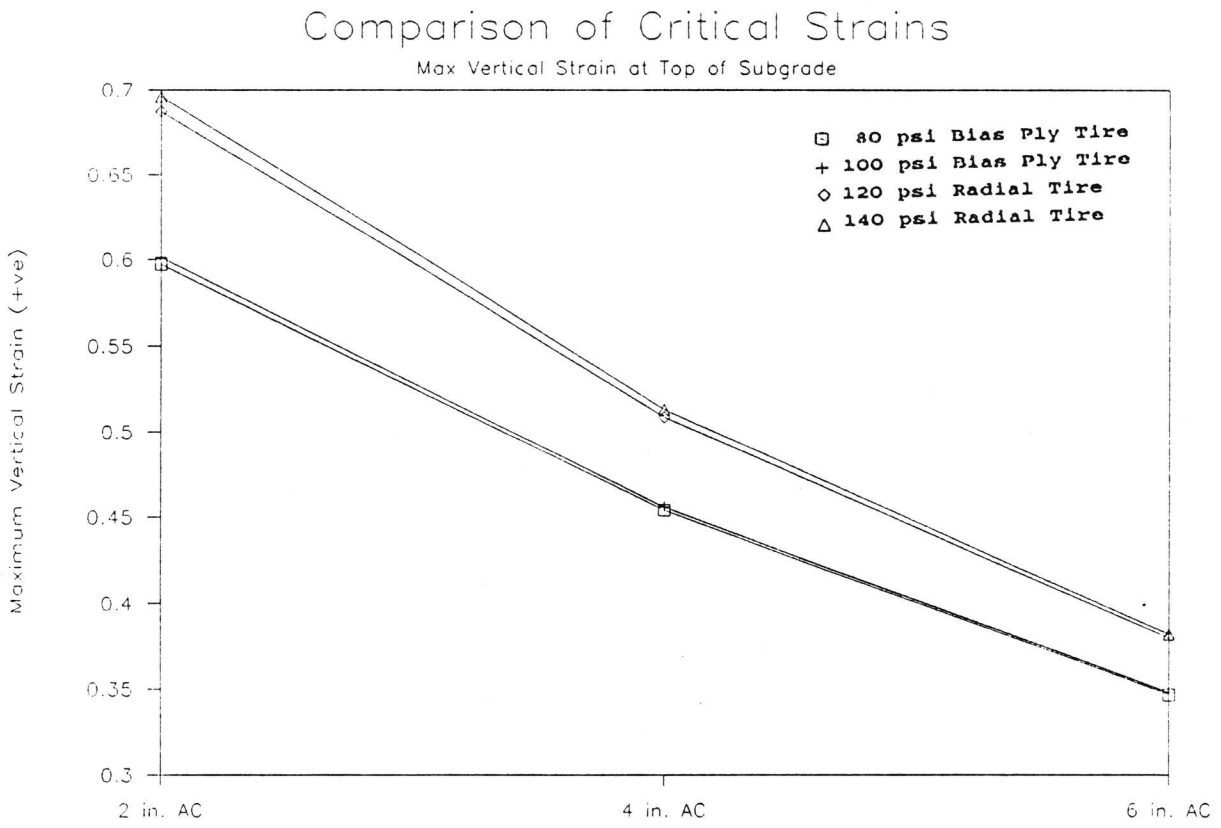

Figure 5-11. Vertical Strain at Top of Subgrade with E_{ac} = 50 ksi

radial tire are much larger than those of the bias ply tire). Both Figure 5-10 and Figure 5-11 show that thinner pavements (2") are more affected by higher radial tire contact pressures. For a 2" thick AC surface with a modulus of 500 ksi, the vertical strain at the top of the subgrade increased 19% with the 120 psi radial tire and 20% with the 140 psi radial tire. The effect of higher tire pressures on the vertical strain declined with thicker pavements. For the 4" and 6" AC surfaces, the vertical strain increases (with both 120 psi and 140 psi radial tire) were 10% and 5% respectively.

5.3.3 Relative Fatigue Life Analyses.

Relative life analyses using a fatigue transfer function were performed to evaluate the effect of higher tire pressures on pavement performance. The normal critical strains (AC tensile radial strain and subgrade vertical strain) computed from the ILLIPAVE non uniform contact pressure analyses were used in the transfer functions to estimate the relative effect of increased tire pressure on pavement life.

Pavement life analyses based on fatigue cracking criterion were performed using the relationship developed by Finn [9] for 10% alligator cracking (see Eq. 2-5):

$$\log N_f = 15.947 - 3.291 \log e_t - 0.854 \log E$$

or,

$$N_f = 15.947/(e_t^{3.291}\ E^{0.854})$$

where,

N_f = number of load applications to produce up to 10 percent cracking.

e_t = maximum tensile microstrain at the underside of the AC layer, in. per in.

E = complex modulus of asphalt concrete, ksi.

A relative fatigue life factor and the loss of relative life was defined by the ratio of predicted number of load applications to 10 percent cracking:

$$\text{Relative Life (R.L.) Factor} = N_{f@\text{higher pressure}}/N_{f@80\ \text{psi}}$$

$$\text{Relative Life (R.L.) Loss \%} = (1 - \text{R.L. Factor}) \times 100$$

thus,

$$\text{R.L. Factor} = (e_{t@80\ \text{psi}} / e_{t@\text{higher pressure}})^{3.291} \quad \text{[Eq. 5-1]}$$

$$\text{R.L. Loss \%} = (1 - (e_{t@80\ \text{psi}} / e_{t@\text{higher pressure}})^{3.291}) \times 100 \quad \text{[Eq. 5-2]}$$

Table 5.6 shows the results of the R.L. analyses based on the fatigue cracking criterion. The impact of increased tire pressure on pavement performance is observed by the significant reductions in the relative pavement life. It is also noted that the impact is less with thicker AC surfaces. For example, the 120 psi radial tire causes a 65% life loss for the 2" AC surface, a 45% loss for the 4" AC surface, and a 23% loss for the 6" surface.

The actual effect of the increased tire pressures is not as great as these analyses might suggest. The analyses

Table 5.6 Relative Fatigue Life Analysis Using Non-Uniform Contact Pressures.

Eac = 500 ksi									
Tire Type and Pressure	Radial Tensile Microstrain			Relative Life (R.L.) Factor			Relative Life Loss %		
	2"	4"	6"	2"	4"	6"	2"	4"	6"
80 psi Bias Ply	292	218	142	---	---	---	---	---	---
100 psi Bias Ply	328	228	145	0.68	0.86	0.93	32	14	7
120 psi Radial	403	261	154	0.35	0.55	0.77	65	45	23
140 psi Radial	444	274	159	0.25	0.47	0.69	75	53	31
Eac = 50 ksi									
Tire Type and Pressure	Radial Tensile Microstrain			Relative Life (R.L.) Factor			Relative Life Loss %		
	2"	4"	6"	2"	4"	6"	2"	4"	6"
80 psi Bias Ply	376	434	389	---	---	---	---	---	---
100 psi Bias Ply	385	496	435	0.93	0.64	0.69	7	36	31
120 psi Radial	480	519	418	0.45	0.56	0.79	55	44	21
140 psi Radial	548	553	434	0.29	0.45	0.70	71	55	30

R.L. Factor = (Microstrain @ 80 psi/Microstrain @ higher pressure)^3.291

R.L. Loss % = (1 - R.L. Factor) * 100

are based on the extreme pressures found in the field. Less than 10% of the trucks surveyed (Figure 3-4) had tire pressures as high as 120 psi with the average pressure being 105 psi. Nevertheless, the analyses do show that higher tire pressures reduce the life of the pavement and suggest that asphalt surfacing thicknesses should be increased to compensate for the reduction.

5.3.4 Analyses of Vertical and Tensile Strains in AC Layer

Figures 5-12, 5-13, and 5-14 indicate that even though the maximum vertical compressive strain within the AC (E_{AC} = 500 ksi) layer is located at the bottom of the surface, the effect of increased tire pressure is very significant near the top of the AC surfaces regardless of their thicknesses. For a 2" AC surface, Figure 5-12 shows that the increases in tire pressure (compared to the 80 psi bias ply tire) change the vertical strain from a state of tension to a state of compression at a depth of 0.75". For a 4" thick AC surface, the vertical strain increases more at a depth of 1.25" than at a depth of 3.75" (Figure 5-13). Finally, for a 6" thick AC surface, Figure 5-14 shows that the increases in vertical strain near the top of the AC surface are larger than the increases near the bottom of the AC surface. Similar analyses performed on pavements with low AC surface modulus of 50 ksi produced nearly identical results with regard to the effect of higher tire pressures: the top of the AC surfaces

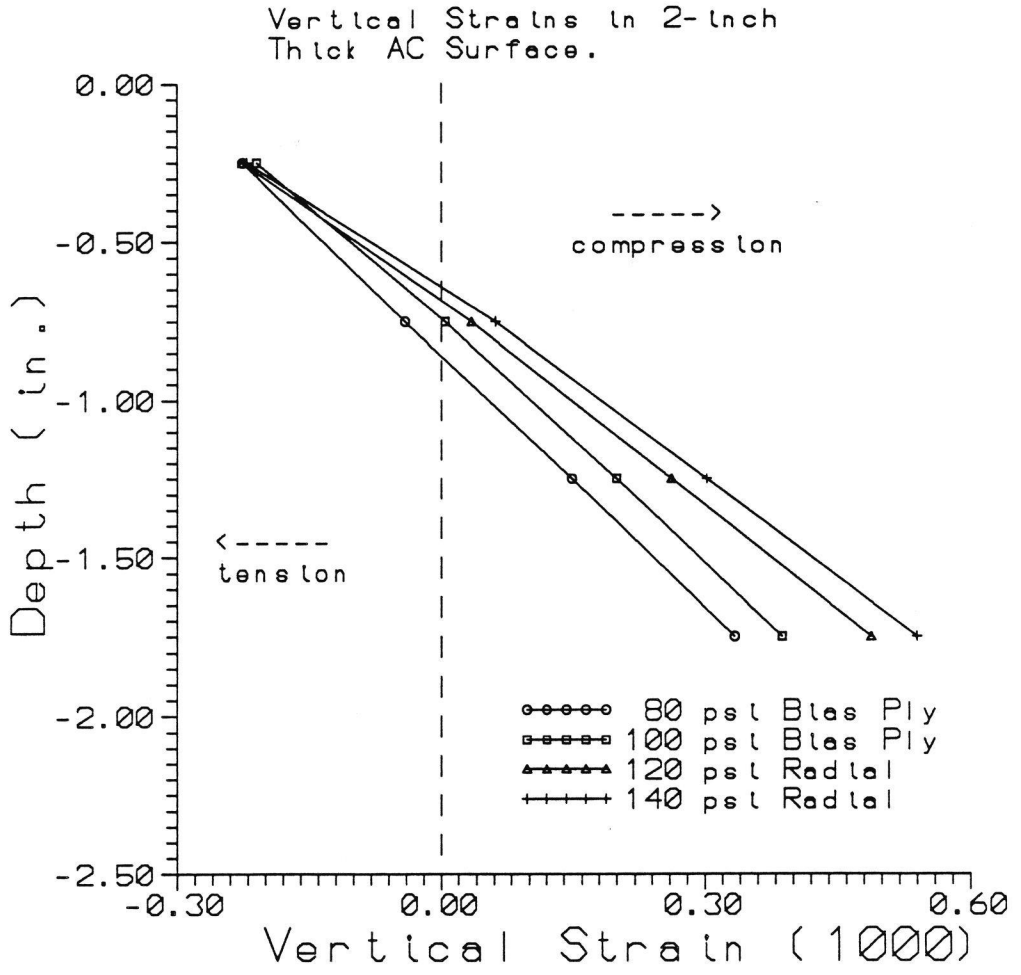

Figure 5-12. Vertical Strains in 2-Inch Thick AC Surface.

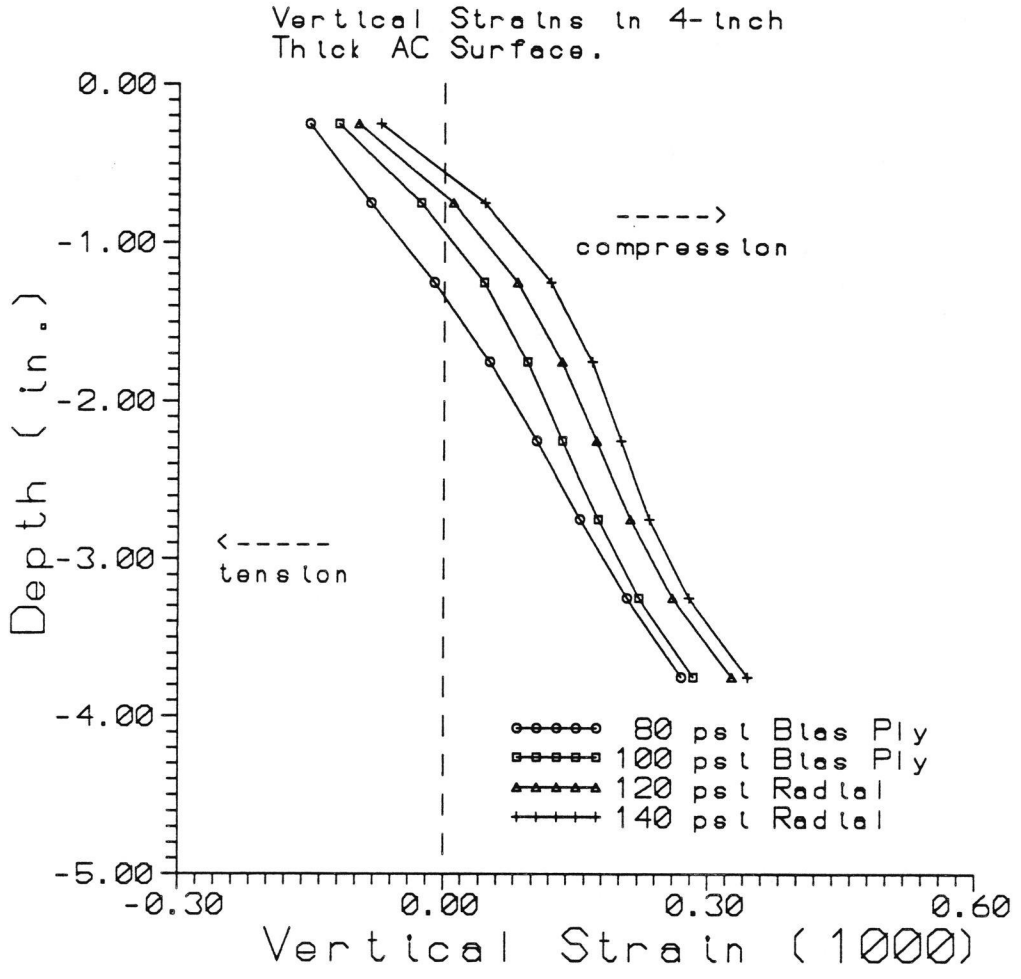

Figure 5-13. Vertical Strains in 4-Inch Thick AC Surface.

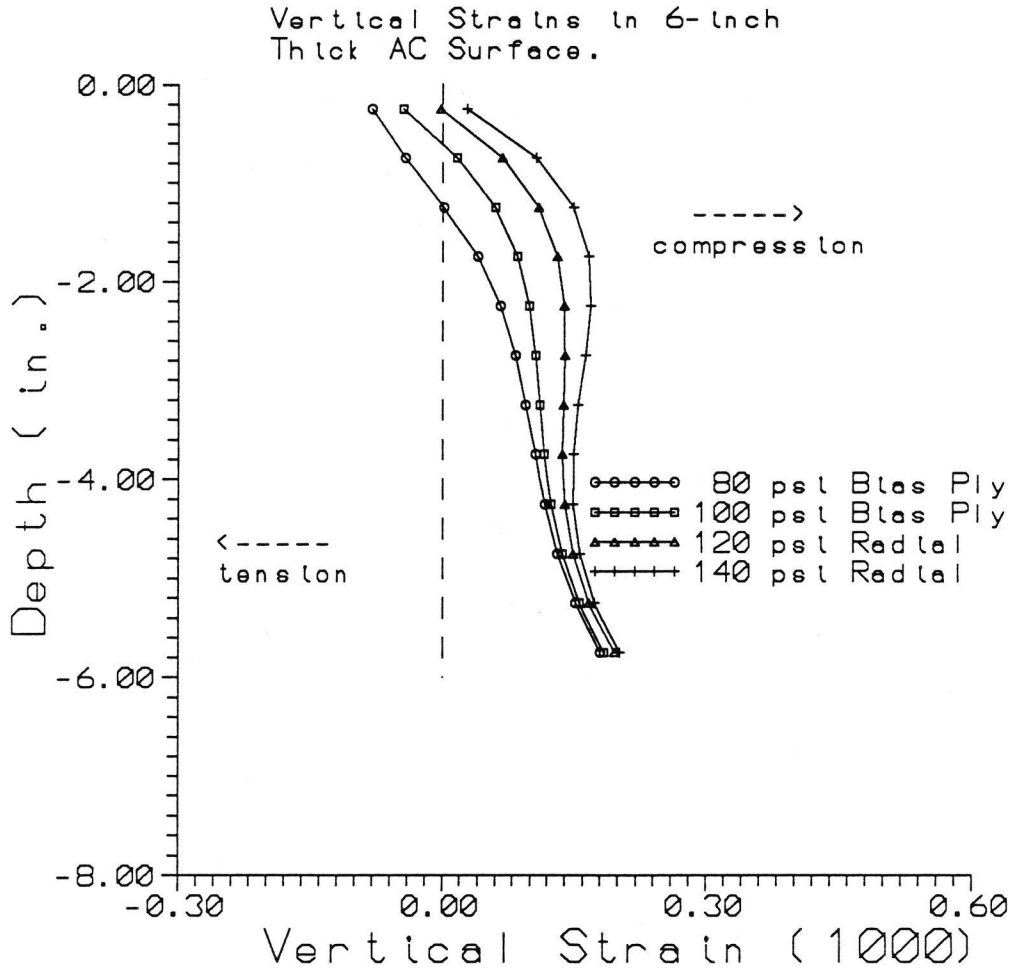

Figure 5-14. Vertical Strains in 6-Inch Thick AC Surface.

is more affected than the bottom. A complete tabulation of the results of the above analyses is shown in Appendix A, Table A.3 to Table A.8.

The above results show that higher tire pressures increase the vertical compressive zone of the AC layer and can lead to an increase in the rutting potential within the AC layer itself. The major effect of higher tire pressures seems to be at a depth of about 2". This suggests that AC rutting due to higher pressure would mostly occur in the upper 2 to 3 inches. It can be concluded that the effect of high tire pressure is more significant around the vicinity of the contact area, and not deep within the pavement section.

Figures 5-15, 5-16, and 5-17 relate the effect of higher tire pressures on the radial strains through the entire AC (E_{AC} = 500 ksi) thickness. Figures 5-15, 5-16, and 5-17 show that the maximum tensile strain always occurs at the bottom of the surface, and that the percentage increases decline with increasing AC thickness. The top portion of the AC layer is more affected by higher tire pressures than the bottom of the AC layer. Figures 5-15, 5-16, and 5-17 show that increases in radial strain (with respect to increased tire pressure) near the top of the AC layer are larger than at the bottom, indicating an increase in tensile zone within the AC layer. For example, for a 6" thick AC surface, the increases in tire pressure result in greater changes in

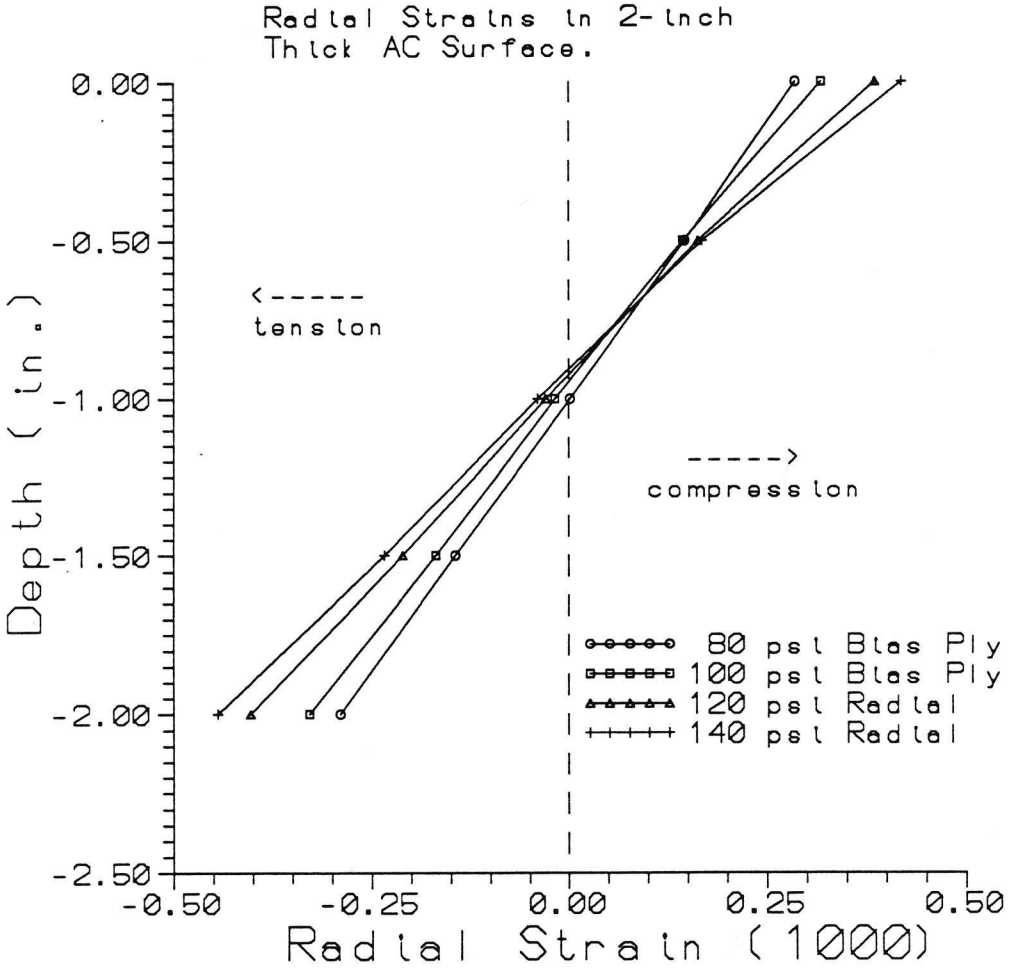

Figure 5-15. Radial Strains in 2-Inch Thick AC Surface.

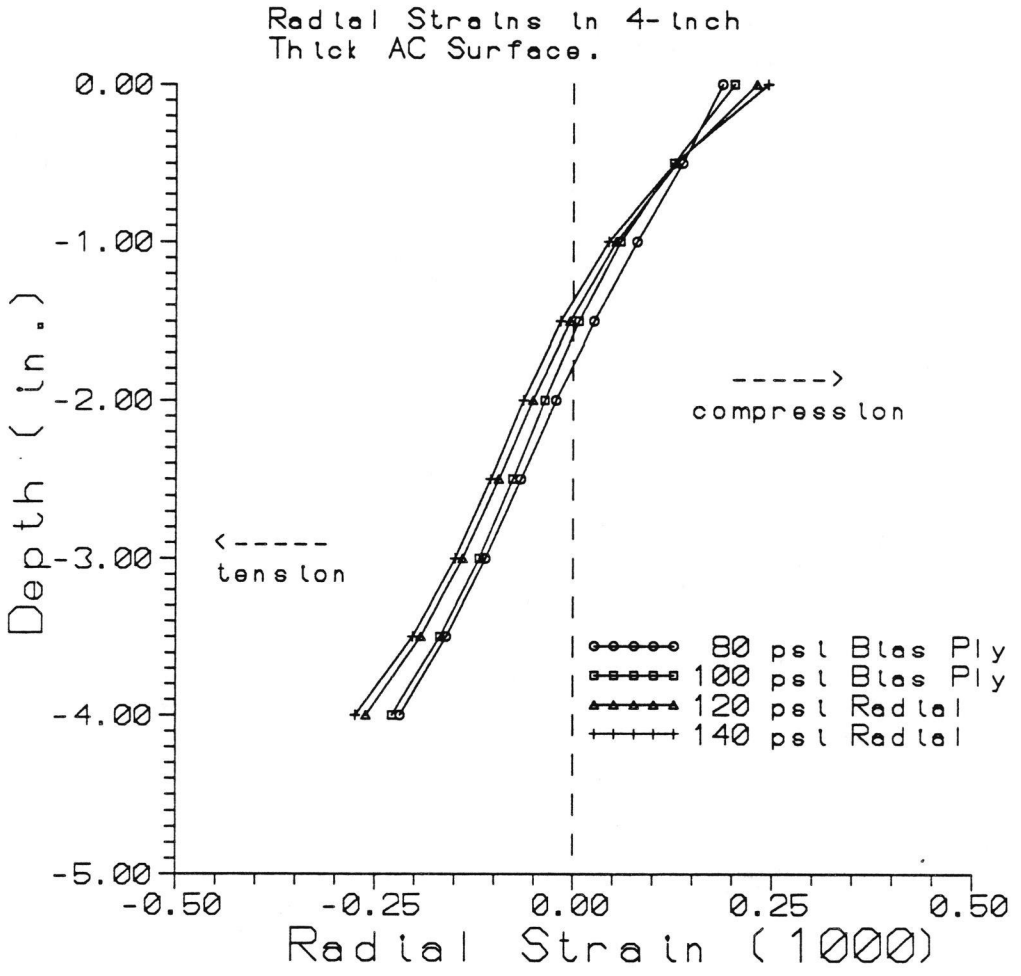

Figure 5-16. Radial Strains in 4-Inch Thick AC Surface.

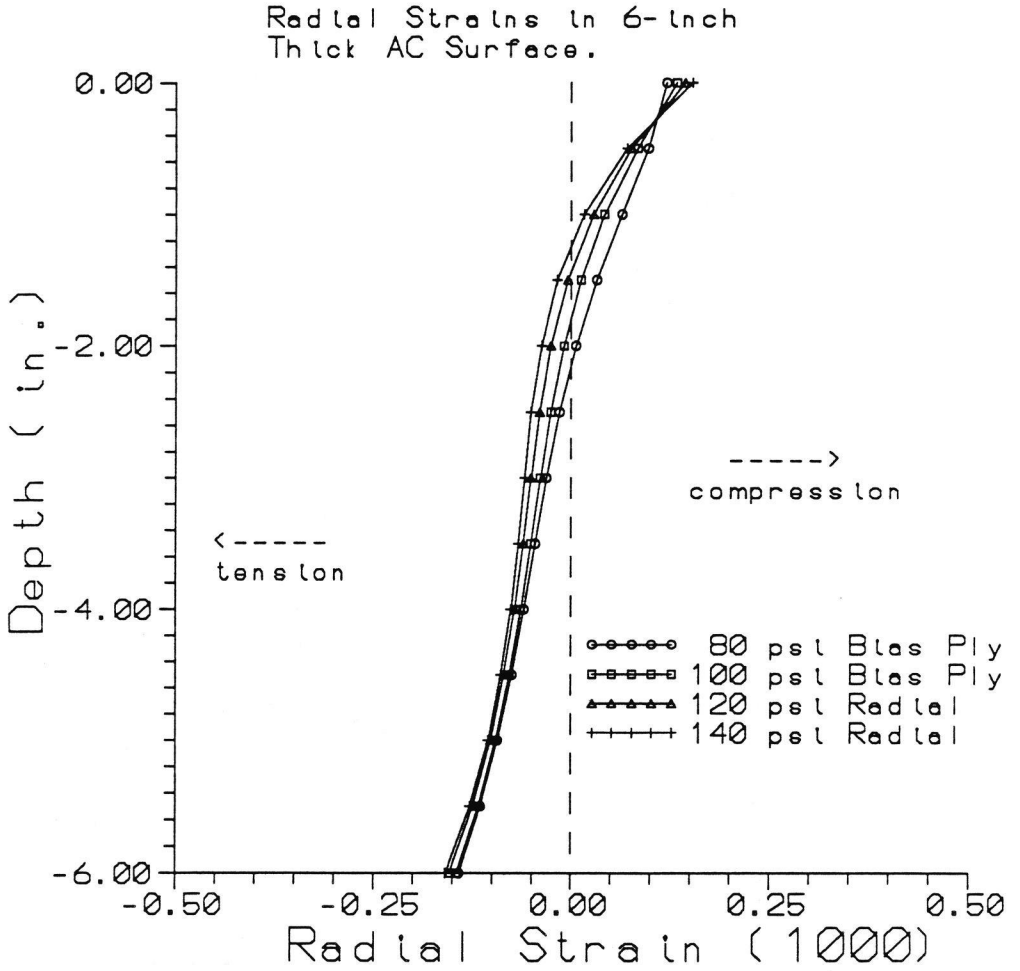

Figure 5-17. Radial Strains in 6-Inch Thick AC Surface.

tensile strain at a depth of less than or equal to 2". A complete tabulation of these analyses is shown in Appendix A, Table A.3 to Table A.8. Based on the results of these analyses, it is concluded that higher tire pressures increase the tensile strain in the AC surface leading to a potential increase in failure due to fatigue cracking. It is also concluded that the effect of higher tire pressures is more severe in thin AC surfaces.

Again, it is stressed that the above analyses are based on extreme pressures found in the field. The actual effect of higher pressures may not be as great; but, the results do suggest that the effect of high tire pressure can be reduced by increasing the AC thickness.

5.3.5 Analyses of Vertical Strain in the Base Layer

Similar to the subgrade, the vertical strain in the base layer is assumed to control the rutting in the base layer. This study analyzed the vertical strains at the top and at the bottom of the base layer to indicate the effect of increased tire pressure on potential rutting in the base layer.

Figures 5-18, 5-19, and 5-20 relate the influence of higher tire pressures on the vertical strains in the 12" thick base layer (E_{ac} = 500 ksi). Relative to an 80 psi bias ply tire, Figure 5-18 shows that for a 2" thick AC surface, the vertical strains at the top of the base increase by 6%

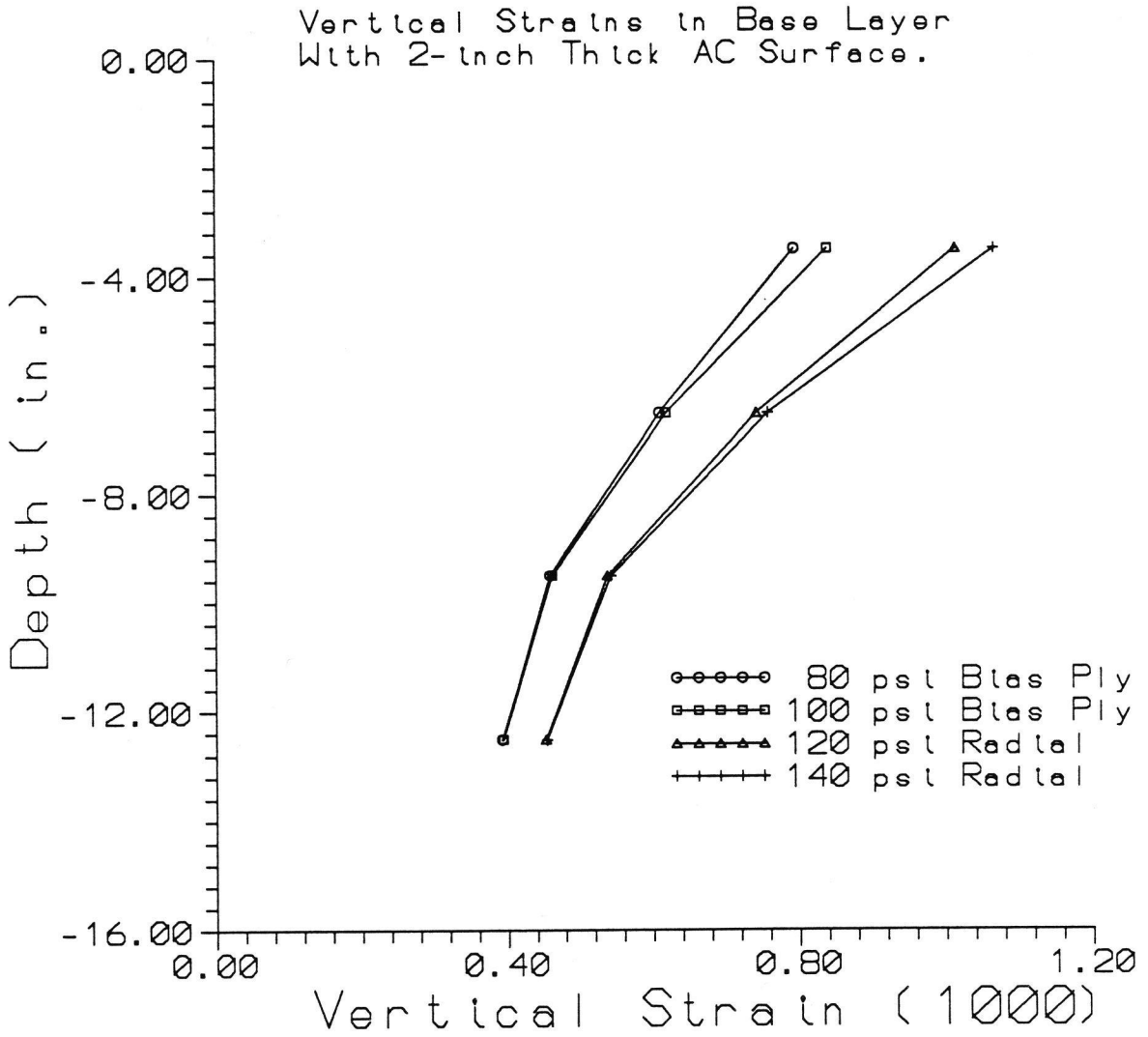

Figure 5.18 Vertical Strain in Base Layer with 2-Inch Thick AC Surface.

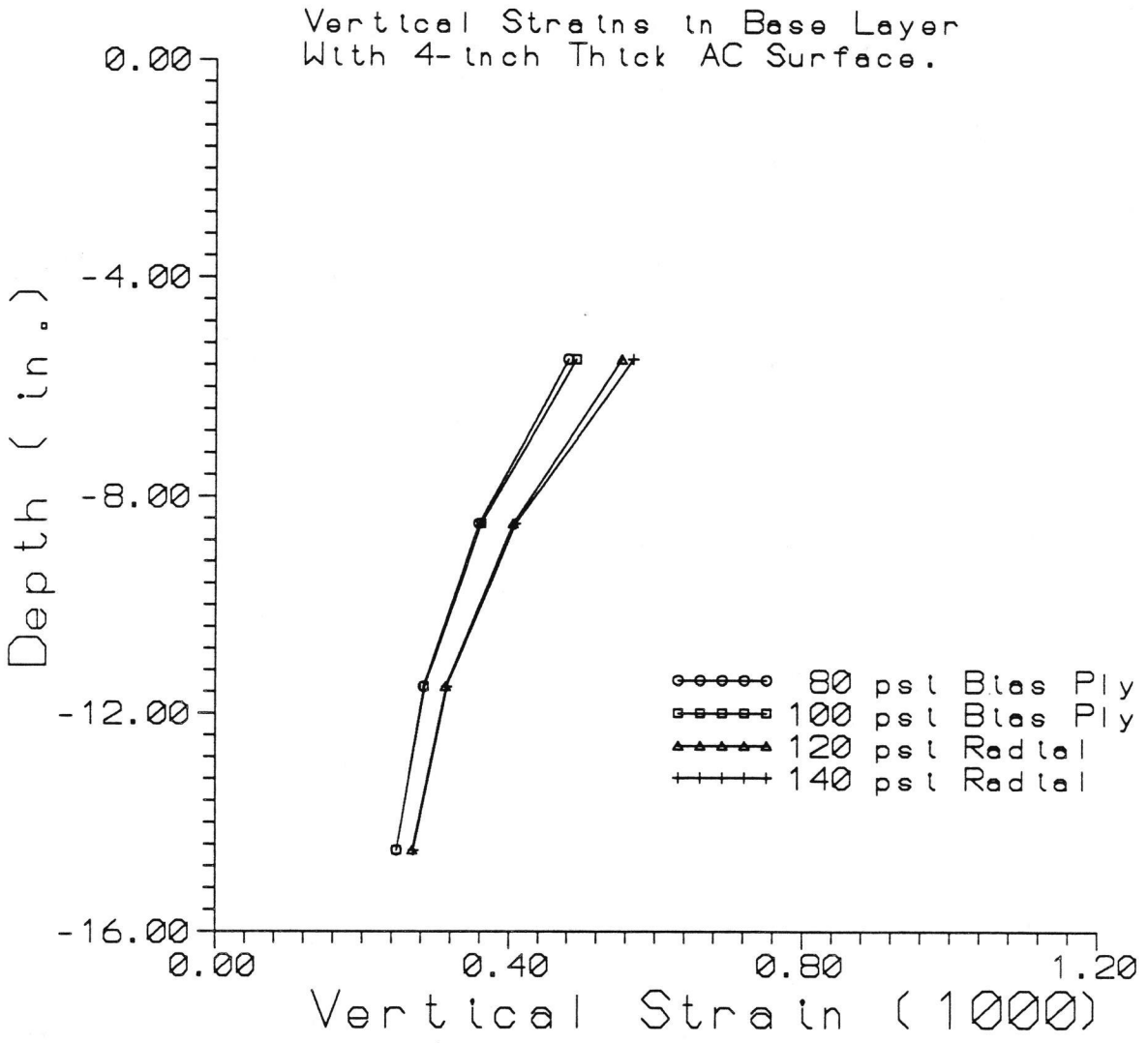

Figure 5.19 Vertical Strain in Base Layer with 4-Inch Thick AC Surface.

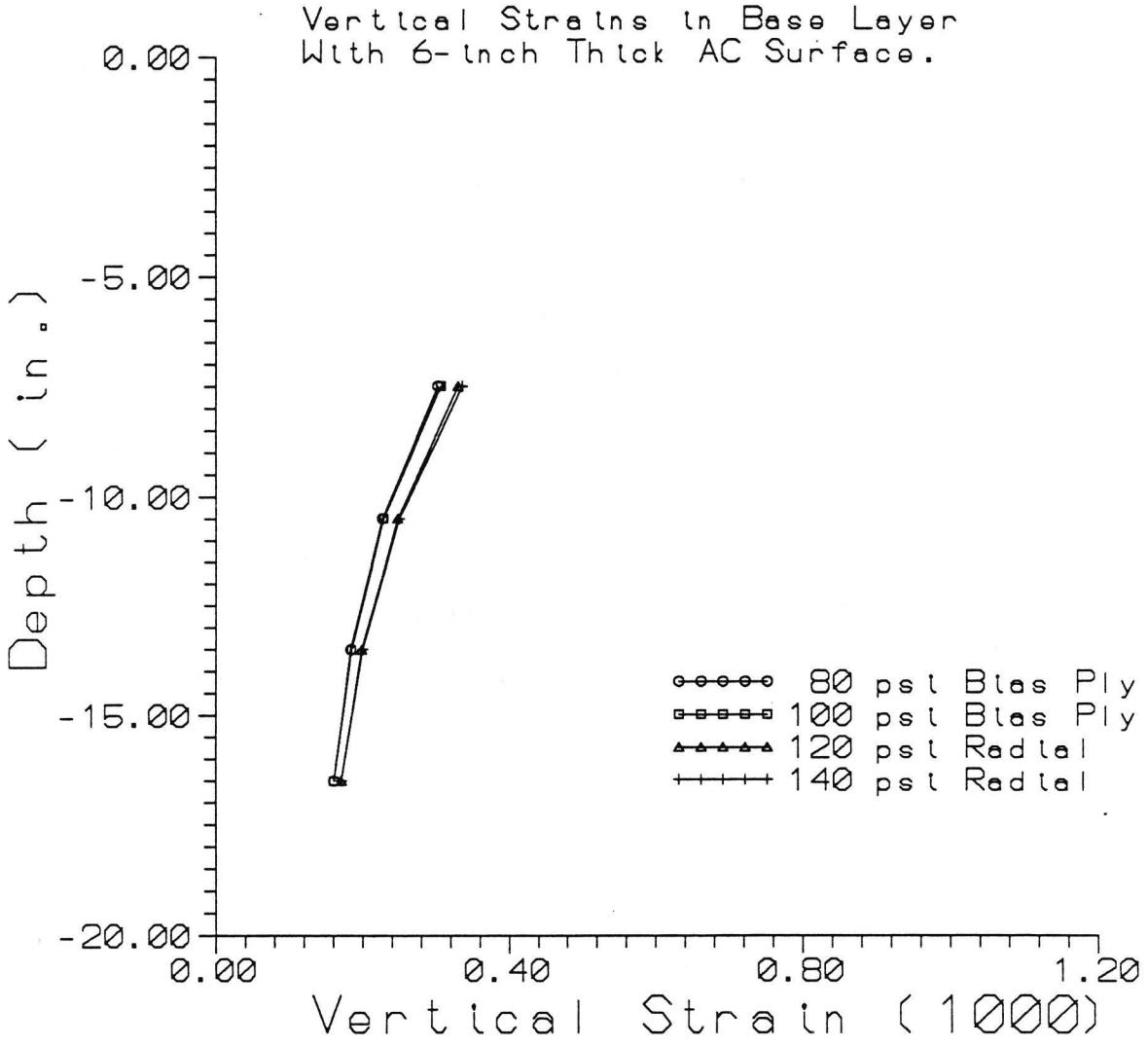

Figure 5.20 Vertical Strain in Base Layer with 6-Inch Thick AC Surface.

for the 100 psi bias ply tire, 28% for the 120 psi radial tire, and 34% for the 140 psi radial tire. These effects are reduced to 2%, 15%, and 18% respectively for the 4" AC surface (Figure 5-19); and are only 1%, 9%, and 11% increases are observed for the 6" thick AC surface (Figure 5-20). Figures 5-18, 5-19, and 5-20 also show that the increase in bias ply tire pressure (from 80 psi to 100 psi) does not have much affect on the vertical strains at the bottom of the base layer. On the other hand, a change to higher pressures and a radial tire (from 80 psi bias ply to 120 psi radial and 140 psi radial) increases the vertical strains by about 16% for the 2" AC surface, 9% for the 4" AC surface, and 7% for the 6" AC surface. Analyses of the effect of higher tire pressures on the base layer of lower AC surface modulus (E_{AC} = 50 ksi) also show similar behavior; thicker AC surface reduces the effect of high tire pressure. A complete tabulation of the above analyses can be referred to Appendix A, Table A.3 to Table A.8.

5.4 ILLIPAVE Uniform Contact Pressure Analyses

A series of ILLIPAVE analyses were performed using the normal assumption of a uniform contact pressure. The purpose of these analyses was to investigate whether or not such the uniform tire contact pressure assumption can be used without arriving at erroneous conclusions. The analyses were performed assuming uniform tire contact pressures at 80 psi,

120 psi, and 140 psi. The effects of increased uniform tire contact pressure on the normal critical strains and on the relative pavement life were analyzed. These effects were then compared to the effects reported in Sections 5.3.2 and 5.3.3.

The relative increases in normal critical strains are tabulated in Appendix A, Table A.9 and Table A.10. The relative increases in strains at other locations are tabulated in Appendix A, Table A.11 to Table A.16. Table 5.7 compares the relative increases in normal critical strains due to the uniform tire contact pressure increases to those due to non-uniform tire contact pressure increases. With the exception of the relative percentage increase in vertical subgrade strain with an AC modulus of 50 ksi (e.g. 6% vs 15%), Table 5.7 shows that increases in uniform tire contact pressure yield a slightly greater relative increase than the non-uniform (actual) contact pressure (e.g. 21% vs 19%).

Uniform tire contact pressure analyses produce a lower estimate of the actual magnitude of the tensile and vertical strains (e.g. -.226 vs -.190 and .793 vs .753) even though the relative effect of pressure increases appears greater. Nevertheless, both analyses (uniform and non-uniform pressure) arrive at similar conclusions: 1) the thin AC surfaced pavements are more significantly affected by high tire pressure, 2) the top portion of the AC surface (regardless of the total AC thickness) experiences a much greater in-

TABLE 5.7 EFFECT OF PRESSURE INCREASE ON CRITICAL PAVEMENT STRAINS UNDER UNIFORM AND NON-UNIFORM CONTACT PRESSURES.

Asphalt Thickness	% Strain Increase Contact Pressure Type Uniform	Non-Uniform	% Difference Uniform to Non-Uniform
PRESSURE INCREASE FROM 80 TO 120 PSI			
	Radial Strain at Bottom of AC		
2"	38	38	0
4"	24	20	-17
6"	12	9	-25
	Vertical Strain at Top of Subgrade		
2"	21	19	-10
4"	11	10	-9
6"	6	5	-17
PRESSURE INCREASE FROM 80 TO 140 PSI			
	Radial Strain at Bottom of AC		
2"	51	52	2
4"	30	26	-13
6"	15	12	-20
	Vertical Strain at Top of Subgrade		
2"	22	20	-9
4"	12	10	-17
6"	7	6	-14

crease in radial and vertical strains than does the lower portion, and 3) the base layer, usually ignored in most studies of the effect of high tire pressure, is affected by high tire pressure.

The results of the relative fatigue life analyses are tabulated in Table 5.8. The results shown in Table 5.8 are compared to those shown in Table 5.6 (non-uniform contact pressure). Table 5.6 and Table 5.8 show little difference in the computed R.L. losses based on the fatigue criterion. The maximum difference observed is 13% (55% and 68%) for pavement with low AC modulus (50 ksi). In most cases, uniform contact pressure analyses yield slightly higher R.L. losses than non-uniform contact pressure analyses.

The results from the uniform tire contact pressure analyses indicate higher increases in critical radial and vertical strains relative to non-uniform contact pressure analyses. Analyses at the AC surface and base layer show that both uniform and non-uniform contact pressure analyses produce similar behavior of high tire contact pressure effect on pavements. Even though uniform tire contact pressure analyses produce lower magnitude of normal critical strains, relative life analyses usually yield higher reductions in pavement life. This demonstrates that the assumption of a uniform tire contact pressure is reasonable and may be used in pavement structural analyses.

Table 5.8 Relative Fatigue Life Analysis Using Uniform Contact Pressures.

Eac = 500 ksi									
Tire Type and Pressure	Radial Tensile Microstrain			Relative Life (R.L.) Factor			Relative Life Loss %		
	2"	4"	6"	2"	4"	6"	2"	4"	6"
80 psi Bias Ply	268	202	135	---	---	---	---	---	---
120 psi Radial	369	250	151	0.35	0.50	0.69	65	50	31
140 psi Radial	403	263	156	0.26	0.42	0.62	74	58	38
Eac = 50 ksi									
Tire Type and Pressure	Radial Tensile Microstrain			Relative Life (R.L.) Factor			Relative Life Loss %		
	2"	4"	6"	2"	4"	6"	2"	4"	6"
80 psi Bias Ply	294	402	361	---	---	---	---	---	---
120 psi Radial	416	491	407	0.32	0.52	0.67	68	48	33
140 psi Radial	473	523	422	0.21	0.42	0.60	79	58	40

CHAPTER 6

CONCLUSIONS AND RECOMMENDATIONS

6.1 Conclusions

The following conclusions were made on the basis of the data and analyses from this study:

1. Truck tire pressures and tire types used on Arkansas highways are similar to those reported in other states.
2. Radial tires are more commonly used on Arkansas highways than bias ply tires.
3. Truck tire inflation pressures have increased to an average of 105 psi with pressures in excess of 120 psi not being uncommon.
4. Truck tire pressure and tire type distributions vary some by highway class and geographic region but not to the extent that consideration needs to be given in pavement design.
5. Higher tire pressures usually increase the radial and vertical strains of conventional flexible pavements, thus increasing the potential for rutting and fatigue cracking.
6. The effect of tire pressure is more significant within the upper 2 to 3 inches of the pavement section.

7. Relative life analyses show that thin pavements are affected by higher tire pressure more than are thick pavements.
8. Analyses show that the single tire model commonly used in pavement analyses is adequate to represent the relative effect of pressure increases.
9. The assumption of a uniform tire contact pressure equal to the tire inflation pressure is conservative and may be used for routine, practical pavement analyses.

6.2 Recommendation Development

From the study it is quite obvious that a major effect of the higher tire pressures is an increase in the potential for rutting within the asphalt surface layers (conclusion 4). This effect cannot be accommodated within the thickness design process but should be considered in mix design and material selection. In this respect, research under TRC-8903 suggests that consideration should be given to increasing the use of manufactured sands in asphalt concrete binder and surface mixes.

Nevertheless, other effects noted in the study can be considered during thickness design. In particular, the potential decrease in asphalt fatigue life and the increase in base and subgrade rutting potential can be accommodated by modifying the design thicknesses. Additional analyses

were performed to develop specific recommendations for design modifications to account for these effects of higher tire pressures.

The obvious method for countering the fatigue and subgrade rutting effects is to increase the asphalt surfacing thickness. The greater thickness will reduce the radial strain at the bottom of the AC to account for fatigue and also reduce the vertical subgrade strain to reduce subgrade rutting. The objective of the analyses was to determine how much the AC should be thickened and what adjustment might be needed in the design Structural Number (SN).

Taking advantage of conclusions 8 and 9 above, the analyses used the linear elastic ELSYM5 program and assumed a single 9,000 pound wheel load with the contact pressure equal to the inflation pressure. Two inflation pressures were used - 80 psi as representative of pressures at the time of the Road Test and 110 psi as representative of pressures today.

Each pavement configuration studied was analyzed in the following manner. First, the AC radial strain and subgrade vertical strain due to the 80 psi pressure was determined. Next, the AC and base thicknesses that resulted in the same strain values under the 110 psi pressure were determined by trial and error. These thicknesses were then converted to a Structural Number which was compared with the Structural Number of the pavement thicknesses used in the 80 psi analy-

sis.

The pavements analyzed had AC thicknesses ranging from 2 inches to 8 inches and base thicknesses of 12 inches and 18 inches. The Structural Numbers ranged from 2.56 to 5.60. Each pavement design was analyzed with three levels of subgrade support. The subgrade resilient modulus values used were 5, 7.5, and 10 ksi . Resilient modulus values of 500 ksi and 30 ksi were used to represent the asphalt concrete and base materials respectively.

Figure 6-1 is a plot of the AC thickness increase required versus the "normal" AC thickness. In these figures, the "normal" AC thickness is the thickness used in the 80 psi analysis. The thickness increase is the additional thickness needed in the 100 psi analysis to reduce the AC radial strain to the same level as determined in the 80 psi analysis. As should be expected, the required additional thickness reduces as the "normal" thickness increases.

The AC thickness increase is plotted versus initial Structural Number in Figure 6-2. Similar to the trend observed in Figure 6-1, the thickness increase decreases with Structural Number increases. In comparing the two figures, greater scatter is noted Figure 6-2. This shows that the required thickness increase is more a function of the "normal" AC thickness than a function of the Structural Number.

As the AC thickness increased, the base thickness had to be decreased to keep the strains under 100 psi the same

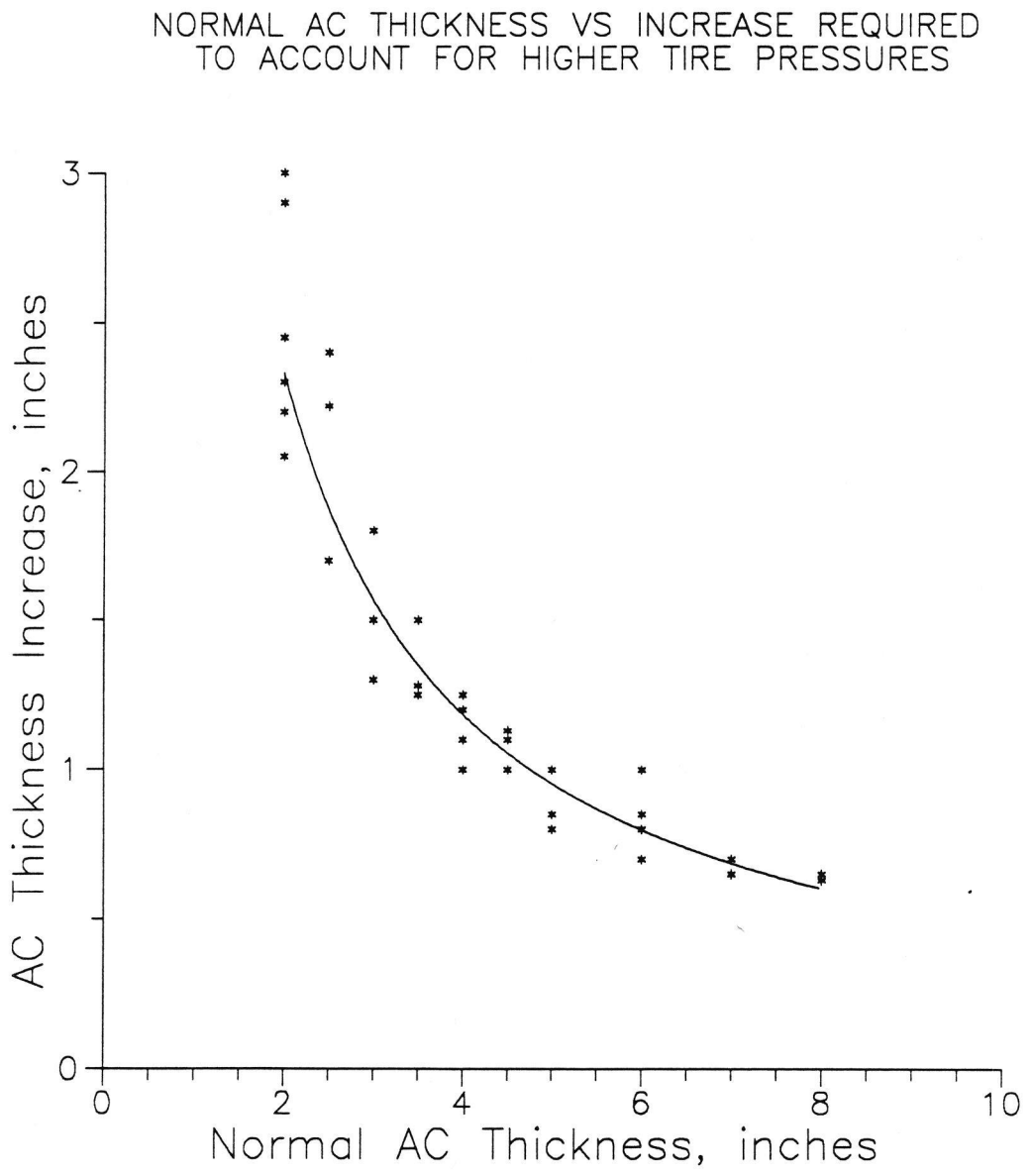

Figure 6-1. Asphalt Thickness Increase Needed to Account for Effects of Higher Tire Pressure on Fatigue.

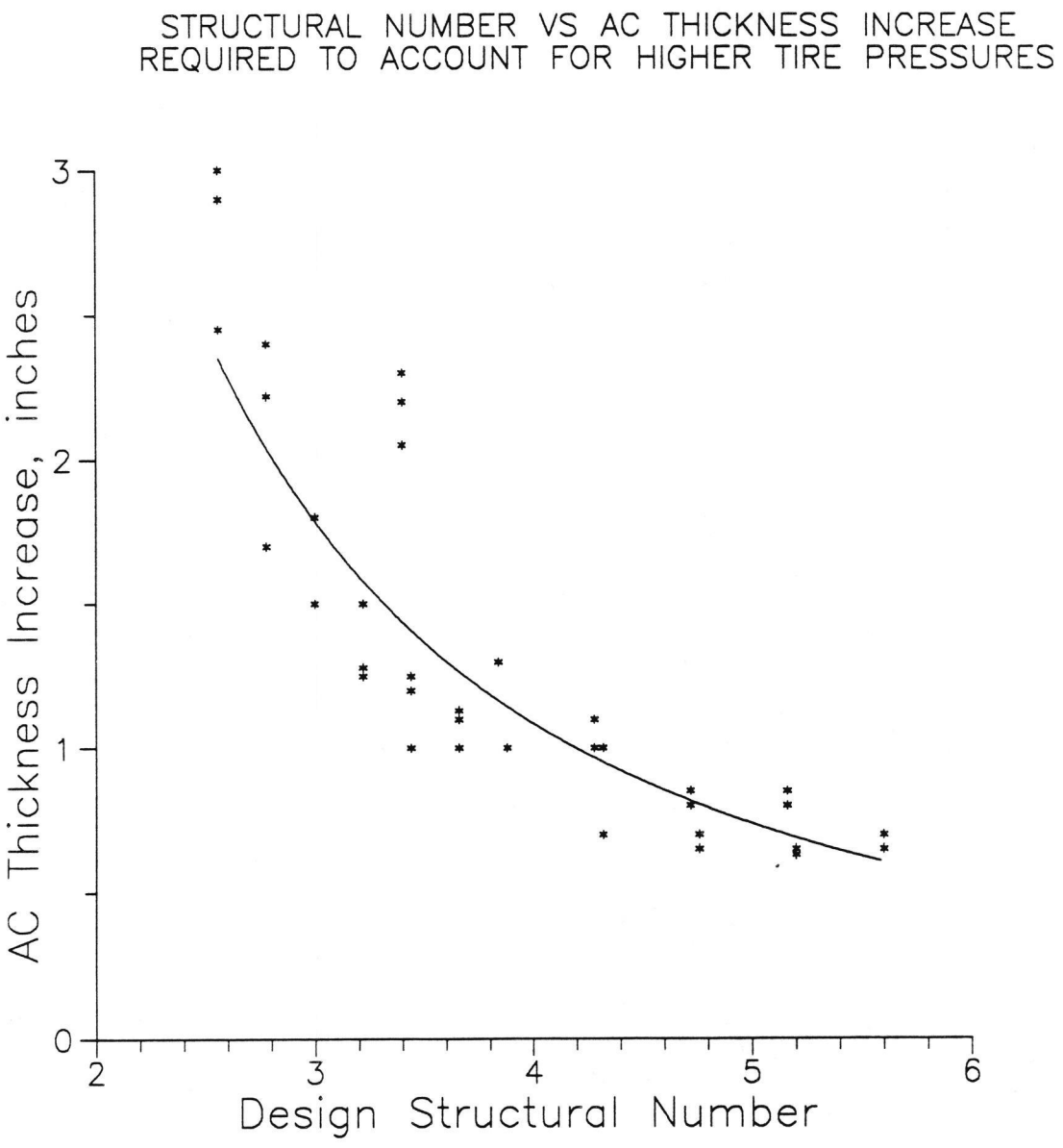

Figure 6-2. Asphalt Thickness Increase versus Design Structural Number.

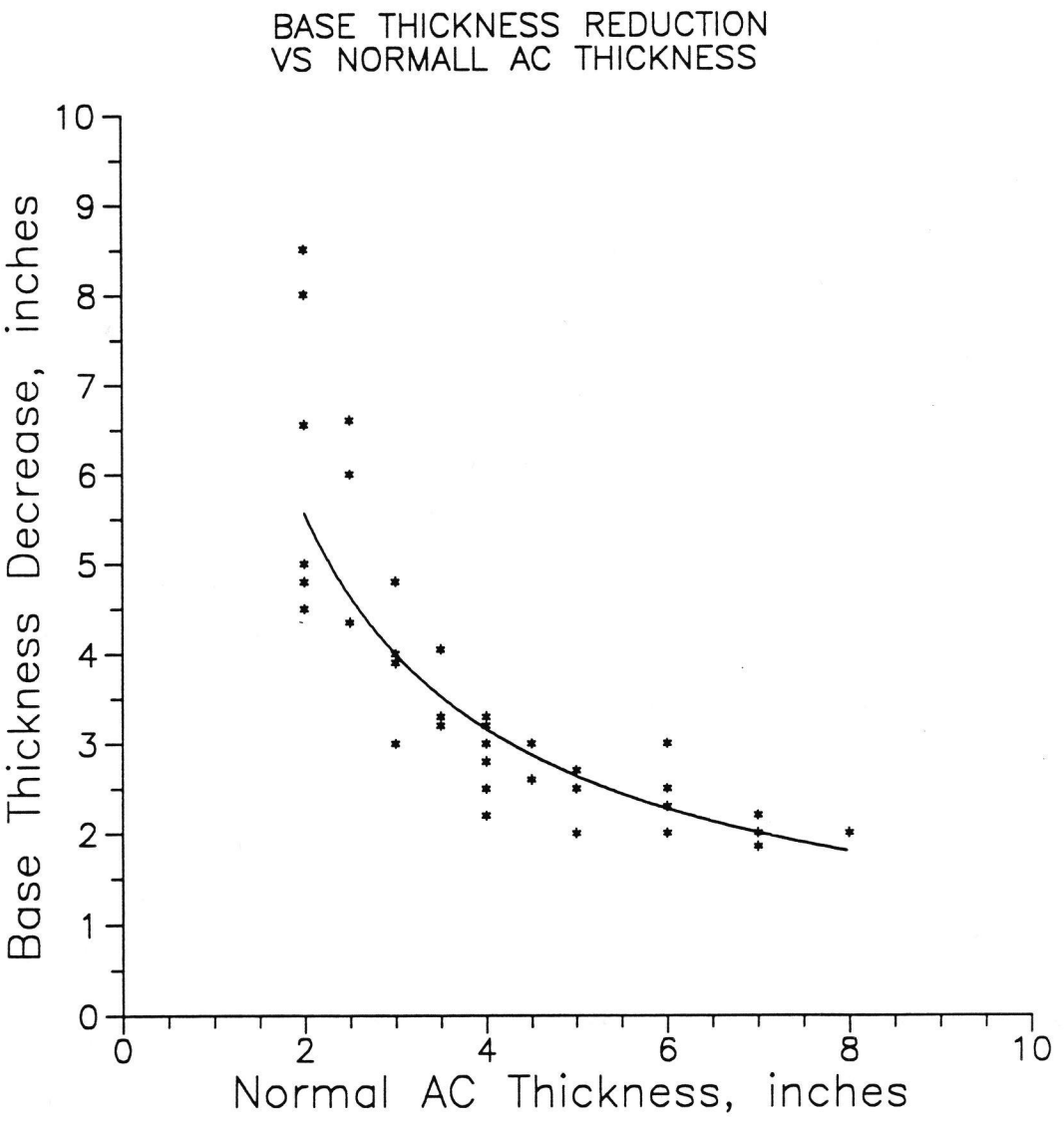

Figure 6-3. Base Thickness Decrease versus the "Normal" Asphalt Design Thickness.

as they are under 80 psi. Figure 6-3 is a plot of the base thickness decrease versus the "normal" AC thickness. The base decrease is greater with lower "normal" AC thicknesses. This also is as should be expected since the lower "normal" AC thickness would require a greater AC increase which should be matched with a greater base thickness decrease.

The thickness changes, of course, result in a change in the pavement's Structural Number. In all cases the Structural Number was increased somewhat. Figure 6-4 is a plot of the Structural Number increase versus the Structural Number of the thicknesses used in the 80 psi analysis. The most striking feature of this figure is the scatter and apparent lack of any pattern or trend. This confirms that the effect of the higher tire pressures cannot be accounted for simply by changing the design Structural Number.

From these analyses, it is apparent that a practical method of account for tire pressure effects in thickness design is to increase the "normal" AC thickness and to make a commensurate decrease in the base thickness. Figure 6-5 is a plot of the AC thickness increase versus the base thickness decrease. This plot coupled with the plot in Figure 6-1 can be used as the basis for selecting the thickness changes.

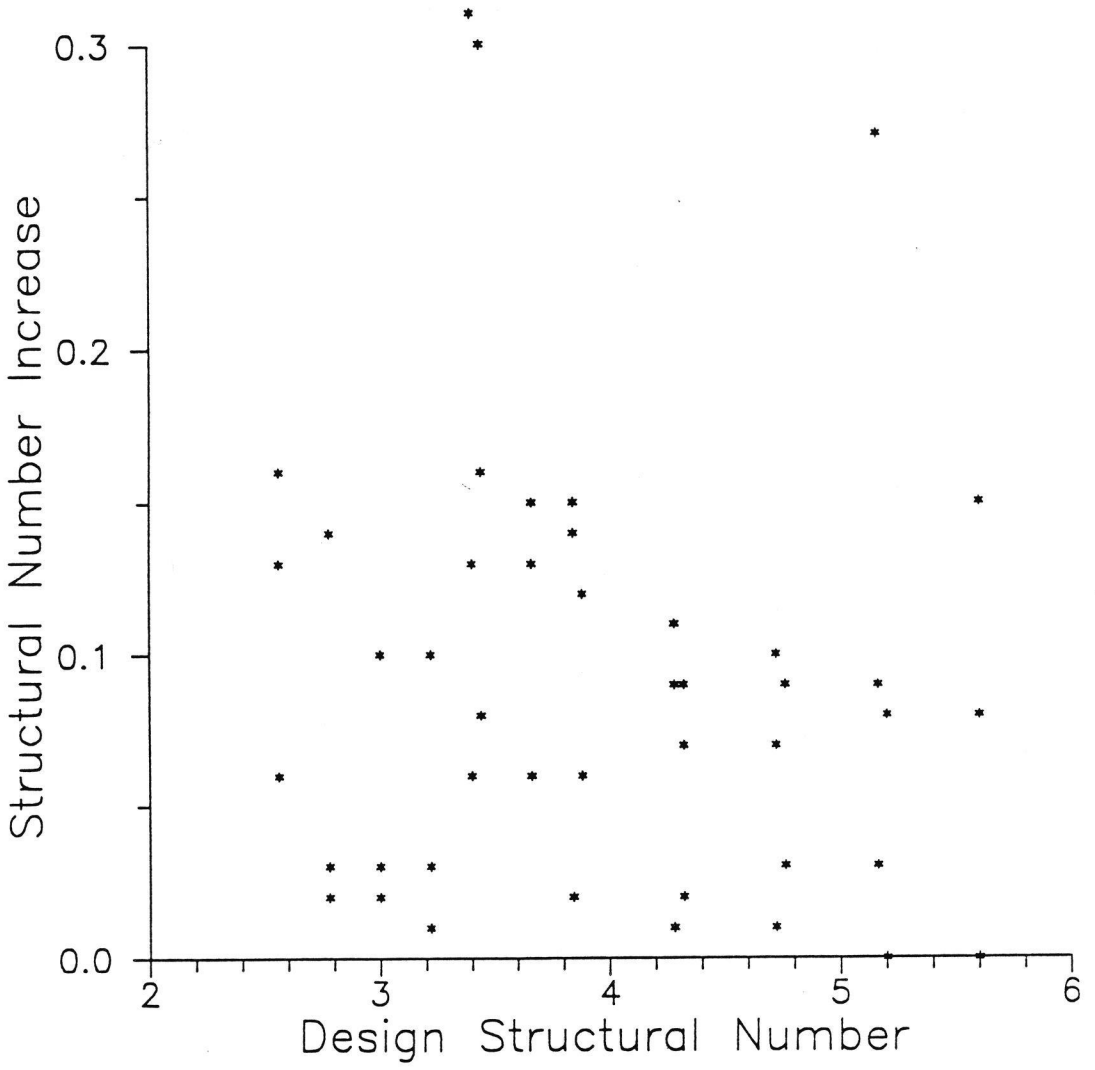

Figure 6-4. Structural Number Increase versus "Normal" Design Structural Number.

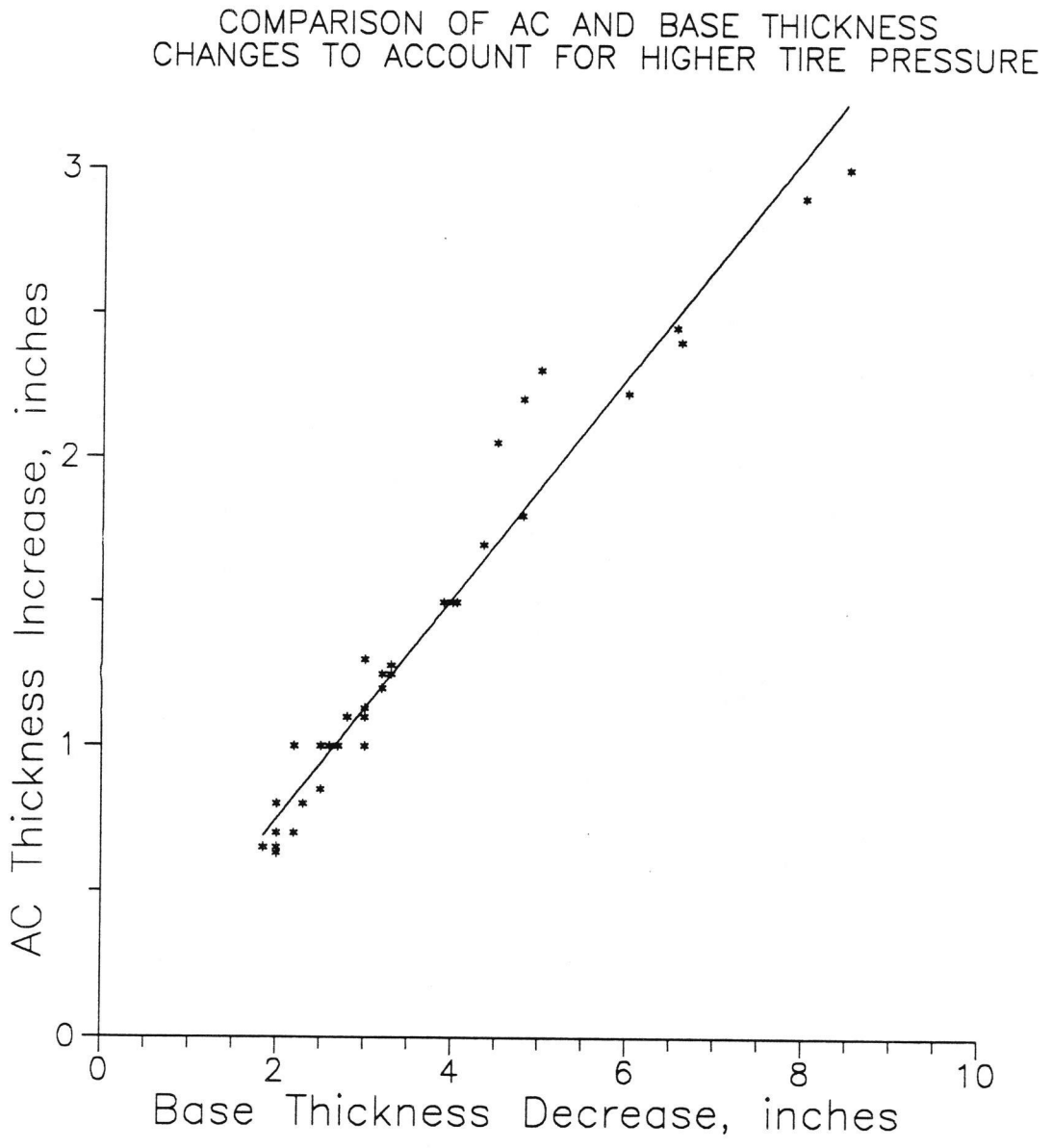

Figure 6-5. Asphalt Thickness Increase versus Base Thickness Decrease.

6.3 Recommendations

Based on these analyses, the following specific design procedure modifications are recommended:

1. The minimum design AC thickness should be 4 inches. This is based on Figure 6-1 which shows a thickness increase of 2 to 3 inches being required for a 2 inch "normal" thickness.
2. If the "normal" AC thickness (the thickness normally used in the past) is less than 4 inches, increase the design AC thickness by 1.5 inches.
3. If the "normal" AC thickness is between 4 and 6 inches, increase the design AC thickness by 1.0 inches.
4. If the "normal" AC thickness is greater than 6 inches, increase the design AC thickness by 0.5 inches.
5. If the design Structural Number is less than 4.0, increase the Structural Number by 0.1. In all other cases, make no change to the Structural Number.
6. The base (and/or subbase) thickness should be determined in the usual manner using the design Structural Number (+0.1 if < 4.0) and the design AC thickness.

The following examples are offered to help clarify the above recommendations.

EXAMPLE 1 - The Structural Number required by the AASHTO Guide for a given pavement is 2.5. In the past, an AC thickness of 2 inches would have been used. With a 2 inch AC thickness, the minimum base thickness would have been 11.6 inches. To follow the above recommendations, the design AC thickness will be increased to 4 inches and the design Structural Number will be increased by 0.10 to 2.6. The required base thickness will be 6.0 inches.

Normal Design	Recommended Design
Design SN = 2.5	SN = 2.5 + 0.1 = 2.6
Normal T_{ac} = 2"	T_{ac} = 4" (minimum)
T_{base} = (2.5-2*.44)/.14	T_{base} = (2.5-4*.44)/.14
= 11.6"	= 6.0"

EXAMPLE 2 - The Structural Number required in this example is 3.5. In the past, an AC thickness of 3 inches would have been used. With a 3 inch AC thickness, the minimum base thickness would have been 15.6 inches. Following the above recommendations, the design AC thickness will be increased 1.5 inches to 4.5 inches and the design Structural Number will be increased by 0.10 to 3.6. The required base thickness will be 11.6 inches.

Normal Design	Recommended Design
Design SN = 3.5	SN = 3.5 + 0.1 = 3.6
Normal T_{ac} = 3"	T_{ac} = 3 + 1.5 = 4.5"
T_{base} = (3.5-3*.44)/.14	T_{base} = (3.6-4.5*.44)/.14
= 15.6"	= 11.6"

EXAMPLE 3 - The Structural Number required in this example is 5.0. and the AC thickness "normally" used in the past is 5 inches. With a 5 inch AC thickness, the minimum base thickness would have been 20 inches. To follow these recommendations, the design AC thickness will be increased 1.0 inches to 6 inches and the design Structural Number will remain unchanged. The required base thickness will be 16.9 inches.

Normal Design	Recommended Design
Design SN = 5.0	SN = 5.0
Normal T_{ac} = 5"	T_{ac} = 5 + 1 = 6"
T_{base} = (5.0-5*.44)/.14	T_{base} = (5.0-6*.44)/.14
= 20.0"	= 16.9"

REFERENCES

1. ————————, "AASHTO Guide for Design of Pavement Structures," American Association of State, Highway, and Transportation Officials, Washington, D.C., 1986.

2. Asa Sharp, "Truck Tire Pavement Interaction," Proceedings of a Symposium/Workshop on High Pressure Truck Tires, Austin, Texas, 1987.

3. E. Stuart III, E. Gililland, and L. Della-Moretta, "The Use of Central Tire Inflation Systems on Low-Volume Roads," Fourth International Conference on Low-Volume Roads, Transportation Research Record 1106, 1987.

4. T.L. Ford, Impact of Truck Tire Selection on Contact Pressures, The Goodyear Tire & Rubber Company, Beijing, China Conference, Sept 11 - 26, 1988.

5. N.W. Lister and D.E. Nunn, "Contact Areas of Commercial Vehicle Tyres," RRL Report LR 172, Road Research Laboratory, England, 1968.

6. Pedro Yap, Truck Tire Types and Road Contact Pressures, The Goodyear Tire & Rubber Company. Paper prepared for Presentation at the Second International Symposium on Heavy Vehicle Weights and Dimensions.

7. J.T. Tielking, "A Finite Element Tire Model," Tire Science and Technology, Vol. 11, Nos. 1-4, pp. 50-63, 1983.

8. J. Craus, R. Yuce, and C.L. Monismith, "Fatique Behavior of Thin Asphalt Concrete in Flexible Pavement Structures," Proceedings Association of Asphalt Paving Technologists Technical Sessions, Vol. 53, 1984.

9. F.N. Finn, C. Saraf, R. Kulkarni, K. Nair, W. Smith, and A. Abdullah, "The Use of Distress Prediction Subsystems for the Design of Pavement Structures," Proceedings of the Fourth International Conference on the Structural Design of Asphalt Pavements, Vol. I, University of Michigan, Ann Arbor (August 1977), pp. 3-38 (PSAD).

10. C. Saraf, K. Marshek, H. Chen, R. Conell, and W.R. Hudson, "The Effect of Truck Tire Contact Pressure Distribution on The Design of Flexible Pavements," The Sixth International Conference for the Structural Design of Asphalt Pavements, The University of Michigan, Ann Arbor, Michigan 1987, pp. 180-190.

11. F.L. Roberts, J.T. Tielking, D. Middleton, R.L. Lytton, and K. Tseng, "Effects of Tire Pressures on Flexible Pavements," Research Report 372-1F, Texas Transportation Institute, The Texas A&M University System, College Station, TX, 1986.

12. M.R. Thompson, "Analytical Methods for Considering Tire Pressure Effects in Pavement Design," Proceedings of a Symposium/Workshop on High Pressure Truck Tires, Sponsored by AASHTO, Austin, Texas, 1987.

13. W.D.O. Patterson, Review of Equivalent Single Wheel Mass Concept and Damaging Effect of Wheel Loads, Report to National Institute for Transport and Road Research, Pretoria, South Africa (August 1979), 47 pp.

14. J. Eisenmann and A. Hilmer, "Influence of Wheel Load and Inflation Pressure on the Rutting Effect at Asphalt Pavements: Experiments and Theoretical Investigations," Sixth International Conference, Structural Design of Asphalt Pavements, 1987. pp. 393-403.

15. R.C.G. Haas and A.T. Papagianakis, "Understanding Pavement Rutting," Roads and Transportation Association of Canada, Toronto, Ontario, 1986.

16. P. Sebaaly and N. Tabatabaee, "Effect of Tire Pressure and Types on the Response of Flexible Pavement," Pennsylvania Transportation Institute, Presented at the 68th. Annual TRB meeting, Report No. 880230, Jan. 1989.

17. S.W. Hudson & S.B. Seeds, "Evaluation of Increased Pavement Loading and Tire Pressures," Transportation Research Record 1207.

18. R.F. Bonaquist, C.J. Churilla, and D.M. Freund, "Effect of Load, Tire Pressure, and Tire Type on Flexible Pavement Response," Transportation Research Record 1207.

19. R.P. Elliott, "Design Transfer Functions For Asphalt Pavements," Unpublished paper.

20. ————————, "Predictive Design Procedure, VESYS Users Manual," Federal Highway Administration, Report No. FHWA-RD-77-154, 1978.

21. ————————, "Thickness Design - Asphalt Pavements for Highways and Streets," Manual Series No. 1, The Asphalt Institute, 1981.

22. ————————, "Shell Pavement Design Manual," Shell International Petroleum Company Limited, London, 1978.

23. R.D. Pavlovich and T.S. Shuler, "Shear Models for Pavement Rutting," Proceedings Twenty-Fifth Paving and Transportation Conference, Civil Engineering Department, University of New Mexico, Albuquerque, New Mexico, 1988.

24. E.R. Brown, "Mix Design and Construction of Asphalt Concrete to Support High Tire Pressures," Proceedings Twenty-Fifth Paving and Transportation Conference, Civil Engineering Department, University of New Mexico, Albuquerque, New Mexico, 1988.

25. O.K. Kim, C.A. Bell, J.E. Wilson, and G. Boyle, "Study on Mix Design Criteria for Controlling the Effect of Increased Tire Pressure on Asphalt Pavement," Transportation Research Record 1171, 1988.

26. O.K. Kim, C.A. Bell, and J.E. Wilson, "Effect of Increased Truck Tire Pressure on Asphalt Concrete Pavement," Journal of Transportation Engineering, Vol. 115, No. 4, July, 1989.

27. S.K. Wong, "Comparison of Dynamic Loading Test Versus Static Loading Test to Evaluate Rutting Potential of Asphalt Concrete," University of Arkansas, Fayetteville, Arkansas.

APPENDIX A

Table A.1 Comparison of Critical Strains and Stresses (Eac = 500 ksi).

Pavement Type: Conventional AC Pavement

Comparison of Critical Strains and Stresses Date: 6/19/90

Eac = 500000 psi AC Layer: Radial Strain 10^3

Pavement Type	Bias Ply 80 psi	Bias Ply 100 psi	% Increase	Radial 120 psi	% Increase	Radial 140 psi	% Increase
2 in. AC	-0.292	-0.328	12.58	-0.403	38.28	-0.444	52.18
4 in. AC	-0.218	-0.228	4.49	-0.261	19.58	-0.274	25.85
6 in. AC	-0.142	-0.145	2.29	-0.154	8.55	-0.159	11.92

Eac = 500000 psi Subgrade: Vertical Strain 10^3

Pavement Type	Bias Ply 80 psi	Bias Ply 100 psi	% Increase	Radial 120 psi	% Increase	Radial 140 psi	% Increase
2 in. AC	0.438	0.440	0.51	0.522	19.19	0.526	20.08
4 in. AC	0.246	0.247	0.31	0.271	9.99	0.271	10.28
6 in. AC	0.147	0.147	0.09	0.155	5.31	0.155	5.46

Eac = 500000 psi AC Layer: Radial Stress

Pavement Type	Bias Ply 80 psi	Bias Ply 100 psi	% Increase	Radial 120 psi	% Increase	Radial 140 psi	% Increase
2 in. AC	-145.00	-166.00	14.48	-202.00	39.31	-222.00	53.10
4 in. AC	-145.00	-151.00	4.14	-173.00	19.31	-181.00	24.83
6 in. AC	-102.00	-104.00	1.96	-110.00	7.84	-113.00	10.78

Eac = 500000 psi Subgrade: Vertical Stress

Pavement Type	Bias Ply 80 psi	Bias Ply 100 psi	% Increase	Radial 120 psi	% Increase	Radial 140 psi	% Increase
2 in. AC	5.98	6.00	0.33	6.98	16.72	7.01	17.22
4 in. AC	4.44	4.45	0.23	4.89	10.14	4.89	10.14
6 in. AC	3.53	3.53	0.00	3.76	6.52	3.76	6.52

Table A.2 Comparison of Critical Strains and Stresses (Eac = 50 ksi).

Pavement Type: Conventional AC Pavement

Comparison of Critical Strains and Stresses Date: 6/19/90

Eac = 50000 psi AC Layer: Radial Strain 10^3

Pavement Type	Bias Ply 80 psi	Bias Ply 100 psi	% Increase	Radial 120 psi	% Increase	Radial 140 psi	% Increase
2 in. AC	-0.376	-0.385	2.53	-0.480	27.76	-0.548	45.98
4 in. AC	-0.434	-0.496	14.50	-0.519	19.62	-0.553	27.49
6 in. AC	-0.389	-0.435	11.76	-0.418	7.60	-0.434	11.59

Eac = 50000 psi Subgrade: Vertical Strain 10^3

Pavement Type	Bias Ply 80 psi	Bias Ply 100 psi	% Increase	Radial 120 psi	% Increase	Radial 140 psi	% Increase
2 in. AC	0.597	0.601	0.68	0.687	15.15	0.696	16.62
4 in. AC	0.454	0.456	0.46	0.509	12.06	0.513	13.04
6 in. AC	0.347	0.348	0.35	0.380	9.51	0.382	10.22

Eac = 50000 psi AC Layer: Radial Stress

Pavement Type	Bias Ply 80 psi	Bias Ply 100 psi	% Increase	Radial 120 psi	% Increase	Radial 140 psi	% Increase
2 in. AC	36.30	41.50	14.33	49.80	37.19	56.60	55.92
4 in. AC	4.99	5.29	6.01	6.41	28.46	7.07	41.68
6 in. AC	-7.42	-7.57	2.02	-7.28	-1.89	-7.49	0.94

Eac = 50000 psi Subgrade: Vertical Stress

Pavement Type	Bias Ply 80 psi	Bias Ply 100 psi	% Increase	Radial 120 psi	% Increase	Radial 140 psi	% Increase
2 in. AC	7.15	7.18	0.42	8.24	15.24	8.30	16.08
4 in. AC	6.19	6.21	0.32	7.02	13.41	7.05	13.89
6 in. AC	5.41	5.42	0.18	6.00	10.91	6.03	11.46

Table A.3 Radial and Vertical Strains in AC (2", Eac = 500 ksi) and Base Layers.

Pavement Type 1 AC thkness: 2 in. Date: 6/19/90
Eac: 500000 psi

AC layer Vertical Strain 10^3

Depth in.	Nodal Point	Bias Ply 80 psi	Bias Ply 100 psi	% Increase	Radial 120 psi	% Increase	Radial 140 psi	% Increase
-0.25	1-17	-0.226	-0.210	-6.80	-0.226	0.29	-0.221	-2.16
-0.75	17-33	-0.041	0.005	-113.05	0.035	-185.66	0.062	-252.78
-1.25	33-49	0.149	0.200	34.39	0.262	76.02	0.302	102.71
-1.75	49-65	0.333	0.387	16.17	0.488	46.22	0.539	61.77

Base Layer Vertical Strain 10^3

Depth in.	Nodal Point	Bias Ply 80 psi	Bias Ply 100 psi	% Increase	Radial 120 psi	% Increase	Radial 140 psi	% Increase
-3.5	65-81	0.793	0.838	5.66	1.012	27.64	1.065	34.34
-6.5	81-97	0.609	0.618	1.58	0.741	21.83	0.757	24.40
-9.5	97-113	0.458	0.461	0.69	0.537	17.36	0.542	18.41
-12.5	113-129	0.392	0.394	0.53	0.452	15.19	0.454	15.89

AC Layer Radial Strain 10^3

Depth in.	Nodal Point	Bias Ply 80 psi	Bias Ply 100 psi	% Increase	Radial 120 psi	% Increase	Radial 140 psi	% Increase
0.0	1-2	0.285	0.317	11.31	0.385	35.01	0.418	46.52
-0.5	17-18	0.146	0.143	-2.39	0.162	10.75	0.168	14.67
-1.0	33-34	0.001	-0.018	-1471.17	-0.030	-2408.54	-0.040	-3251.48
-1.5	49-50	-0.144	-0.169	17.50	-0.211	46.52	-0.234	63.00
-2.0	65-66	-0.289	-0.328	13.83	-0.403	39.81	-0.444	53.86

Base Layer Radial Strain 10^3

Depth in.	Nodal Point	Bias Ply 80 psi	Bias Ply 100 psi	% Increase	Radial 120 psi	% Increase	Radial 140 psi	% Increase
-5.0	81-82	-0.275	-0.284	3.05	-0.351	27.56	-0.364	32.28
-8.0	97-98	-0.210	-0.212	0.94	-0.252	20.10	-0.256	21.85
-11.0	113-114	-0.178	-0.179	0.63	-0.205	15.56	-0.207	16.57
-14.0	129-130	-0.199	-0.200	0.57	-0.232	16.38	-0.234	17.28

Table A.4 Radial and Vertical Strains in AC (4", Eac = 500 ksi) and Base Layers

Pavement Type 2 AC thkness: 4 in. Date: 6/19/90
Eac: 500000 psi

AC layer Vertical Strain 10^3

Depth in.	Nodal Point	Bias Ply 80 psi	Bias Ply 100 psi	% Increase	Radial 120 psi	% Increase	Radial 140 psi	% Increase
-0.25	1-17	-0.152	-0.119	-21.75	-0.097	-36.01	-0.072	-52.45
-0.75	17-33	-0.083	-0.026	-68.64	0.010	-112.13	0.046	-155.41
-1.25	33-49	-0.011	0.045	-498.54	0.083	-841.96	0.121	-1174.07
-1.75	49-65	0.052	0.095	83.98	0.134	160.33	0.168	224.94
-2.25	65-81	0.105	0.135	28.69	0.173	65.05	0.201	90.89
-2.75	81-97	0.155	0.175	13.06	0.212	36.91	0.233	50.77
-3.25	97-113	0.208	0.222	6.89	0.260	24.91	0.278	33.53
-3.75	113-129	0.270	0.283	4.84	0.327	21.11	0.345	27.69

Base Layer Vertical Strain 10^3

Depth in.	Nodal Point	Bias Ply 80 psi	Bias Ply 100 psi	% Increase	Radial 120 psi	% Increase	Radial 140 psi	% Increase
-5.5	129-145	0.481	0.492	2.18	0.554	15.17	0.570	18.34
-8.5	145-161	0.359	0.362	0.73	0.405	12.79	0.409	13.87
-11.5	161-177	0.284	0.285	0.37	0.314	10.65	0.315	11.07
-14.5	177-193	0.247	0.247	0.28	0.269	9.04	0.270	9.29

AC Layer Radial Strain 10^3

Depth in.	Nodal Point	Bias Ply 80 psi	Bias Ply 100 psi	% Increase	Radial 120 psi	% Increase	Radial 140 psi	% Increase
0.00	1-2	0.187	0.202	8.35	0.230	23.48	0.244	30.76
-0.50	17-18	0.137	0.126	-8.06	0.130	-5.17	0.127	-7.03
-1.00	33-34	0.080	0.059	-25.86	0.054	-32.62	0.044	-45.24
-1.50	49-50	0.026	0.007	-72.34	-0.004	-115.78	-0.016	-162.88
-2.00	65-66	-0.022	-0.036	65.04	-0.051	132.16	-0.063	185.58
-2.50	81-82	-0.066	-0.077	15.57	-0.094	41.48	-0.104	57.31
-3.00	97-98	-0.111	-0.119	7.07	-0.139	25.00	-0.149	33.78
-3.50	113-114	-0.160	-0.168	4.59	-0.192	19.76	-0.202	26.26
-4.00	129-130	-0.218	-0.228	4.49	-0.261	19.58	-0.274	25.85

Base Layer Radial Strain 10^3

Depth in.	Nodal Point	Bias Ply 80 psi	Bias Ply 100 psi	% Increase	Radial 120 psi	% Increase	Radial 140 psi	% Increase
-7.00	145-146	-0.158	-0.160	1.29	-0.181	14.81	-0.184	16.97
-10.00	161-162	-0.123	-0.124	0.55	-0.137	11.30	-0.138	12.13
-13.00	177-178	-0.106	-0.107	0.37	-0.115	8.49	-0.116	8.93
-16.00	193-194	-0.111	-0.111	0.34	-0.119	7.51	-0.119	7.82

Table A.5 Radial and Vertical Strains in AC (6", Eac = 500 ksi) and Base Layers

Pavement Type 3 AC thkness: 6 in. Date: 6/19/90
Eac: 500000 psi

AC layer Vertical Strain 10^3

Depth in.	Nodal Point	Bias Ply 80 psi	Bias Ply 100 psi	% Increase	Radial 120 psi	% Increase	Radial 140 psi	% Increase
-0.25	1-17	-0.080	-0.044	-44.45	-0.002	-97.97	0.028	-134.63
-0.75	17-33	-0.042	0.017	-140.96	0.068	-263.54	0.107	-357.77
-1.25	33-49	0.002	0.060	2397.18	0.110	4437.87	0.150	6102.70
-1.75	49-65	0.040	0.085	114.79	0.131	231.06	0.167	321.86
-2.25	65-81	0.066	0.099	49.44	0.139	110.84	0.169	155.50
-2.75	81-97	0.083	0.106	27.03	0.140	67.60	0.163	94.97
-3.25	97-113	0.095	0.111	16.10	0.138	44.47	0.155	62.36
-3.75	113-129	0.106	0.116	9.90	0.137	29.85	0.150	41.75
-4.25	129-145	0.117	0.124	6.15	0.140	20.05	0.149	28.01
-4.75	145-161	0.131	0.137	3.89	0.149	13.66	0.157	19.11
-5.25	161-177	0.152	0.156	2.70	0.167	10.02	0.173	14.07
-5.75	177-193	0.180	0.184	2.31	0.196	9.16	0.202	12.57

Base Layer Vertical Strain 10^3

Depth in.	Nodal Point	Bias Ply 80 psi	Bias Ply 100 psi	% Increase	Radial 120 psi	% Increase	Radial 140 psi	% Increase
-7.5	193-209	0.303	0.307	1.45	0.330	9.19	0.336	10.97
-10.5	209-225	0.227	0.229	0.68	0.248	9.24	0.250	9.88
-13.5	225-241	0.184	0.185	0.43	0.199	8.25	0.200	8.50
-16.5	241-257	0.161	0.161	0.27	0.171	6.51	0.171	6.62

AC Layer Radial Strain 10^3

Depth in.	Nodal Point	Bias Ply 80 psi	Bias Ply 100 psi	% Increase	Radial 120 psi	% Increase	Radial 140 psi	% Increase
0.0	1-2	0.120	0.133	11.35	0.143	19.93	0.153	28.21
-0.5	17-18	0.097	0.084	-12.72	0.076	-21.69	0.070	-26.97
-1.0	33-34	0.064	0.042	-33.90	0.028	-56.07	0.016	-74.67
-1.5	49-50	0.032	0.012	-61.78	-0.004	-113.68	-0.018	-155.97
-2.0	65-66	0.006	-0.009	-267.75	-0.026	-559.00	-0.038	-779.20
-2.5	81-82	-0.015	-0.026	72.41	-0.040	170.91	-0.051	239.98
-3.0	97-98	-0.031	-0.039	24.05	-0.051	63.27	-0.059	89.13
-3.5	113-114	-0.046	-0.051	11.54	-0.061	33.29	-0.067	47.01
-4.0	129-130	-0.060	-0.064	6.31	-0.072	19.67	-0.077	27.88
-4.5	145-146	-0.075	-0.078	3.79	-0.085	12.65	-0.089	18.05
-5.0	161-162	-0.093	-0.096	2.60	-0.102	9.16	-0.105	13.15
-5.5	177-178	-0.115	-0.117	2.17	-0.124	7.92	-0.128	11.32
-6.0	193-194	-0.142	-0.145	2.29	-0.154	8.55	-0.159	11.92

Base Layer Radial Strain 10^3

Depth in.	Nodal Point	Bias Ply 80 psi	Bias Ply 100 psi	% Increase	Radial 120 psi	% Increase	Radial 140 psi	% Increase
-9.0	209-210	-0.098	-0.098	0.92	-0.105	7.61	-0.106	8.96
-12.0	225-226	-0.077	-0.077	0.52	-0.081	6.49	-0.082	7.08
-15.0	241-242	-0.067	-0.067	0.28	-0.070	4.23	-0.070	4.50
-18.0	257-258	-0.066	-0.066	0.11	-0.067	2.43	-0.067	2.60

Table A.6 Radial and Vertical Strains in AC (2", Eac = 50 ksi) and Base Layers.

Pavement Type 4 AC thkness: 2 in. Date: 6/19/90
Eac: 50000 psi

AC layer Vertical Strain 10^3

Depth in.	Nodal Point	Bias Ply 80 psi	Bias Ply 100 psi	% Increase	Radial 120 psi	% Increase	Radial 140 psi	% Increase
-0.25	1-17	0.345	0.744	115.65	1.253	263.07	1.604	364.83
-0.75	17-33	0.514	1.133	120.57	1.679	226.92	2.112	311.24
-1.25	33-49	0.786	1.390	76.79	1.891	140.57	2.321	195.32
-1.75	49-65	1.034	1.466	41.72	1.890	82.75	2.239	116.42

Base Layer Vertical Strain 10^3

Depth in.	Nodal Point	Bias Ply 80 psi	Bias Ply 100 psi	% Increase	Radial 120 psi	% Increase	Radial 140 psi	% Increase
-3.5	65-81	1.022	1.135	11.03	1.303	27.46	1.409	37.86
-6.5	81-97	0.836	0.862	3.14	0.947	13.32	0.982	17.53
-9.5	97-113	0.608	0.614	1.03	0.663	9.01	0.673	10.79
-12.5	113-129	0.504	0.508	0.69	0.554	9.91	0.560	11.11

AC Layer Radial Strain 10^3

Depth in.	Nodal Point	Bias Ply 80 psi	Bias Ply 100 psi	% Increase	Radial 120 psi	% Increase	Radial 140 psi	% Increase
0.0	1-2	0.249	0.345	38.96	0.372	49.65	0.418	68.27
-0.5	17-18	0.213	0.070	-67.09	-0.048	-122.49	-0.126	-159.46
-1.0	33-34	0.043	-0.183	-528.55	-0.330	-870.09	-0.461	-1177.47
-1.5	49-50	-0.143	-0.330	130.83	-0.471	229.50	-0.597	317.67
-2.0	65-66	-0.304	-0.385	26.81	-0.480	58.01	-0.548	80.55

Base Layer Radial Strain 10^3

Depth in.	Nodal Point	Bias Ply 80 psi	Bias Ply 100 psi	% Increase	Radial 120 psi	% Increase	Radial 140 psi	% Increase
-5.0	81-82	-0.384	-0.408	6.44	-0.460	19.90	-0.489	27.30
-8.0	97-98	-0.292	-0.296	1.49	-0.318	8.93	-0.326	11.62
-11.0	113-114	-0.236	-0.238	0.80	-0.255	8.17	-0.259	9.74
-14.0	129-130	-0.272	-0.274	0.73	-0.303	11.35	-0.307	12.83

Table A.7 Radial and Vertical Strains in AC (4", Eac = 50 ksi) and Base Layers.

Pavement Type 5 AC thkness: 4 in. Date: 6/19/90
Eac: 50000 psi

AC layer Vertical Strain 10^3

Depth in.	Nodal Point	Bias Ply 80 psi	Bias Ply 100 psi	% Increase	Radial 120 psi	% Increase	Radial 140 psi	% Increase
-0.25	1-17	0.223	0.587	163.99	1.042	368.20	1.351	507.22
-0.75	17-33	0.426	1.020	139.32	1.544	262.18	1.951	357.70
-1.25	33-49	0.722	1.310	81.55	1.819	152.06	2.238	210.14
-1.75	49-65	0.976	1.442	47.68	1.925	97.17	2.304	136.00
-2.25	65-81	1.135	1.473	29.88	1.911	68.47	2.229	96.45
-2.75	81-97	1.202	1.442	19.95	1.822	51.60	2.075	72.69
-3.25	97-113	1.197	1.363	13.94	1.677	40.17	1.871	56.35
-3.75	113-129	1.137	1.246	9.60	1.484	30.56	1.620	42.47

Base Layer Vertical Strain 10^3

Depth in.	Nodal Point	Bias Ply 80 psi	Bias Ply 100 psi	% Increase	Radial 120 psi	% Increase	Radial 140 psi	% Increase
-5.5	129-145	0.931	0.968	3.92	1.078	15.81	1.125	20.79
-8.5	145-161	0.664	0.675	1.62	0.735	10.74	0.751	13.08
-11.5	161-177	0.487	0.490	0.77	0.527	8.36	0.533	9.56
-14.5	177-193	0.408	0.410	0.50	0.442	8.40	0.445	9.22

AC Layer Radial Strain 10^3

Depth in.	Nodal Point	Bias Ply 80 psi	Bias Ply 100 psi	% Increase	Radial 120 psi	% Increase	Radial 140 psi	% Increase
0.00	1-2	0.356	0.483	35.70	0.560	57.42	0.646	81.32
-0.50	17-18	0.286	0.157	-45.16	0.060	-79.01	-0.002	-100.80
-1.00	33-34	0.092	-0.129	-239.75	-0.274	-398.06	-0.402	-537.04
-1.50	49-50	-0.110	-0.311	183.27	-0.479	336.67	-0.622	467.50
-2.00	65-66	-0.264	-0.419	58.74	-0.587	122.51	-0.720	172.80
-2.50	81-82	-0.363	-0.476	30.96	-0.630	73.31	-0.742	104.05
-3.00	97-98	-0.417	-0.496	19.05	-0.628	50.51	-0.716	71.66
-3.50	113-114	-0.434	-0.487	12.24	-0.589	35.91	-0.653	50.51
-4.00	129-130	-0.426	-0.453	6.45	-0.519	21.85	-0.553	29.87

Base Layer Radial Strain 10^3

Depth in.	Nodal Point	Bias Ply 80 psi	Bias Ply 100 psi	% Increase	Radial 120 psi	% Increase	Radial 140 psi	% Increase
-7.00	145-146	-0.322	-0.330	2.63	-0.364	13.24	-0.376	16.97
-10.00	161-162	-0.233	-0.236	1.07	-0.252	8.13	-0.256	9.93
-13.00	177-178	-0.191	-0.192	0.60	-0.203	6.64	-0.205	7.75
-16.00	193-194	-0.210	-0.211	0.51	-0.227	8.18	-0.229	9.16

Table A.8 Radial and Vertical Strains in AC (6", Eac = 50 ksi) and Base Layers

Pavement Type 6 AC thkness: 6 in. Date: 6/19/90
Eac: 50000 psi

AC layer Vertical Strain 10^3

Depth in.	Nodal Point	Bias Ply 80 psi	Bias Ply 100 psi	% Increase	Radial 120 psi	% Increase	Radial 140 psi	% Increas
-0.25	1-17	0.202	0.565	179.87	1.012	401.25	1.319	552.96
-0.75	17-33	0.394	0.987	150.18	1.506	281.87	1.910	384.29
-1.25	33-49	0.670	1.256	87.49	1.761	162.87	2.175	224.67
-1.75	49-65	0.901	1.363	51.24	1.842	104.37	2.213	145.56
-2.25	65-81	1.038	1.372	32.18	1.805	73.94	2.112	103.53
-2.75	81-97	1.091	1.325	21.49	1.703	56.20	1.946	78.42
-3.25	97-113	1.087	1.251	15.08	1.573	44.75	1.760	61.90
-3.75	113-129	1.051	1.167	11.02	1.438	36.77	1.580	50.30
-4.25	129-145	1.001	1.085	8.31	1.310	30.81	1.418	41.64
-4.75	145-161	0.947	1.007	6.42	1.193	26.01	1.276	34.76
-5.25	161-177	0.889	0.934	5.03	1.082	21.76	1.145	28.85
-5.75	177-193	0.829	0.861	3.87	0.975	17.62	1.021	23.18

Base Layer Vertical Strain 10^3

Depth in.	Nodal Point	Bias Ply 80 psi	Bias Ply 100 psi	% Increase	Radial 120 psi	% Increase	Radial 140 psi	% Increas
-7.5	193-209	0.735	0.750	1.96	0.817	11.13	0.838	13.90
-10.5	209-225	0.517	0.522	0.99	0.566	9.46	0.574	10.95
-13.5	225-241	0.388	0.390	0.54	0.419	8.01	0.422	8.85
-16.5	241-257	0.328	0.329	0.36	0.352	7.41	0.354	8.01

AC Layer Radial Strain 10^3

Depth in.	Nodal Point	Bias Ply 80 psi	Bias Ply 100 psi	% Increase	Radial 120 psi	% Increase	Radial 140 psi	% Increas
0.0	1-2	0.369	0.497	34.83	0.581	57.49	0.668	81.24
-0.5	17-18	0.301	0.173	-42.62	0.079	-73.79	0.018	-93.99
-1.0	33-34	0.116	-0.104	-188.96	-0.248	-313.32	-0.375	-421.80
-1.5	49-50	-0.073	-0.273	273.45	-0.441	503.75	-0.582	696.65
-2.0	65-66	-0.215	-0.368	71.46	-0.538	150.28	-0.667	210.53
-2.5	81-82	-0.305	-0.415	36.42	-0.572	87.82	-0.680	123.37
-3.0	97-98	-0.354	-0.433	22.20	-0.571	61.00	-0.657	85.40
-3.5	113-114	-0.379	-0.435	14.79	-0.552	45.82	-0.620	63.69
-4.0	129-130	-0.388	-0.428	10.40	-0.527	35.80	-0.579	49.34
-4.5	145-146	-0.389	-0.418	7.59	-0.500	28.47	-0.540	38.94
-5.0	161-162	-0.385	-0.407	5.66	-0.473	22.65	-0.504	30.76
-5.5	177-178	-0.378	-0.394	4.21	-0.445	17.64	-0.468	23.73
-6.0	193-194	-0.372	-0.383	2.91	-0.418	12.33	-0.434	16.49

Base Layer Radial Strain 10^3

Depth in.	Nodal Point	Bias Ply 80 psi	Bias Ply 100 psi	% Increase	Radial 120 psi	% Increase	Radial 140 psi	% Increas
-9.0	209-210	-0.253	-0.257	1.44	-0.279	10.17	-0.285	12.45
-12.0	225-226	-0.185	-0.186	0.75	-0.198	7.26	-0.201	8.56
-15.0	241-242	-0.153	-0.153	0.44	-0.161	5.55	-0.162	6.38
-18.0	257-258	-0.161	-0.162	0.38	-0.170	5.91	-0.172	6.62

Table A.9 Comparison of Critical Strains and Stresses (Eac = 500 ksi) (Uniform Tire Pressure).

Pavement Type: Conventional AC Pavement

Comparison of Critical Strains and Stresses Date: 6/19/90

Uniform Tire Pressure

Eac = 500000 psi AC Layer: Radial Strain 10^3

Pavement Type	80 psi	120 psi	% Increase	140 psi	% Increase
2 in. AC	-0.268	-0.369	37.87	-0.403	50.63
4 in. AC	-0.202	-0.250	23.66	-0.263	29.88
6 in. AC	-0.135	-0.151	11.87	-0.156	15.32

Eac = 500000 psi Subgrade: Vertical Strain 10^3

Pavement Type	80 psi	120 psi	% Increase	140 psi	% Increase
2 in. AC	0.429	0.519	21.04	0.524	22.04
4 in. AC	0.243	0.270	11.31	0.271	11.70
6 in. AC	0.146	0.155	6.29	0.155	6.55

Eac = 500000 psi AC Layer: Radial Stress

Pavement Type	80 psi	120 psi	% Increase	140 psi	% Increase
2 in. AC	-134.00	-183.00	36.57	-200.00	49.25
4 in. AC	-135.00	-166.00	22.96	-174.00	28.89
6 in. AC	-96.40	-107.00	11.00	-111.00	15.15

Eac = 500000 psi Subgrade: Vertical Stress

Pavement Type	80 psi	120 psi	% Increase	140 psi	% Increase
2 in. AC	5.92	6.96	17.57	7.00	18.24
4 in. AC	4.42	4.89	10.63	4.90	10.86
6 in. AC	3.51	3.76	7.12	3.75	6.84

Table A.10 Comparison of Critical Strains and Stresses (Eac = 50 ksi) (Uniform Tire Pressure)

Pavement Type: Conventional AC Pavement

Comparison of Critical Strains and Stresses Date: 6/19/90

Uniform Tire Pressure

Eac = 50000 psi AC Layer: Radial Strain 10^3

Pavement Type	80 psi	120 psi	% Increase	140 psi	% Increase
2 in. AC	-0.294	-0.416	41.56	-0.473	60.82
4 in. AC	-0.402	-0.491	22.17	-0.523	29.98
6 in. AC	-0.361	-0.407	12.76	-0.422	16.92

Eac = 50000 psi Subgrade: Vertical Strain 10^3

Pavement Type	80 psi	120 psi	% Increase	140 psi	% Increase
2 in. AC	0.643	0.683	6.21	0.692	7.64
4 in. AC	0.482	0.507	5.07	0.512	6.08
6 in. AC	0.365	0.379	3.82	0.382	4.58

Eac = 50000 psi AC Layer: Radial Stress

Pavement Type	80 psi	120 psi	% Increase	140 psi	% Increase
2 in. AC	32.70	44.50	36.09	50.10	53.21
4 in. AC	4.71	6.08	29.09	6.66	41.40
6 in. AC	-6.49	-7.09	9.24	-7.28	12.17

Eac = 50000 psi Subgrade: Vertical Stress

Pavement Type	80 psi	120 psi	% Increase	140 psi	% Increase
2 in. AC	7.89	8.20	3.93	8.27	4.82
4 in. AC	6.74	7.00	3.86	7.04	4.45
6 in. AC	5.82	6.00	3.09	6.02	3.44

Table A.11 Radial and Vertical Strains in AC (2", Eac = 500 ksi) and Base Layers (Uniform Tire Pressure).

Pavement Type 1 AC thkness: 2 in. Date: 6/19/90
Eac: 500000 psi

Uniform Tire Pressure

AC layer Vertical Strain 10^3

Depth in.	Nodal Point	80 psi	120 psi	% Increase	140 psi	% Increase
-0.25	1-17	-0.190	-0.239	26.20	-0.246	29.92
-0.75	17-33	-0.016	0.000	-101.65	0.012	-178.01
-1.25	33-49	0.151	0.222	47.61	0.250	65.88
-1.75	49-65	0.312	0.441	41.17	0.483	54.56

Base Layer Vertical Strain 10^3

Depth in.	Nodal Point	80 psi	120 psi	% Increase	140 psi	% Increase
-3.5	65-81	0.753	0.969	28.62	1.016	34.89
-6.5	81-97	0.589	0.730	23.96	0.745	26.61
-9.5	97-113	0.449	0.534	18.95	0.539	20.09
-12.5	113-129	0.386	0.450	16.56	0.453	17.33

AC Layer Radial Strain 10^3

Depth in.	Nodal Point	80 psi	120 psi	% Increase	140 psi	% Increase
0.0	1-2	0.266	0.356	34.18	0.384	44.61
-0.5	17-18	0.126	0.162	28.08	0.171	35.33
-1.0	33-34	-0.006	-0.017	177.15	-0.023	272.49
-1.5	49-50	-0.135	-0.190	40.36	-0.209	54.36
-2.0	65-66	-0.267	-0.369	38.27	-0.403	51.06

Base Layer Radial Strain 10^3

Depth in.	Nodal Point	80 psi	120 psi	% Increase	140 psi	% Increase
-5.0	81-82	-0.262	-0.342	30.36	-0.354	35.11
-8.0	97-98	-0.204	-0.250	22.34	-0.253	24.23
-11.0	113-114	-0.174	-0.204	17.24	-0.206	18.34
-14.0	129-130	-0.195	-0.231	18.26	-0.233	19.26

Table A.12 Radial and Vertical Strains in AC (4", Eac = 500 ksi) and Base Layers (Uniform Tire Pressure).

Pavement Type 2 AC thkness: 4 in. Date: 6/19/90
Eac: 500000 psi

Uniform Tire Pressure

AC layer Vertical Strain 10^3

Depth in.	Nodal Point	80 psi	120 psi	% Increase	140 psi	% Increase
-0.25	1-17	-0.127	-0.127	0.47	-0.118	-7.32
-0.75	17-33	-0.057	-0.033	-41.68	-0.015	-74.37
-1.25	33-49	0.003	0.042	1138.33	0.065	1818.46
-1.75	49-65	0.054	0.100	86.25	0.124	129.38
-2.25	65-81	0.099	0.148	49.61	0.169	70.55
-2.75	81-97	0.144	0.194	34.77	0.211	47.05
-3.25	97-113	0.193	0.246	27.20	0.262	35.34
-3.75	113-129	0.251	0.314	24.77	0.330	31.23

Base Layer Vertical Strain 10^3

Depth in.	Nodal Point	80 psi	120 psi	% Increase	140 psi	% Increase
-5.5	129-145	0.463	0.543	17.35	0.558	20.49
-8.5	145-161	0.353	0.402	14.06	0.406	15.21
-11.5	161-177	0.281	0.313	11.64	0.315	12.14
-14.5	177-193	0.244	0.269	10.02	0.269	10.35

AC Layer Radial Strain 10^3

Depth in.	Nodal Point	80 psi	120 psi	% Increase	140 psi	% Increase
0.00	1-2	0.179	0.218	21.43	0.229	27.39
-0.50	17-18	0.120	0.136	13.53	0.138	15.20
-1.00	33-34	0.067	0.067	-0.16	0.063	-6.73
-1.50	49-50	0.020	0.009	-55.51	0.001	-92.92
-2.00	65-66	-0.022	-0.040	85.68	-0.049	125.60
-2.50	81-82	-0.062	-0.085	37.86	-0.094	51.67
-3.00	97-98	-0.103	-0.131	27.33	-0.140	35.60
-3.50	113-114	-0.149	-0.184	23.63	-0.194	30.04
-4.00	129-130	-0.202	-0.250	23.66	-0.263	29.88

Base Layer Radial Strain 10^3

Depth in.	Nodal Point	80 psi	120 psi	% Increase	140 psi	% Increase
-7.00	145-146	-0.153	-0.179	16.60	-0.182	18.83
-10.00	161-162	-0.121	-0.136	12.59	-0.137	13.52
-13.00	177-178	-0.105	-0.115	9.63	-0.116	10.16
-16.00	193-194	-0.109	-0.119	8.86	-0.119	9.27

Table A.13 Radial and Vertical Strains in AC (6", Eac = 500 ksi) and Base Layers (Uniform Tire Pressure).

Pavement Type 3 AC thkness: 6 in. Date: 6/19/90
Eac: 500000 psi

Uniform Tire Pressure

AC layer Vertical Strain 10^3

Depth in.	Nodal Point	80 psi	120 psi	% Increase	140 psi	% Increase
-0.25	1-17	-0.060	-0.035	-42.43	-0.021	-65.71
-0.75	17-33	-0.020	0.023	-215.23	0.044	-326.83
-1.25	33-49	0.015	0.066	354.05	0.092	531.22
-1.75	49-65	0.041	0.095	133.88	0.121	196.89
-2.25	65-81	0.060	0.111	86.16	0.134	123.96
-2.75	81-97	0.074	0.119	61.35	0.138	86.34
-3.25	97-113	0.085	0.123	44.53	0.138	61.40
-3.75	113-129	0.096	0.127	32.21	0.138	43.61
-4.25	129-145	0.108	0.133	23.23	0.141	30.95
-4.75	145-161	0.123	0.144	17.06	0.151	22.45
-5.25	161-177	0.144	0.163	13.41	0.169	17.50
-5.75	177-193	0.171	0.192	12.46	0.198	15.94

Base Layer Vertical Strain 10^3

Depth in.	Nodal Point	80 psi	120 psi	% Increase	140 psi	% Increase
-7.5	193-209	0.294	0.327	10.96	0.332	12.79
-10.5	209-225	0.225	0.247	10.18	0.249	10.90
-13.5	225-241	0.182	0.199	9.16	0.200	9.49
-16.5	241-257	0.159	0.171	7.39	0.171	7.59

AC Layer Radial Strain 10^3

Depth in.	Nodal Point	80 psi	120 psi	% Increase	140 psi	% Increase
0.0	1-2	0.118	0.133	13.49	0.141	19.53
-0.5	17-18	0.083	0.084	0.87	0.084	0.27
-1.0	33-34	0.053	0.042	-19.81	0.036	-31.36
-1.5	49-50	0.027	0.010	-63.55	0.001	-95.99
-2.0	65-66	0.006	-0.014	-349.86	-0.023	-511.89
-2.5	81-82	-0.012	-0.031	157.98	-0.039	225.02
-3.0	97-98	-0.027	-0.044	62.85	-0.051	87.51
-3.5	113-114	-0.041	-0.056	35.91	-0.061	49.04
-4.0	129-130	-0.055	-0.068	23.15	-0.072	31.10
-4.5	145-146	-0.070	-0.082	16.30	-0.086	21.64
-5.0	161-162	-0.088	-0.099	12.75	-0.103	16.77
-5.5	177-178	-0.109	-0.121	11.35	-0.125	14.84
-6.0	193-194	-0.135	-0.151	11.87	-0.156	15.32

Base Layer Radial Strain 10^3

Depth in.	Nodal Point	80 psi	120 psi	% Increase	140 psi	% Increase
-9.0	209-210	-0.096	-0.104	8.75	-0.106	10.20
-12.0	225-226	-0.076	-0.081	7.56	-0.082	8.24
-15.0	241-242	-0.066	-0.070	5.28	-0.070	5.63
-18.0	257-258	-0.065	-0.067	3.43	-0.067	3.70

Table A.14 Radial and Vertical Strains in AC (2", Eac = 50 ksi) and Base Layers (Uniform Tire Pressure).

Pavement Type 4 AC thkness: 2 in. Date: 6/19/90
Eac: 50000 psi

Uniform Tire Pressure

AC layer Vertical Strain 10^3

Depth in.	Nodal Point	80 psi	120 psi	% Increase	140 psi	% Increase
-0.25	1-17	0.513	0.878	71.27	1.067	108.08
-0.75	17-33	0.720	1.194	65.96	1.445	100.79
-1.25	33-49	0.900	1.435	59.42	1.711	90.18
-1.75	49-65	1.032	1.549	50.00	1.798	74.14

Base Layer Vertical Strain 10^3

Depth in.	Nodal Point	80 psi	120 psi	% Increase	140 psi	% Increase
-3.5	65-81	0.976	1.206	23.62	1.297	32.98
-6.5	81-97	0.820	0.919	12.12	0.953	16.22
-9.5	97-113	0.618	0.655	6.00	0.667	7.81
-12.5	113-129	0.529	0.551	4.15	0.557	5.34

AC Layer Radial Strain 10^3

Depth in.	Nodal Point	80 psi	120 psi	% Increase	140 psi	% Increase
0.0	1-2	0.257	0.311	20.87	0.337	31.21
-0.5	17-18	0.966	0.057	-94.14	0.028	-97.12
-1.0	33-34	-0.058	-0.177	206.64	-0.249	330.48
-1.5	49-50	-0.187	-0.338	81.07	-0.419	124.44
-2.0	65-66	-0.281	-0.416	47.80	-0.473	67.96

Base Layer Radial Strain 10^3

Depth in.	Nodal Point	80 psi	120 psi	% Increase	140 psi	% Increase
-5.0	81-82	-0.366	-0.437	19.33	-0.463	26.36
-8.0	97-98	-0.287	-0.313	8.92	-0.321	11.71
-11.0	113-114	-0.241	-0.253	5.15	-0.257	6.74
-14.0	129-130	-0.286	-0.301	5.14	-0.305	6.60

Table A.15 Radial and Vertical Strains in AC (4", Eac = 50 ksi) and Base Layers (Uniform Tire Pressure).

Pavement Type 5 AC thkness: 4 in. Date: 6/19/90
Eac: 50000 psi

Uniform Tire Pressure

AC layer Vertical Strain 10^3

Depth in.	Nodal Point	80 psi	120 psi	% Increase	140 psi	% Increase
-0.25	1-17	0.393	0.702	78.34	0.859	118.34
-0.75	17-33	0.630	1.082	71.64	1.316	108.81
-1.25	33-49	0.831	1.374	65.36	1.649	98.42
-1.75	49-65	0.983	1.552	57.97	1.827	85.94
-2.25	65-81	1.077	1.619	50.28	1.867	73.26
-2.75	81-97	1.120	1.601	42.92	1.809	61.51
-3.25	97-113	1.114	1.514	35.90	1.679	50.69
-3.75	113-129	1.069	1.374	28.57	1.493	39.71

Base Layer Vertical Strain 10^3

Depth in.	Nodal Point	80 psi	120 psi	% Increase	140 psi	% Increase
-5.5	129-145	0.913	1.041	13.97	1.084	18.73
-8.5	145-161	0.675	0.724	7.28	0.739	9.57
-11.5	161-177	0.503	0.524	4.05	0.530	5.27
-14.5	177-193	0.427	0.440	3.09	0.444	3.93

AC Layer Radial Strain 10^3

Depth in.	Nodal Point	80 psi	120 psi	% Increase	140 psi	% Increase
0.00	1-2	0.358	0.469	30.88	0.526	46.74
-0.50	17-18	0.169	0.152	-10.45	0.135	-20.26
-1.00	33-34	-0.005	-0.126	2622.49	-0.197	4150.11
-1.50	49-50	-0.150	-0.333	121.52	-0.429	185.70
-2.00	65-66	-0.261	-0.464	77.94	-0.563	116.03
-2.50	81-82	-0.337	-0.533	58.10	-0.622	84.63
-3.00	97-98	-0.383	-0.554	44.77	-0.628	64.02
-3.50	113-114	-0.403	-0.538	33.63	-0.592	47.20
-4.00	129-130	-0.402	-0.491	22.17	-0.523	29.98

Base Layer Radial Strain 10^3

Depth in.	Nodal Point	80 psi	120 psi	% Increase	140 psi	% Increase
-7.00	145-146	-0.320	-0.356	11.05	-0.367	14.68
-10.00	161-162	-0.236	-0.250	5.80	-0.254	7.63
-13.00	177-178	-0.195	-0.202	3.60	-0.205	4.76
-16.00	193-194	-0.218	-0.226	3.64	-0.228	4.67

Table A.16 Radial and Vertical Strains in AC (6", Eac = 50 ksi) and Base Layers (Uniform Tire Pressure).

Pavement Type 6 AC thkness: 6 in. Date: 6/19/90
Eac: 50000 psi

Uniform Tire Pressure

AC layer Vertical Strain 10^3

Depth in.	Nodal Point	80 psi	120 psi	% Increase	140 psi	% Increase
-0.25	1-17	0.373	0.674	80.64	0.829	122.10
-0.75	17-33	0.602	1.046	73.81	1.277	112.25
-1.25	33-49	0.787	1.319	67.63	1.589	101.94
-1.75	49-65	0.920	1.474	60.18	1.742	89.29
-2.25	65-81	0.998	1.520	52.31	1.758	76.22
-2.75	81-97	1.029	1.489	44.76	1.688	64.07
-3.25	97-113	1.025	1.414	37.99	1.573	53.49
-3.75	113-129	0.999	1.320	32.16	1.445	44.66
-4.25	129-145	0.961	1.223	27.23	1.320	37.38
-4.75	145-161	0.916	1.128	23.07	1.204	31.37
-5.25	161-177	0.866	1.034	19.40	1.093	26.19
-5.75	177-193	0.812	0.941	15.81	0.985	21.20

Base Layer Vertical Strain 10^3

Depth in.	Nodal Point	80 psi	120 psi	% Increase	140 psi	% Increase
-7.5	193-209	0.739	0.802	8.51	0.822	11.23
-10.5	209-225	0.536	0.561	4.73	0.569	6.21
-13.5	225-241	0.406	0.417	2.88	0.421	3.76
-16.5	241-257	0.343	0.351	2.29	0.353	2.92

AC Layer Radial Strain 10^3

Depth in.	Nodal Point	80 psi	120 psi	% Increase	140 psi	% Increase
0.0	1-2	0.371	0.488	31.49	0.547	47.40
-0.5	17-18	0.184	0.169	-7.66	0.154	-16.00
-1.0	33-34	0.017	-0.101	-706.66	-0.170	-1122.47
-1.5	49-50	-0.119	-0.296	148.79	-0.390	227.79
-2.0	65-66	-0.219	-0.416	89.63	-0.513	133.53
-2.5	81-82	-0.287	-0.477	65.96	-0.563	96.03
-3.0	97-98	-0.329	-0.498	51.35	-0.571	73.32
-3.5	113-114	-0.353	-0.497	40.96	-0.556	57.55
-4.0	129-130	-0.365	-0.485	33.10	-0.532	45.89
-4.5	145-146	-0.369	-0.468	26.89	-0.505	36.89
-5.0	161-162	-0.369	-0.449	21.76	-0.478	29.59
-5.5	177-178	-0.365	-0.428	17.13	-0.449	23.06
-6.0	193-194	-0.361	-0.407	12.76	-0.422	16.92

Base Layer Radial Strain 10^3

Depth in.	Nodal Point	80 psi	120 psi	% Increase	140 psi	% Increase
-9.0	209-210	-0.258	-0.275	6.95	-0.281	9.20
-12.0	225-226	-0.190	-0.197	4.00	-0.200	5.33
-15.0	241-242	-0.157	-0.161	2.54	-0.162	3.42
-18.0	257-258	-0.166	-0.170	2.51	-0.171	3.29